

University of Alberta
Department of Civil &
Environmental Engineering



Structural Engineering Report No. 217

CONNECTION OF INFILL PANELS IN STEEL PLATE SHEAR WALLS

by
Ann Schumacher
Gilbert Y. Grondin
and
Geoffrey L. Kulak

August 1997

CONNECTION OF INFILL PANELS IN STEEL PLATE SHEAR WALLS

by

**Ann Schumacher
Gilbert Y. Grondin
and
Geoffrey L. Kulak**

Structural Engineering Report No. 217

**Department of Civil Engineering
University of Alberta
Edmonton, Alberta, Canada T6G 2G7**

August 1997

Abstract

Steel plate shear walls are a very ductile and stable lateral force-resisting system. The ability of a steel plate shear wall to resist effectively lateral loads on a structure—such as wind loading and earthquake loading—will depend in part on the transfer of forces from the infill panel to the beams and the columns. This is especially critical in unstiffened steel plate shear walls, where the development of a tension field within a shear panel requires proper anchorage of the infill plate.

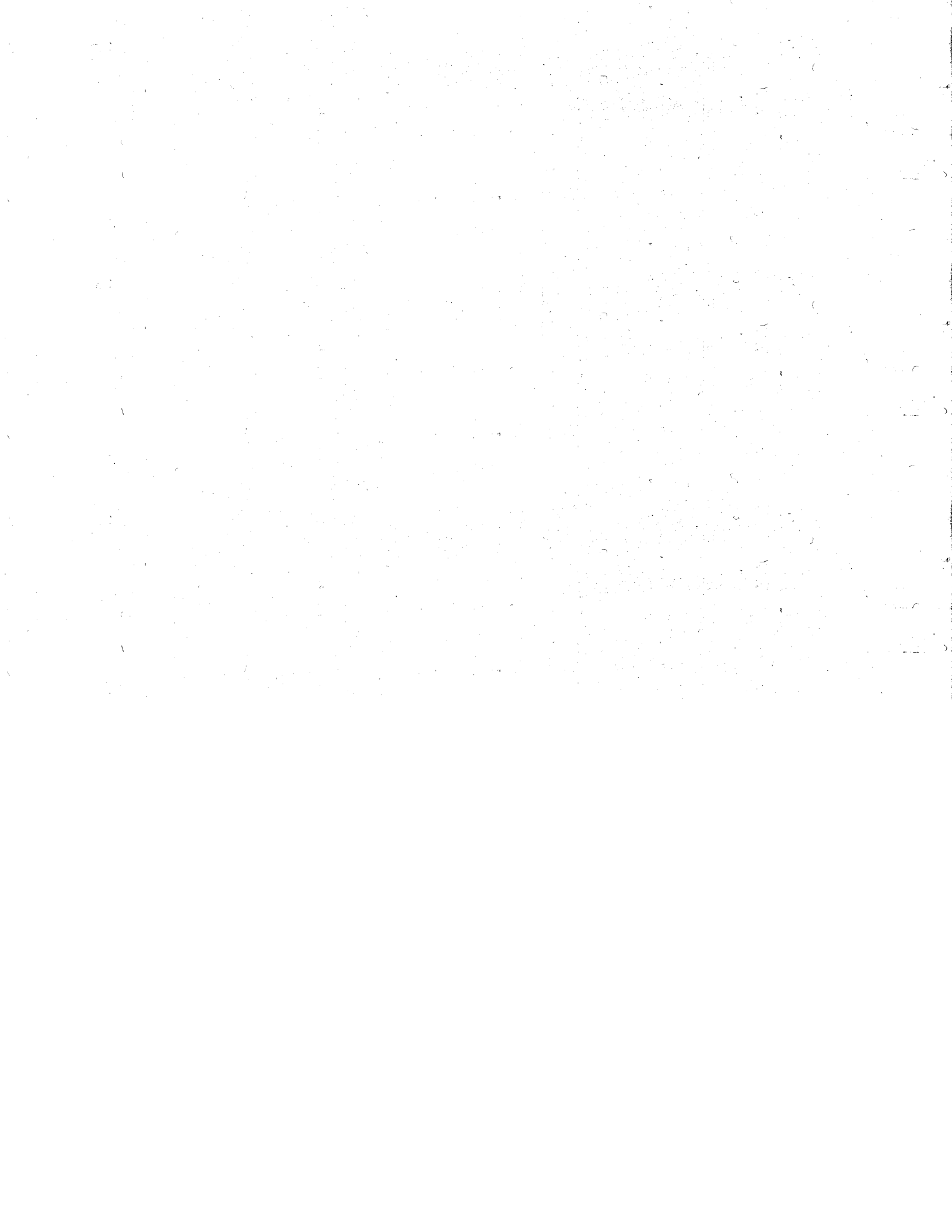
Four different infill panel connection details were tested in order to examine and compare their response to quasi-static cyclic loading. The load versus displacement response of the details showed gradual and stable deterioration at higher loads. The formation of tears in the connection details did not result in a loss of load-carrying capacity. In addition to the experimental program, a finite element model was developed to predict the behaviour of one of the infill plate corner connection specimens. Results from the analysis showed that the finite element method can be used to predict reliably the load versus displacement behaviour of an infill panel-to-boundary member arrangement.

Acknowledgements

Funding for this research was provided by the Natural Sciences and Engineering Research Council of Canada. Thanks are extended to Mr. Larry Burden and Mr. Richard Helfrich, technicians in the Morrison Structural Engineering Laboratory, who were instrumental during the experimental portion of the work. Mr. Richard Vincent of Canam Manac Group Incorporated, Boucherville, PQ gave helpful technical advice on some of the connection details investigated in the research program. Thanks are also extended to Dr. D.J.L. Kennedy for his advice and input at numerous occasions during the course of this project.

Table of Contents

1.	Introduction	1
	1.1 Steel Plate Shear Walls	1
	1.2 Statement of the Problem	2
	1.3 Scope and Objectives	3
2.	Literature Review	5
	2.1 Introduction	5
	2.2 Bolted Infill Plate Connections	6
	2.3 Welded Infill Plate Connections	7
	2.3.1 Testing of Welded Steel Plate Shear Walls	7
	2.3.2 Recent Tests Done by Driver <i>et al.</i> [1997]	10
3.	Experimental Program	17
	3.1 Objectives of the Test Program	17
	3.2 Loading Concept	18
	3.3 Testing of Material Properties	19
	3.4 Infill Plate Connection Specimens	19
	3.5 Test Set-Up	21
	3.5.1 Test Frame	21
	3.5.2 Placement of the Specimen	22
	3.5.3 Test Control and Data Acquisition	23
	3.6 Test Procedure	24
4.	Experimental Results	39
	4.1 General	39
	4.2 Material Properties	39
	4.3 Test Data and Observations	40
	4.3.1 Out-of-Plane Measurements	40
	4.3.2 Deterioration of the Infill Plate Connection Specimens	40
	4.3.2.1 Specimen Buckling	40
	4.3.2.2 Hysteresis Behaviour	41
	4.3.2.3 Specimen Tearing	43
	4.4 Strain Gauge Data	46
5.	Finite Element Analysis	63
	5.1 General	63
	5.2 Description of Model	63
	5.2.1 Elements and Mesh	63
	5.2.2 Initial Conditions	65
	5.2.3 Material Model	66
	5.3 Analysis	67
	5.4 Results of the Analysis	68
6.	Discussion	76



6.1	Experimental Results of Infill Plate Connection Specimens	76
6.1.1	Buckling of Specimens	76
6.1.2	Load Versus Displacement Response	77
6.1.3	Tearing of Specimens	78
6.1.4	Summary of Specimen Behaviour and Response.....	80
6.2	Comparison with the Results of Earlier Studies.....	82
6.3	Finite Element Analysis	82
6.3.1	Load Versus Displacement Comparison	83
6.3.2	Strains in the Infill Plate	84
6.3.2.1	Comparison with Strain Gauge Data	84
6.3.2.2	Correlation of Strains with Specimen Tearing	85
7.	Summary, Conclusions, and Recommendations.....	99
7.1	Summary and Conclusions.....	99
7.2	Recommendations	100
	List of References	102
	Appendix A – Results of Tension Coupon Tests.....	105
	Appendix B – Demec Point Data	107
	Appendix C – Experimental Strain Results	115
	Appendix D – Loading Block Data	121

List of Tables

Table 3.1	Plate Material and Weld Data	27
Table 3.2	Load History Followed for Infill Plate Connection Specimen Tests	28
Table 4.1	Material Properties	47
Table 4.2	Measured Strains from Specimen 2	48
Table 6.1	Comparison of Loading Blocks for Specimen 2	88
Table A.1	Coupon Test Results	106
Table B.1	Demec Point Data for Specimen 1	109
Table B.2a	Demec Point Data for Specimen 2	110
Table B.2b	Demec Point Data for Specimen 2 (con't)	111
Table B.3	Demec Point Data for Specimen 3	112
Table B.4	Demec Point Data for Specimen 4.....	113
Table C.1	Measured Strains from Specimen 1.....	116
Table C.2	Measured Strains from Specimen 2.....	117
Table C.3	Measured Strains from Specimen 3.....	118
Table C.4	Measured Strains from Specimen 4.....	119
Table D.1	Comparison of Loading Blocks for Specimen 1	122
Table D.2	Comparison of Loading Blocks for Specimen 2	123
Table D.3	Comparison of Loading Blocks for Specimen 3	124
Table D.4	Comparison of Loading Blocks for Specimen 4	125

List of Figures

Figure 1.1	Steel Plate Shear Wall Panel Using Fish Plates	4
Figure 2.1	Bolted Infill Plate Connection Details.....	13
Figure 2.2	Welded Infill Plate Connection Detail	13
Figure 2.3	Timler and Kulak [1983] Test Specimen	14
Figure 2.4	Tear Observed in Timler and Kulak [1983] Specimen	14
Figure 2.5	Tromposch and Kulak [1987] Corner Detail	15
Figure 2.6	Tear Observed in Tromposch and Kulak [1987] Specimen	15
Figure 2.7	Corner Detail Specimen [Driver <i>et al.</i> 1997].....	16
Figure 3.1	One Storey of Driver <i>et al.</i> [1997] Four-Strey Steel Plate Shear Wall	29
Figure 3.2	Steel Plate Shear Wall Panel Using Two Fish Plates	29
Figure 3.3	Loading Concept for Infill Plate Connection Tests	30
Figure 3.4	Infill Plate Connection Specimen 1.....	31
Figure 3.5	Infill Plate Connection Specimen 2.....	32
Figure 3.6	Infill Plate Connection Specimen 3.....	33
Figure 3.7	Infill Plate Connection Specimen 4.....	34
Figure 3.8	Test Set-Up	35
Figure 3.9	South Side of Test Set-Up—Looking Eastward	36
Figure 3.10	South Side of Test Set-Up—Looking Westward	37
Figure 3.11	Strain Rosette Locations	38
Figure 4.1	Buckling of Infill Plate	49
Figure 4.2	Yielding of Specimen 4 Due to Buckling	50
Figure 4.3	Hysteresis Curves for Specimen 1	51
Figure 4.4	Hysteresis Curves for Specimen 2	51
Figure 4.5	Hysteresis Curves for Specimen 3.....	52
Figure 4.6	Hysteresis Curves for Specimen 4.....	52
Figure 4.7	V-Frame Load Versus Displacement Response.....	53
Figure 4.8	Yielding Observed on North and South Sides of Specimen 1	54
Figure 4.9	Yielding Observed on North Side of Specimen 1	54
Figure 4.10	Tears Noted on Specimen 2	55

Figure 4.11	Specimen 2 Corner Detail at End of Testing	56
Figure 4.12	Tears Noted on Specimen 3	57
Figure 4.13	Specimen 3 Corner Detail at End of Testing	58
Figure 4.14	Tears Noted on Specimen 4	59
Figure 4.15	Specimen 4 Corner Detail at End of Testing	60
Figure 4.16	Axes for Strain Orientation	61
Figure 4.17	Measured Normal and Shear Strains	62
Figure 5.1	V-Frame Finite Element Model	70
Figure 5.2	Coarse Finite Element Mesh	71
Figure 5.3	Fine Finite Element Mesh	72
Figure 5.4	Material Model	73
Figure 5.5	V-Frame Stiffness—Experimental Versus Analytical	74
Figure 5.6	Finite Element Analysis Results for Coarse and Fine Meshes	75
Figure 6.1	Load Versus Displacement Envelopes	89
Figure 6.2	Specimen 2 and Specimen 4 at End of Testing	90
Figure 6.3	Specimen 2 Response Compared to Analysis Results	91
Figure 6.4	Test Specimen 2 – Comparison of the Observed Deformed Shape with the Predicted Deformed Shape	92
Figure 6.5	Strain Comparison at Inward V-Frame Displacement.....	93
Figure 6.6	Strain Comparison at Outward V-Frame Displacement	94
Figure 6.7	Major Principal Strain Distribution at Maximum Inward V-Frame Displacement	95
Figure 6.8	Major Principal Strain Vector Plot at Maximum Inward V-Frame Displacement	96
Figure 6.9	Major Principal Strain Distribution at Maximum Outward V-Frame Displacement	97
Figure 6.10	Major Principal Strain Vector Plot at Maximum Outward V-Frame Displacement	98
Figure B.1	Location of Demec Points on Specimens	108

1. Introduction

1.1 Steel Plate Shear Walls

A multi-storey structure must be able to absorb wind and earthquake loads through some kind of lateral force-resisting system. Factors contributing to the choice of a particular lateral bracing system range from architectural requirements—floor space, building aesthetics—to economic considerations. The most commonly used lateral force-resisting systems in tall structures are: moment-resisting frames, braced frames, shear walls, and tubular systems.

Moment-resisting frames have proven to be efficient for structures up to about 20 storeys. On the other end of the building height spectrum, a tubular system, that is, a system of closely spaced columns around the perimeter of a structure, will provide bracing for buildings with over 40 storeys. Braced frames and shear walls are generally found in structures up to 40 storeys. In some cases, moment resisting or braced frames are interconnected with shear walls, thereby combining the structural advantages of the two systems and optimizing the overall lateral load resisting behaviour.

The concept of shear walls is that of a series of plane walls that can be idealized as vertical cantilevers supported at the foundation of a structure. Typically, a series of shear walls will form a core that surrounds a central service area in a multi-storey building. Wind loads acting on the building exterior are transferred through the floors to the shear core. In the case of dynamic earthquake loading, the shear core is displaced laterally at the ground level.

In recent years, it has been demonstrated that steel plate shear walls can act as an effective and economical lateral bracing system. In particular, steel plate shear walls will respond to seismically-induced loading with a high degree of stiffness, stable load versus deflection behaviour, and a capacity for significant energy dissipation [Driver *et al.* 1997]. The economic advantages of a steel plate shear wall system are realized through its speed of erection and the elimination of trade interdependence in an all-steel system. As compared with conventional reinforced concrete shear walls, steel plate shear walls have a reduced mass, which lowers the dynamic forces and gravity loads transmitted to the building foundation. For the same strength requirement, steel plate

shear walls will have a much smaller wall thickness than heavily reinforced concrete walls. This results in more rentable space for the owner.

A steel plate shear wall assemblage consist of columns intersected at the floor levels by beams, thereby forming a vertical stack of rectangular bays that are then filled with steel plates. These are also referred to as *infill* plates. The connections between the beams and the columns can range from simple to moment-resisting, and the steel infill panels can be either stiffened or unstiffened. In the former case, lateral and longitudinal stiffeners are applied to the steel panels to prevent buckling of the infill plate. Unstiffened steel panels rely on the post-buckling strength of the thin steel plates, which is provided by the formation of a diagonal tension field. The application of this concept was first seen in the analysis and design of aircraft; in civil engineering practice, the tension field concept is used in the design of steel plate girder webs. It is judged that stiffened steel plate shear walls are not economical in the North American market, and the work described herein concentrates on research pertaining to unstiffened steel plate shear walls.

A single bay in a steel plate shear wall consists of a vertical steel panel framed by beams and columns. In an unstiffened steel plate shear wall, a thin steel panel will buckle under small compressive loads. The formation of a tension field in the infill plate in the direction orthogonal to buckling depends on the transfer of forces from the steel panel to the stiffer beams and columns. Therefore, proper anchorage of the steel plate to the boundary members is critical in areas of high stress. For example, the effect of reversing lateral loads on a structure—such as wind loading and earthquake loading—will cause the angle between the beams and the columns at their intersection to increase and decrease. This relative movement between the boundary members can result in large reversing strains in the corner region of the infill plate where it connects into the beam-to-column joint.

1.2 Statement of the Problem

The most obvious scheme for connecting the infill panel to the boundary members is to weld the steel plate directly to the beams and the columns. This does not represent a practical solution, however, since it would require precise fitting of the infill

plate into the rectangle formed by the beams and the columns in a given bay and storey. An alternative scheme uses connection plates, also referred to as *fish* plates, connected to the boundary members. The use of fish plates in a steel plate shear wall panel can be seen in Figure 1.1. The fish plate detail facilitates the placement of the infill plate in the frame and permits reasonable fabrication tolerances.

The fish plate connection shown in Figure 1.1, which has been used in much of the experimental work on steel plate shear walls, is only one possible infill panel-to-boundary member arrangement. In order to produce economical designs, both designers and fabricators should have access to several methods for infill panel-to-boundary member connections in the construction of steel plate shear walls. Therefore, it is considered appropriate to examine and compare the behaviour of various infill plate connection details.

1.3 Scope and Objectives

The scope and objectives of this study are to:

1. Investigate four welded infill plate-to-boundary member corner connection details experimentally;
2. Examine the effect of corner detail deterioration on the load-carrying capacity of the infill plate;
3. Compare the behaviour of the four infill plate corner connection details;
4. Explore the potential of using the finite element method to predict reliably the behaviour of infill plate connection details.

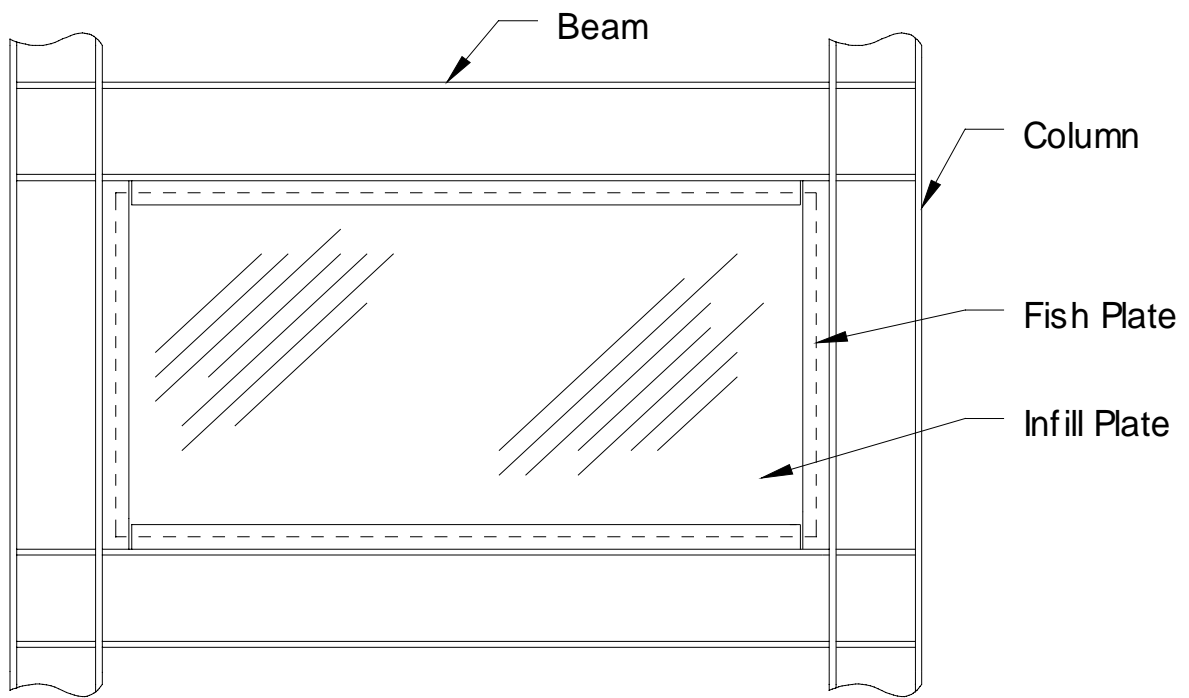


Figure 1.1 Steel Plate Shear Wall Panel Using Fish Plates

2. Literature Review

2.1 Introduction

The emergence of steel plate shear walls, both as a topic of research and in actual construction, began in the early 1970's. Most of the structures constructed during this period that employed steel shear walls were built in Japan and the United States, and they were generally a substitute for conventional reinforced concrete shear walls. As a result, the earliest research came from Japan and the United States, the Japanese being the first to study the overall behaviour of steel plate shear walls [Takahashi *et al.*, 1973]. The design approach used by the Japanese concentrated on preventing the steel plate shear panels from buckling prior to the attainment of shear yield. This was achieved by reinforcing the thin panels with a relatively large number of longitudinal and transverse stiffeners, a solution that is considered uneconomical in North America. In the United States, the design concept also was to prevent elastic buckling in the panels of the steel plate shear walls. However, in American practice this was most commonly achieved by using sufficiently thick steel plate panels. This solution also had economic implications, both with respect to material cost and erection.

The judgement of Thorburn *et al.* [1983] was that the prevention of shear buckling in a steel plate shear wall panel would generally lead to an overly conservative solution. As a result, they developed a model recognizing that thin steel plate panels have considerable post-buckling strength. The so-called strip-model is a reflection of the fact that allowing the formation of a tension field within a buckled panel adds substantial resistance to the shear wall. Since permitting the panel to buckle does not require the addition of stiffeners or the use of thickened plates, it seemed to offer both strength and cost advantages. Experimental research that started in the 1980's [Timler and Kulak, 1983; Tromposch and Kulak, 1987; and Driver *et al.*, 1997] led to the validation and further refinement of the original analytical work presented by Thorburn *et al.* The experimental work concentrated first on the overall behaviour under monotonic loading, and later considered the hysteretic performance of thin steel plate shear panels when subjected to reversing cyclic loads. In addition to the analytical and experimental work, Thorburn *et al.* and Driver *et al.* also present extensive reviews of previous research and

construction of steel plate shear walls.

In both the construction of steel plate shear walls and in the associated research, not much attention has been given to the behaviour of the shear panel-to-boundary member connections used. The connection between the shear panel and boundary members is critical in the force transfer from the infill plate (or web plate) to the stiffer boundary members—the beams and columns. Two types of infill plate connections have been used in the design and construction of steel plate shear walls: bolted connections and welded connections.

2.2 Bolted Infill Plate Connections

A typical bolted connection consists of fish plates, or angles, shop-welded to the boundary members and an infill plate bolted to the fish plates or angles in the field. Figure 2.1 shows each of these details. The infill plate is lapped over and bolted to the fish plate, or passed between a pair of angles. The bolts must form a slip-critical connection, because the development of a tension field in an infill panel requires that these connections do not slip.

The use of bolted infill plate connections has been documented for several buildings. For example, the Hyatt Regency Hotel in Dallas, Texas used thick steel plate sections in the construction of steel plate shear walls to resist wind load [Troy and Richard, 1988]. The steel plate walls were connected to columns using a bolted double angle arrangement like the one shown in Figure 2.1. Steel plates from successive storeys were connected with a field-bolted splice just above each floor line. Two horizontally oriented channels were welded to the steel plates to form a closed tube section at the floor level. The torsionally stiff closed tube sections acted as floor beams, and provided significant restraint to the steel panels against out-of-plane buckling. A hospital in California (Olive View Medical Center) used a combination of concrete shear walls and bolted steel plate shear walls in order to meet the stringent California earthquake regulations. In this application, similar to the one used for the Hyatt Regency Hotel, wall panel assemblies were again connected to columns with high strength bolts. Adjacent panel storeys were connected with a field-bolted splice above the channel floor beams [Troy and Richard 1988].

One of the earliest Japanese high-rises that employed steel plate shear walls as the lateral force-resisting system, the Shinjuku Nomura Building, was built using bolted infill plate connections [Anon. 1978]. Stiffened, rectangular steel infill plates were bolted to connection plates, thereby forming the panels of the shear wall. Each panel required between 200 to 500 bolts depending on the forces in the panel. The connection scheme required precise drilling and placement, resulting in increased time and expense in the construction of the shear walls.

2.3 Welded Infill Plate Connections

A more practical method of joining shear wall panels to boundary members is to use an all-welded infill plate connection. The most significant advantage of all-welded connections is that they eliminate the need for the precise drilling of holes and the bolt placement required for bolted infill plate connections. An example of a typical welded infill plate connection is shown in Figure 2.2. First, fish plates are shop-welded to the boundary members. Then, in the field, the infill plate is lapped over the fish plates and held in place with a few erection bolts or tack welds. Once the structure has been plumbed and aligned, the infill plate is welded to the fish plates with continuous fillet welds. The infill plate need not be aligned precisely; the only requirement is that there be sufficient overlap of the infill plate and fish plates so that the welding can be properly executed.

2.3.1 Testing of Welded Steel Plate Shear Walls

Welded steel plate shear walls have been investigated both experimentally and analytically. As mentioned above, Japanese researchers were among the first to study the behaviour of steel plate shear panels. The all-welded specimens—steel panels were welded directly to pin-connected framing members—tested by Takahashi *et al.* [1973] were heavily stiffened steel plates designed to prevent buckling of the shear panels. A more recent Japanese study examined the energy dissipation behaviour of shear panels made of low yield strength steel [Nakashima *et al.* 1994]. Specimens consisted again of a steel web plate welded directly to the surrounding framing members. Six shear panels with different stiffener spacings (one specimen had no stiffeners) were subjected to

various loading conditions. The behaviour of panels with both horizontal and vertical stiffeners exhibited stable hysteresis loops and a large energy dissipation capacity. In literature from the Japanese tests mentioned above, Takahashi *et al.* and Nakashima *et al.* report the overall behaviour of the steel plate test specimens. However, no descriptions of the steel plate-to-boundary member connection performance are given.

An experimental study of thin steel plate shear walls under cyclic load was conducted using 1:4 scale, single bay, three-storey specimens [Caccese *et al.* 1993]. The all-welded specimens used unstiffened steel plates welded directly to the steel frame members. A steel frame with no infill plate was also tested. Experimental results showed that the addition of unstiffened thin steel plates to a steel frame gave a substantial increase in stiffness, load-carrying capacity and energy absorption to the overall system. However, the connection detail used in these tests—direct connection of the infill panel to the boundary members—is not a practical one. The research performed by Caccese *et al.* examined the behaviour of steel plate shear wall systems as a whole. The contribution of the infill plate connections, although essential to the behaviour of steel plate shear walls, was not mentioned in discussions about the performance of shear walls, as affected by load, material, and design variables.

Two experimental programs at the University of Alberta closely followed the analytical study done by Thorburn *et al.* [1983]. In the first, Timler and Kulak [1983] examined the behaviour of a single, full-scale, unstiffened steel plate shear wall—first under reversing loads sufficient to reach the allowable serviceability deflection, and then under ultimate load. The symmetric specimen, shown in Figure 2.3, consisted of two adjacent shear panels. In the orientation depicted in the figure the columns are positioned horizontally, and the beams—two exterior beams and one interior beam separating the infill panels—are positioned vertically in the test set-up. A welded fish plate arrangement, similar to the one shown in Figure 2.2, connected the infill panels to the boundary members. Moment-resisting connections were used between the interior beam and the columns. The joints between the exterior beams and the columns were pin-connected. The entire specimen was supported by two pin reactions located at the base of the exterior beams. Loads (equivalent to a storey shear force) were applied vertically to the structure through the midpoint of the top column.

The Timler and Kulak specimen responded elastically to reversed serviceability level loading. Subsequently, during monotonic loading to failure, the ultimate load was reached when a weld tear occurred in an infill plate-to-fish plate connection in the corner of a shear panel. Figure 2.4 is a sketch of Detail A (from Figure 2.3) that shows the weld tear. It was thought that the eccentricity of load due to the one-sided fish plate arrangement (refer to Figure 2.2) had precipitated the failure of the weld. However, conclusions made from the Timler and Kulak test stated that this eccentricity would only be a problem at extremely high loads. An alternative detail was suggested in which a double fish plate arrangement is used, thereby creating a symmetrical connection. Another observation arising from the test identified the importance of a stiff, continuous boundary at the corner connections of the steel plate panels in order to provide proper anchoring of the tension field formed in the infill plate. Although the occurrence of a weld tear in the Timler and Kulak specimen led to the completion of testing, the weld failure was a stable and gradual process. This resulted in ductile specimen behaviour, even at loads approaching ultimate.

Tromposch and Kulak [1987] conducted a test similar to that done by Timler and Kulak [1983]. The full-scale, unstiffened steel plate shear wall specimen was first subjected to fully reversed cyclic loading and then to monotonic loading up to the ultimate capacity of the assembly. The two panel, single bay specimen used by Tromposch and Kulak was also tested in the horizontal position. However, an axial preload was applied to the columns to represent better the loads in a typical structure. The bolted beam-to-column joints were designed as bearing-type connections. A welded fish plate arrangement connected the infill panels to the boundary members. However, differing from the Timler and Kulak specimen, in this test the infill plate corner connection details were reinforced by welding a strap plate between orthogonal fish plates at the beam-to-column intersections. Figure 2.5 shows the corner connection detail used by Tromposch and Kulak. A gap was introduced in the corner between the horizontal fish plate and the framing members since construction tolerances may not have allowed for a weld in this region.

Twenty-eight gradually increasing cyclic loads were applied to the Tromposch and Kulak [1987] specimen. The cyclic loads were fully reversed, thereby causing the

opening and closing action that would be expected in the beam-to-column connections during actual seismic loading. Hysteresis curves recorded the behaviour of the specimen during testing. At approximately one-half of the final load the specimen started to show signs of deterioration—both through the pinching of the hysteresis loops and through the yielding of the web plate material. Several tears were noticed at cycle 21 in the fish plates at the top corners of the panels. At the end of 28 cycles, the tears in the fish plates had extended to a length of 25 to 50 mm. A monotonic loading test to ultimate load followed the cyclic loading test. It was observed that monotonic loading slightly lengthened the existing tears in the fish plates and caused a few new weld tears in the top panel corners. Figure 2.6 gives a sketch of the weld tears observed in two corners of the Tromposch and Kulak shear wall specimen.

Tromposch and Kulak [1987] commented on the effect of the one-sided fish plate connection. In contrast to the conclusion reached by Timler and Kulak [1983], it was concluded that the eccentricity of the fish plate with respect to the centre of the boundary members did not noticeably affect the performance of the shear panels. A recommendation was made that the strap plates be connected to the fish plates using fillet welds, and that a minimum thickness of strap plate be used to reduce the probability of inducing tears in the adjacent fish plate material.

2.3.2 Recent Tests Done by Driver *et al.* [1997]

Driver *et al.* [1997] tested a full-scale, four-storey, single bay steel plate shear wall with unstiffened panels. All-welded connections using fish plates were used to join the infill panels to the boundary members. The beam-to-column connections were also welded and were designed to act as fully moment-resisting. The specimen was loaded quasi-statically to determine its behaviour in severe earthquake conditions. Several ancillary tests were conducted prior to testing of the four-storey specimen in order to determine the characteristics of various components of the shear wall. One of these tests, a stand-alone corner detail test, was performed to investigate the adequacy of the selected infill plate connections at the beam-to-column joints. The corner infill plate connection was identified as the critical detail, since it is located in an area of large reversing strains due mainly to the opening and closing action of the beam-to-column joint as described

above.

Tromposch and Kulak [1987] showed that their infill connection detail performed satisfactorily under cyclic loading. This led to the selection of a connection detail for the Driver *et al.* test that included a strap plate welded between two orthogonal fish plates at the panel corners in order to provide continuity. Driver *et al.* took into consideration the recommendation made by Tromposch and Kulak by connecting the strap plate to the fish plates using fillet welds.

In order to test the selected detail, Driver *et al.* subjected a corner detail specimen to reversed cyclic loading. The specimen was, in essence, a corner cut-out of a shear wall panel. First, sections representing a beam and a column were welded at right angles to create a moment-resisting connection. The corner detail specimen—two mutually perpendicular fish plates lapped by a portion of infill plate—was then welded into the beam-to-column joint. A simplified sketch of Driver's corner detail specimen is shown in Figure 2.7.

The corner specimen was tested by applying forces that simulated the opening and closing of a joint in a steel plate shear wall subjected to reversing lateral loads. First, the beam and column were displaced inward simultaneously. At the same time, a tensile load was applied to the infill plate, thereby simulating the tension field formed in an unstiffened steel plate shear wall panel during lateral loading. After the beam, column, and tensile infill plate load had been released, the beam and column were displaced outward simultaneously. A cycle was considered complete once the beam and column had again been brought back to zero load.

The load and displacement criteria used to test the specimen corresponded to movements determined from a finite element analysis of the entire four-storey shear wall at a load level near ultimate. In total, 35 identical loading cycles were applied to the corner specimen.

Observations made during the test identified the presence of tears along welds connecting the strap plate and the fish plates and along welds connecting the infill plate and the fish plates. However, the formation of the tears did not cause a significant change in the overall load response of the test specimen. Since the forces and displacements applied during each cycle were considered to correspond to ultimate conditions, loading

of the corner detail was more severe than would be expected in an actual shear wall. Therefore, it was concluded that this particular corner detail would be adequate and suitable for use in the multi-storey shear wall test [Driver *et al.* 1997].

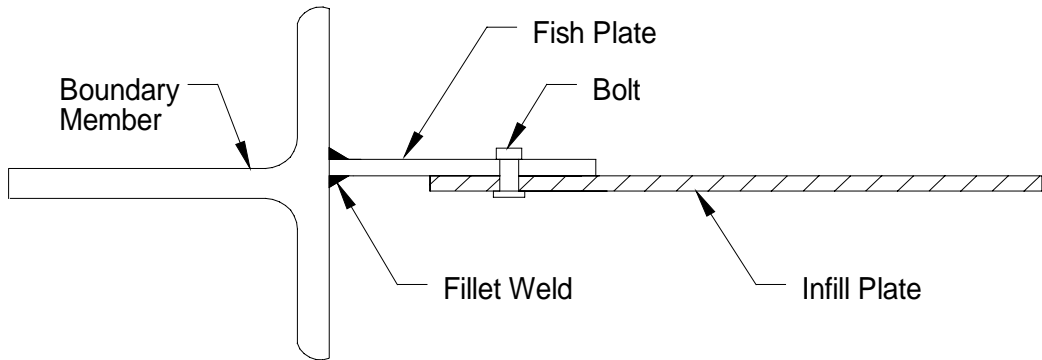
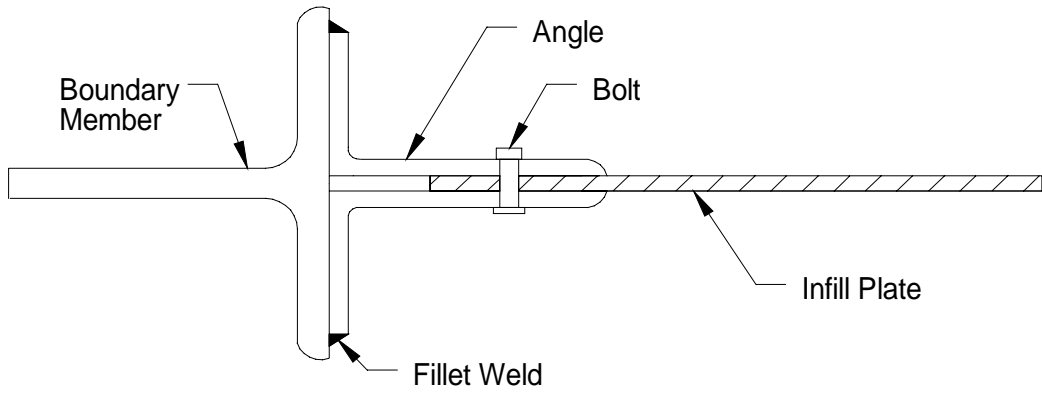


Figure 2.1 Bolted Infill Plate Connection Details

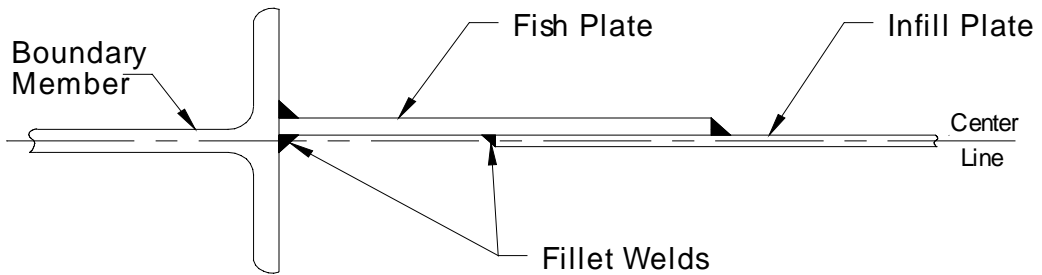


Figure 2.2 Welded Infill Plate Connection Detail

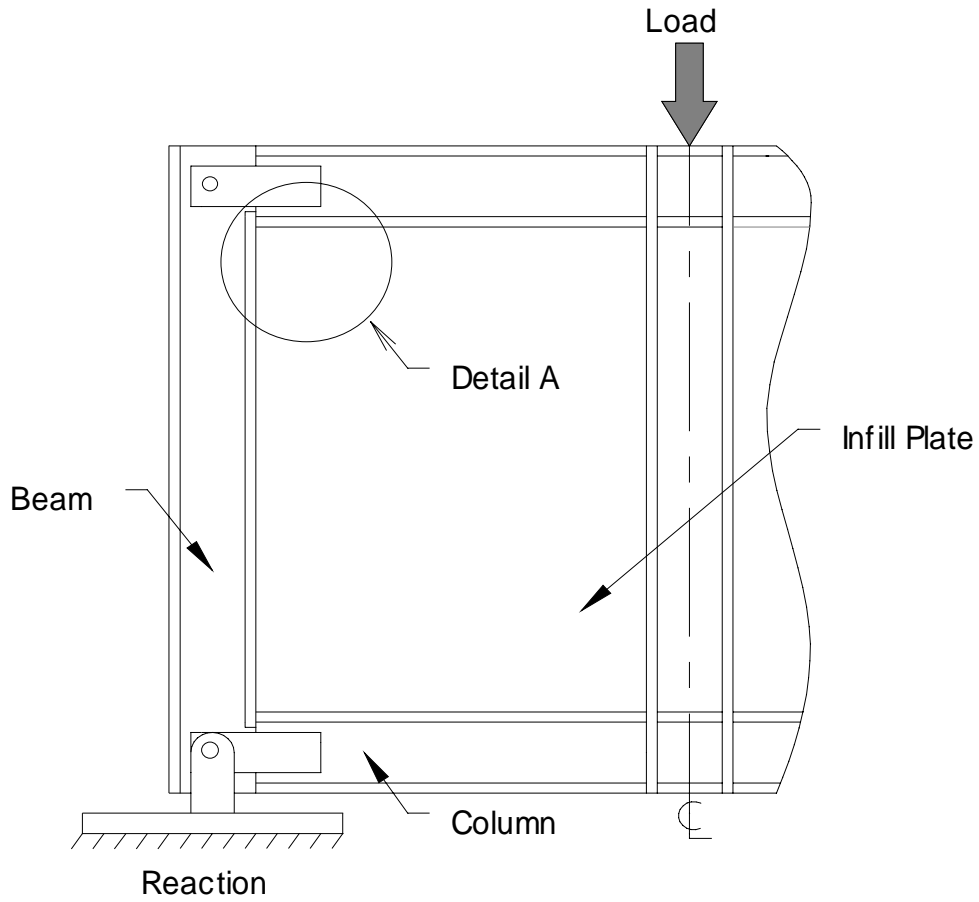


Figure 2.3 Timler and Kulak [1983] Test Specimen

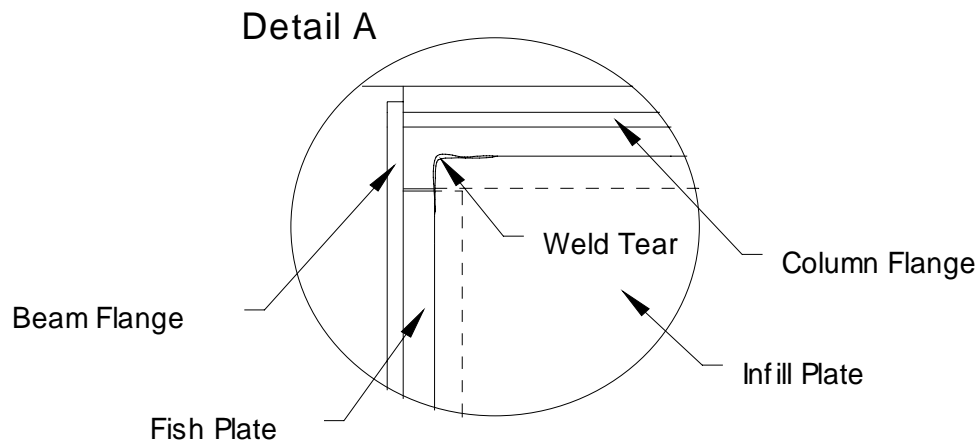


Figure 2.4 Tear Observed in Timler and Kulak [1983] Specimen

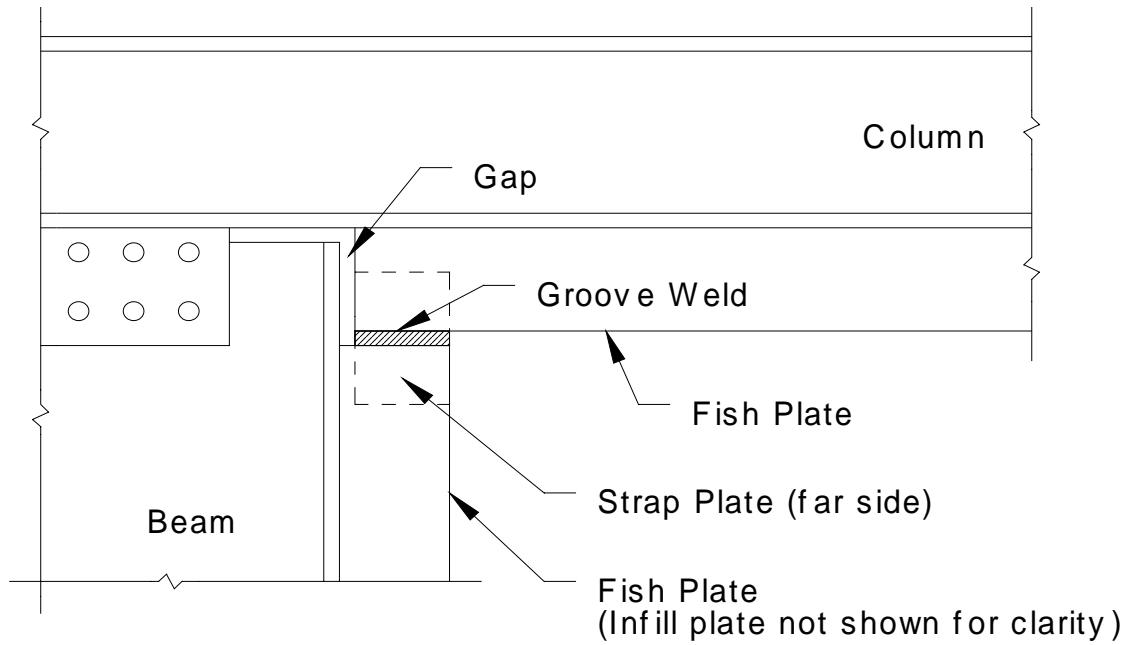


Figure 2.5 Tromposch and Kulak [1987] Corner Detail

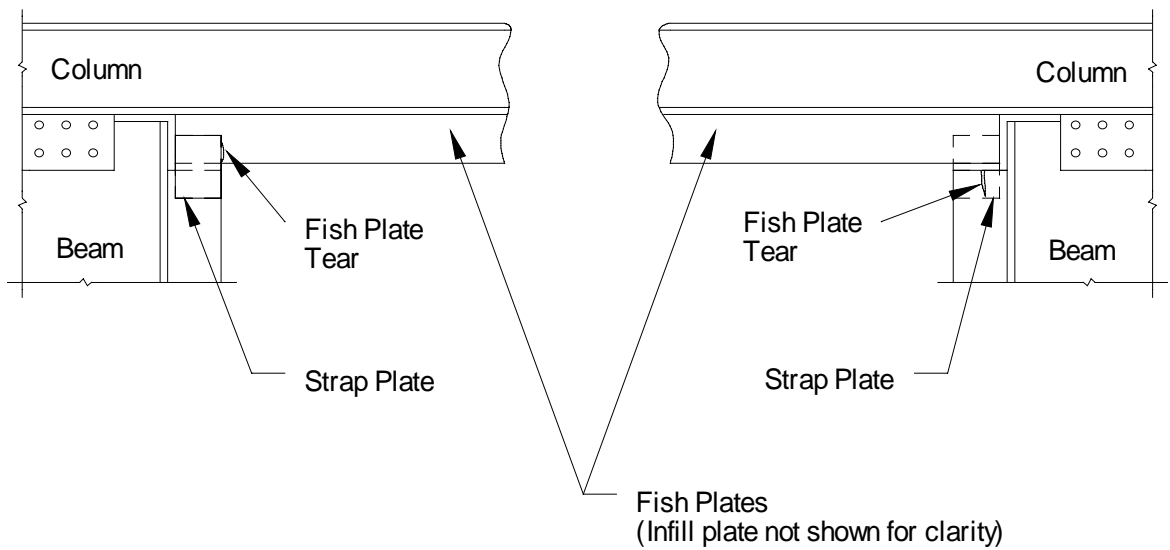


Figure 2.6 Tear Observed in Tromposch and Kulak [1987] Specimen

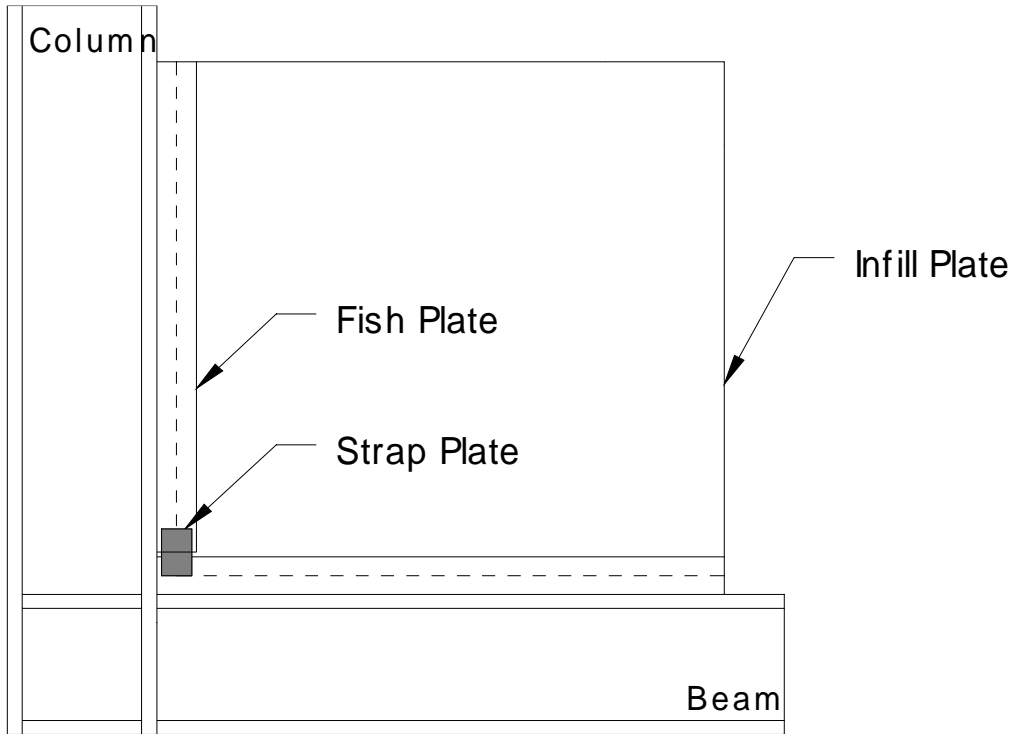


Figure 2.7 Corner Detail Specimen (Driver *et al.*, 1997)

3. Experimental Program

3.1 Objectives of the Test Program

Recent quasi-static testing of a four-storey unstiffened steel plate shear wall [Driver *et al.* 1997] confirmed that the system exhibits excellent performance characteristics. The assembly, which used infill plates that ranged between about 3.5 mm and 4.5 mm in thickness and had moment connections between the beams and columns, demonstrated a high degree of ductility. Deterioration of the shear wall was very slow after the peak load had been reached and large hysteresis loops were developed. The vertical steel infill plates used in this test were connected to the shear wall boundary members—the beams and columns—by means of welded fish plate connections on all four sides of a panel. Figure 3.1 shows one-storey of the four-storey shear wall. (For clarity, the strap plates described in Chapter 2 are not shown in this view.) The fish plate detail facilitates the placement of the infill plate in the frame and allows for reasonable fabrication tolerances.

The goal of the experimental program presented herein was to test various configurations of the infill plate connection under conditions comparable to the large scale test conducted by Driver. This testing enabled comparisons to be made between the behaviour of different corner details.

Figure 3.2 shows a panel with only two fish plates. In this arrangement, the infill plate is welded directly to the beam and the column along two boundaries, and along the other two edges the connection is made using fish plates. In practice, it would be expected that the fish plates are shop welded to the boundary members and the infill plate is aligned in the frame and welded in the field. The two edges of the infill plate in direct contact with the beam and column would be welded first, then the other two edges would be lapped over the fish plates and the welding completed. The use of only two fish plates—as opposed to four fish plates—in a given panel will be attractive to some designers and fabricators. However, this will require increased precision in fabrication of the infill plates because a corner of the infill plate must be fit exactly to the two adjacent boundary members with no fish plates.

Consideration of the steel plate shear wall panel described above led to the selection of the following corner details for the experimental program:

- 1) Infill plate welded to the boundary members (Detail A in Figure 3.2);
- 2) Fish plates welded to each of the boundary members and the infill plate then lapped over the fish plates and welded (Detail B in Figure 3.2);
- 3) Fish plate welded to only one boundary member and then the infill plate welded directly to the other boundary member and lapped and welded onto the fish plate (Detail C in Figure 3.2);
- 4) Two fish plates, with a corner cut-out (chamfer) welded to boundary members and the infill plate then lapped asymmetrically over the fish plates and welded (alternative for Detail B in Figure 3.2).

The corner cut-out in the fourth detail was an attempt to reduce an area of high stresses. The geometric asymmetry in the same detail is intended to be representative of a misalignment that might occur during construction of the steel plate shear wall.

3.2 Loading Concept

Ideally, an experimental program will attempt to duplicate the behaviour of an actual member, or assembly of members, in all aspects—dimensions, loads, and boundary conditions. In reality, testing is often limited by time and cost constraints. Therefore, it becomes necessary to reduce the scope and yet to highlight the particular effects under examination.

An unstiffened steel plate shear wall subjected to cyclic loading (e.g., wind or earthquake) will exhibit two major effects relevant to the infill plate-to-boundary member corner details. The first effect is the repeated opening and closing of the corners as the lateral loads on the structure reverse. The second effect is the development of the tension field that forms diagonally in a panel after the thin plate buckles in the orthogonal direction.

The loading scheme adopted in this experimental program, modelled after that used by Driver *et al.* [1997], applies the two aforementioned effects to an isolated corner

detail. Figure 3.3 shows a simplified diagram depicting the loading scheme. The full-scale corner detail included two boundary members fitted with a portion of infill plate. Opening and closing of the joint was achieved by moving the boundary members outwards and inwards. The tension field was simulated by applying a tensile force diagonally across the infill plate and at 45 degrees to the boundary members.

3.3 Testing of Material Properties

Prior to preparation of the test specimens, tension coupons were taken from the infill plate and fish plate material. Tension tests were conducted in order to confirm the hot-rolled properties of the steel and to establish other basic material properties. It is highly likely that hot-rolled steel would be used in the construction of steel plate shear walls. Therefore, it was important that the relatively thin plates used in this test program also have hot-rolled characteristics, since thin plates often exhibit the characteristics of cold-rolled steel.

Coupons were taken from three individual source pieces of steel plate, designated as Infill Plates 1 and 2, and Fish Plate. Two sets of three coupons (six in total) were cut from each plate. The first set was cut in a direction designated as 1–1, the second set was cut perpendicular to the 1–1 coupons in a direction designated as 1–2. In total, 18 coupons were dimensioned and tested in accordance with the requirements of the American Society for Testing and Materials [ASTM 1992].

3.4 Infill Plate Connection Specimens

The infill plate connection specimens, numbered in the order of testing, were prepared from steel plate that met the requirements of CAN/CSA G40.21-92 grade 300W steel. A total of three different steel source plates were used. Two plates had a nominal thickness of 4.8 mm, and were designated as Infill Plate 1 and Infill Plate 2. The third plate had a nominal thickness of 6.0 mm and was designated as Fish Plate. Table 3.1 lists the steel plates used in individual specimen preparation.

The four infill plate specimens tested are shown in Figures 3.4 to 3.7. Specimen 1, the simplest of the four specimens, was constructed using material from Infill Plate 1 to

form a 1250 mm square specimen[†]. The infill plate was welded directly to the beam and column. Specimens 2, 3 and 4 were also all 1250 mm square specimens, and they involved the use of a 100 mm wide fish plates. Figures 3.4 to 3.7 also show the directions 1–1 and 1–2 in which the tension coupons were cut with respect to the orientation of the specimens relative to the beam and column. These directions are referenced later in Chapter 4.

The present investigation used thin, unstiffened infill plates. This is consistent with the most recent steel plate shear wall research [Driver *et al.* 1997]. Driver showed that quasi-static loading of an unstiffened, steel plate shear wall in a moment-resisting frame exhibits excellent ductility and stability even at very large deformations, thereby supporting the use of thin plates. An important consideration is that thin plates will be more economical than thick or heavily stiffened plates because of lower material and fabrication costs.

A feature in this experimental program was to apply loads sufficiently high such that portions of the infill plate would yield in tension. This behaviour was demonstrated in the Driver *et al.* test. To attain this yielding criterion in the present test, a large area of infill plate was required between the corner detail and the point of application of the tensile force. Thus, the diagonal dimensions of the infill plate were made as large as practicable relative to the test apparatus available, thus, determining the overall dimensions of the infill plate.

In order to accommodate the load needed to develop the tension field, a tension connection was made at one corner of the infill plate specimen. The tension connection, located diagonally from the corner detail in the infill plate, required ten 21 mm drilled bolt holes to accommodate 19 mm diameter A325 bolts. (The bolt holes are shown in Figures 3.4 to 3.7.) The number and configuration of the holes was determined by considering the predicted tensile force needed to yield the infill plate.

All welding of the fish plates to the infill plates and the specimens to the boundary members was done using shielded metal arc welding with E48018, 3.2 mm

[†] This terminology refers to the size of the infill plate, as shown in the figures. The infill plate was not literally square, because a corner of the infill plate was cut off.

diameter electrodes. Weld details for the specimens are shown in Figures 3.4 to 3.7. The welder was instructed to form fillet welds of the specified minimum size, as determined by the thickness of the base metal. For example, infill plate-to-boundary member welds and fish plate-to-boundary member welds were specified as 5 mm and 6 mm in size, respectively, as determined by the thickness of the specimen at the boundary. Measured weld sizes are shown in Table 3.1.

For erection of a steel plate shear wall, the likely sequence is that the fish plates are shop welded to the boundary members and the infill plate is aligned in the frame and welded in the field. For testing of infill specimens, this procedure was altered. The fish plates were welded to the infill plate before being placed into the load frame. This was done to facilitate the welding and handling process in the laboratory. The change in procedure should have no effect on the test results.

3.5 Test Set-Up

For convenience of loading, the boundary members and their associated infill plate were oriented 45 degrees relative to their position in an actual structure, as shown in Figure 3.8. Two 890 kN capacity, double acting hydraulic jacks were used to open and close the beam-to-column joint. The jacks were pin-connected to a tongue attachment welded near the free ends of the beam and column, and were oriented at right angles to the beam and column. The far ends of the jacks were pin-connected to clevis attachments that were bolted to W310x129 reaction columns.

The infill plate was subjected to a vertical tensile load that was transmitted through a tension connection by the MTS 6000—a universal testing machine with 4000 kN capacity in tension. The tension connection consisted of two 10 mm thick tension plates placed on either side of the infill plate and fastened to the infill plate using ten bolts. The upper portion of the tension plates was bolted to a W250x67 tension member that threaded directly into the loading head of the MTS machine.

3.5.1 Test Frame

A drawing of the test frame is shown in Figure 3.8. A WWF400x202 distributing beam was used as a base for the test frame. Two members formed a V-shaped frame: a

2330 mm long W310x129 column connected at 45 degrees to the horizontal distributing beam and a 2050 mm long W530x101 beam connected at 90 degrees to the column. The beam-to-column connection was made rigid by connecting the beam flange and web to the column with fillet welds. Reaction beams were prestressed over the ends of the distributing beam to resist the upward forces applied by the jacks and the MTS machine. Struts were placed between both ends of the distributing beam and the reaction columns in order to prevent in-plane movement resulting from unequal horizontal forces in the jacks.

The test frame was placed in the universal testing machine so that the centre of the V-joint between the beam and column lined up with the centre of the MTS loading head. An increase in out-of-plane movement of the V-frame members during testing of Specimen 2 required the addition of bracing members at the free ends of the beam and column. The bracing reduced the amount of out-of-plane movement, but it did not impede the opening and closing of the V-frame.

3.5.2 Placement of the Specimen

In order to facilitate replacement of the test specimens in the test frame, the infill plate specimens were welded to “foundation plates,” shown in Figure 3.8, which were in turn bolted to the beam and column. New foundation plates were used for each test specimen. Each foundation plate extended a length of 1350 mm from the bottom of the V-joint, along the top flange of a frame member. It was connected to the flange by thirteen pairs of 25 mm diameter A325 bolts. Design calculations showed that 30 mm thick plates were required to prevent prying action in the bolts that connected the foundation plates and the V-frame flanges.

During the placement of a test specimen, the foundation plates were first fastened to the beam and to the column. A specimen was then moved into the test set-up such that the corner detail fit into the V-joint and two edges of the specimen rested against the foundation plates. Centrelines of the foundation plates, which corresponded with the centrelines of the beam and column, acted as references to align the specimen once in the V-frame.

Fillet welds were used to connect both faces of a specimen to the foundation plates using specified minimum weld sizes, as described above. Small stiffeners, shown in Figure 3.8, were welded to the two free edges of each specimen to prevent premature tearing and subsequent loss of strength in an area where high stresses were predicted. Moving specimens out of the test frame simply involved removing the bolts between the foundation plates and frame members and removing the specimen together with the attached foundation plates. Then, for the next test, two new foundation plates were bolted to the boundary members. Using the procedure described greatly reduced the time required between tests.

Once welding of a specimen into the test frame was complete, the two tension plates were bolted to the free corner of the specimen and to the tension member attached to the MTS loading head. About ten percent of the maximum tensile load anticipated was then applied to seat the entire tension connection (the maximum tensile load anticipated was 800 kN), in this way, slip of the tension connection during loading was unlikely. While the load was being held, the bolts in the tension connection were installed to the “snug tight” condition.

Figures 3.9 and 3.10 present photographs showing the test set-up. Whitewash was applied to the specimen and part of the tension connection so that visual identification of yielding regions could be made during the test.

3.5.3 Test Control and Data Acquisition

Tensile loading applied to specimens by the MTS machine was controlled through a microprofiler. The MTS was programmed to load through displacement control since the exact load required to start yielding in the specimen was unknown. At loads close to yield, displacement control will continue to load at the prescribed rate according to the displacement of the MTS cross-head. (On the other hand, load control will respond to the material being loaded, that is, load control will attempt to maintain the load regardless of whether or not the material is yielding.)

Displacement control was also used to regulate the jack loads applied to the V-frame arms. Linear variable displacement transformers (LVDTs) were placed at the free edges of the infill plate to measure and record displacements, thereby making it possible

to adjust jack pressures and to achieve the desired displacements during testing. Jack loads were measured using load cells. LVDTs were also placed at various other locations to monitor the out-of-plane movement of the frame. Figure 3.8 shows locations of the LVDTs on the test set-up.

For each specimen, strains were monitored through ten electrical resistance strain rosettes, and their signals were recorded using an electronic data acquisition unit. Strain rosettes (five on each face of a test specimen) were located in proximity to the boundary between the specimen and the V-frame members, as is shown in Figure 3.11.

Dial gauges were placed at three locations on the distributing beam in order to verify that the test set-up was not moving in-plane. This was a possibility when the jack loads became significantly unequal during loading.

Out-of-plane displacements of the infill specimens were monitored during testing by using a theodolite and a set of seven Demec points mounted on the test specimen. The theodolite was placed approximately three meters from the test set-up and aligned parallel to the specimen prior to loading. Theodolite measurements were taken by simply using a ruler that was held against the Demec points and oriented at right angles to the specimen.

3.6 Test Procedure

A loading strategy for testing was derived by following the method outlined in the Applied Technology Council Handbook (1992), ATC-24 [Applied Technology Council 1992] for experiments using quasi-static cyclic loading. Progressive cyclic loading was adopted, starting with loading in the elastic load range of the specimen and then incrementally increasing into the inelastic load range of the specimen. In the elastic region of behaviour, loading was applied in blocks of three cycles. After the specimen became inelastic, loading was applied in blocks of six cycles. Table 3.2 summarizes the load history followed for each test specimen. The displacements given in Table 3.2 were recorded for both members of the V-frame. The line of action of the displacements was oriented at 45 degrees to the horizontal, that is, in a direction perpendicular to either member. At loading block 4 onwards, each cycle took an average of 40 minutes; typically, forty-two cycles were applied per test. A test was considered complete once

significant damage had occurred in the corner detail or, as in the case of Test 1, when it was judged that a sufficient number of load cycles had been applied.

Cyclic loads of both tension and compression were applied by manually controlled hydraulic jacks. The terms “tension” and “compression” are used only to describe the sense of the load delivered by the jacks. A tensile jack load corresponded to a decrease in the length of the jack, thereby causing the V-frame members to move outwards. A compressive jack load corresponded to an increase in the length of the jack, thus, causing the V-frame members to move inwards. To differentiate between two stages of a single cycle, the joint closure portion of a cycle is referred to as *Part A* and the joint opening portion of a cycle is referred to as *Part B*. Together, Part A and Part B simulate the corner detail of a steel plate shear wall subjected to a lateral load.

A cycle was begun with Part A, that is, the jacks were loaded in compression and the angle between the boundary members decreased. During this phase, the MTS applied an increasing tensile load to the infill plate portion of the specimen. For each loading block, the MTS tensile load was increased, while, simultaneously, the V-frame displacements imposed by the jacks were also increased (refer to Table 3.2). The tensile force in Part A represents the tension field created by the closing of the framing members in an actual shear wall. Once the peak tensile load and compressive displacement had been reached, the specimen was unloaded following the same load and displacement increments that had been followed during loading.

In Part B the jack loads were reversed, that is, the load frame members were pulled open to a prescribed displacement. Opening of a steel plate shear wall corner detail in an actual structure is accompanied by a compressive force corresponding to the compressive force required to buckle the steel plate. For thin plate shear walls this compressive force is very small, and therefore no such force was applied during Part B. The completion of one cycle was reached once unloading in Part B had occurred.

A displacement limit in opening (about 2.5 mm) was reached part-way through the test when the jack attached to the beam—the stiffer of the two V-frame members—attained its capacity. Thereafter, it was necessary to apply subsequent cycles with increased displacement in Part A while displacement in Part B remained at 2.5 mm. Similarly, a tensile load limit was reached because of the strength of the tension plates.

As is seen in Table 3.2, a maximum tensile load of 800 kN applied by the MTS machine—the load predicted necessary to yield the specimen in tension—was reached during loading block 4.

In addition to the cyclic loading applied to specimens, the test procedure included inspection of specimens for tears and yield patterns at different stages during testing. The detection and measurement of tears was carried out with a magnifying glass and a ruler. Demec point readings, described above, were taken throughout the tests in an attempt to record the pattern of specimen movement due to cyclic loading. Data describing the general shape of the specimen facilitated the development of a finite element model.

As testing progressed, plastic deformations were noticed in the V-frame joint during the compressive jack load portion of the cycling. The main consequence of this was seen in the last test (Specimen 4), when tensile jack loads were required to open the V-frame members to allow for specimen placement. This gave a non-zero initial jack load, and resulted in a decreased jack capacity in tension. As a consequence, a maximum of only 1.5 mm in opening was reached for Part B of Test 4.

Table 3.1 Plate Material and Weld Data

Specimen	Plate Material ¹	Weld Location ²	Specified Weld Size (mm)	Average ³ Measured Weld Size ⁴ (mm)
1	Infill Plate 1	North-East	5	5.03
		North-West	5	5.02
		South-East	5	5.49
		South-West	5	4.92
2	Infill Plate 2 Fish Plate	NE	6	5.63
		NW	6	5.68
		SE	6	5.58
		SW	6	5.57
3	Infill Plate 2 Fish Plate	NE	6	5.25
		NW	5	5.20
		SE	6	5.56
		SW	5	5.38
4	Infill Plate 1 Fish Plate	NE	6	5.35
		NW	6	5.11
		SE	6	5.13
		SW	6	5.18

¹Plate material used in specimen preparation.

²Weld location with respect to specimen orientation in the MTS (refer to Figure 3.8).

³Average of four measurements along 1250 mm long weld was taken.

⁴Smaller of two weld legs is reported.

Table 3.2 Load History Followed for Infill Plate Connection Specimen Tests

Block 1 x (3)		Block 2 x (3)		Block 3 x (6)		Block 4 x (6)		Block 5 x (6)		Block 6 x (6)		Block 7 x (6)		Block 8 x (6)	
Jack Displ. (mm)	Tension (kN)														
0.5	67	0.6	67	0.6	67	0.6	67	0.6	53	0.6	44	0.7	38	0.7	33
1.0	67	1.2	78	1.2	81	1.2	78	1.3	68	1.3	57	1.3	51	1.4	47
1.5	100	1.8	117	1.8	122	1.8	117	1.9	101	1.9	85	2.0	76	2.1	71
		2.3	156	2.4	163	2.3	156	2.5	135	2.6	114	2.7	102	2.8	94
		2.9	194	3.1	204	2.9	194	3.2	169	3.2	142	3.3	127	3.5	118
		3.5	233	3.7	244	3.5	233	3.8	203	3.8	170	4.0	152	4.3	142
				4.3	285	4.1	272	4.4	236	4.5	199	4.7	178	5.0	165
				4.9	326	4.7	311	5.1	270	5.1	227	5.3	203	5.7	189
				5.5	367	5.3	350	5.7	304	5.8	256	6.0	229	6.4	213
						5.8	389	6.3	338	6.4	284	6.7	254	7.1	236
						6.4	428	7.0	372	7.0	312	7.3	279	7.8	260
						7.0	467	7.6	405	7.7	341	8.0	305	8.5	283
								8.2	439	8.3	369	8.7	330	9.2	307
								8.9	473	8.9	398	9.3	356	9.9	331
								9.5	507	9.6	426	10.0	381	10.6	354
										10.2	454	10.7	406	11.3	378
										10.9	483	11.3	432	12.0	401
										11.5	511	12.0	457	12.8	425
												12.7	483	13.5	449
												13.3	508	14.2	472
												14.0	533	14.9	496
														15.6	519
														16.3	543
														17.0	567

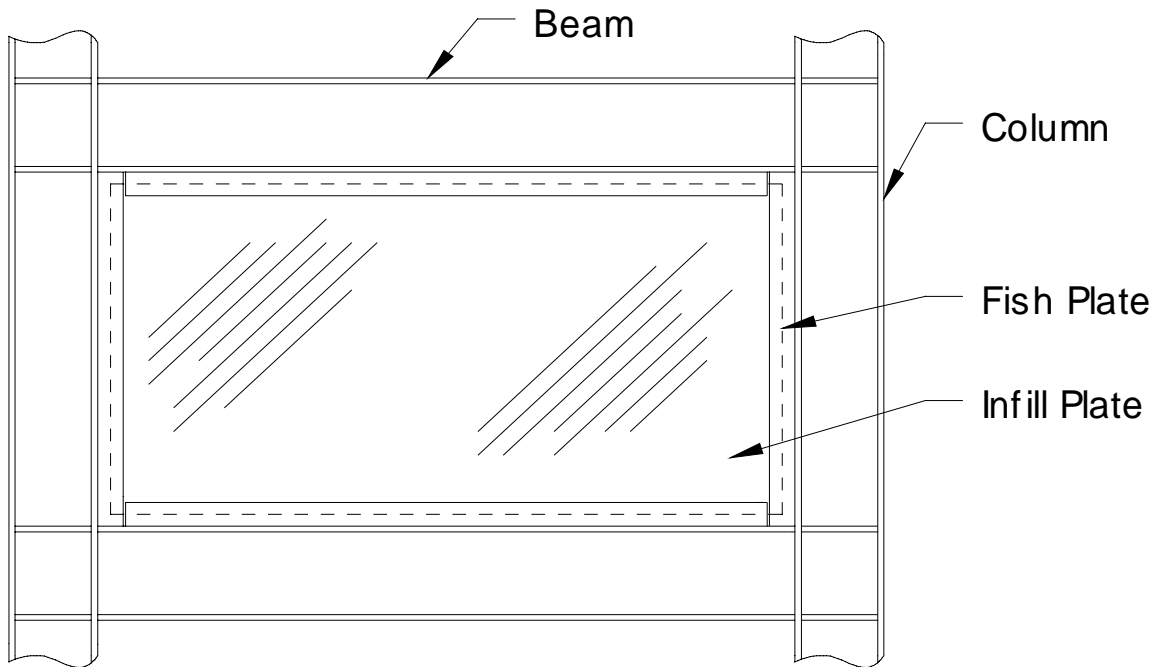


Figure 3.1 One Storey of Driver et al. [1997] Four-Storey Steel Plate Shear Wall

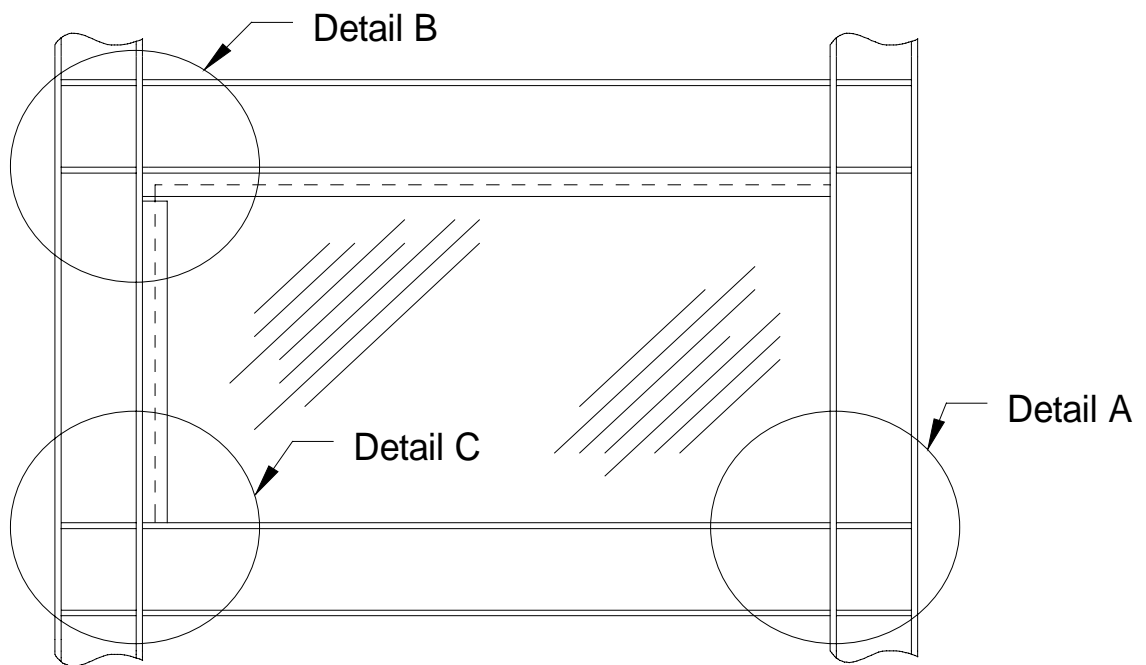


Figure 3.2 Steel Plate Shear Wall Panel Using Two Fish Plates

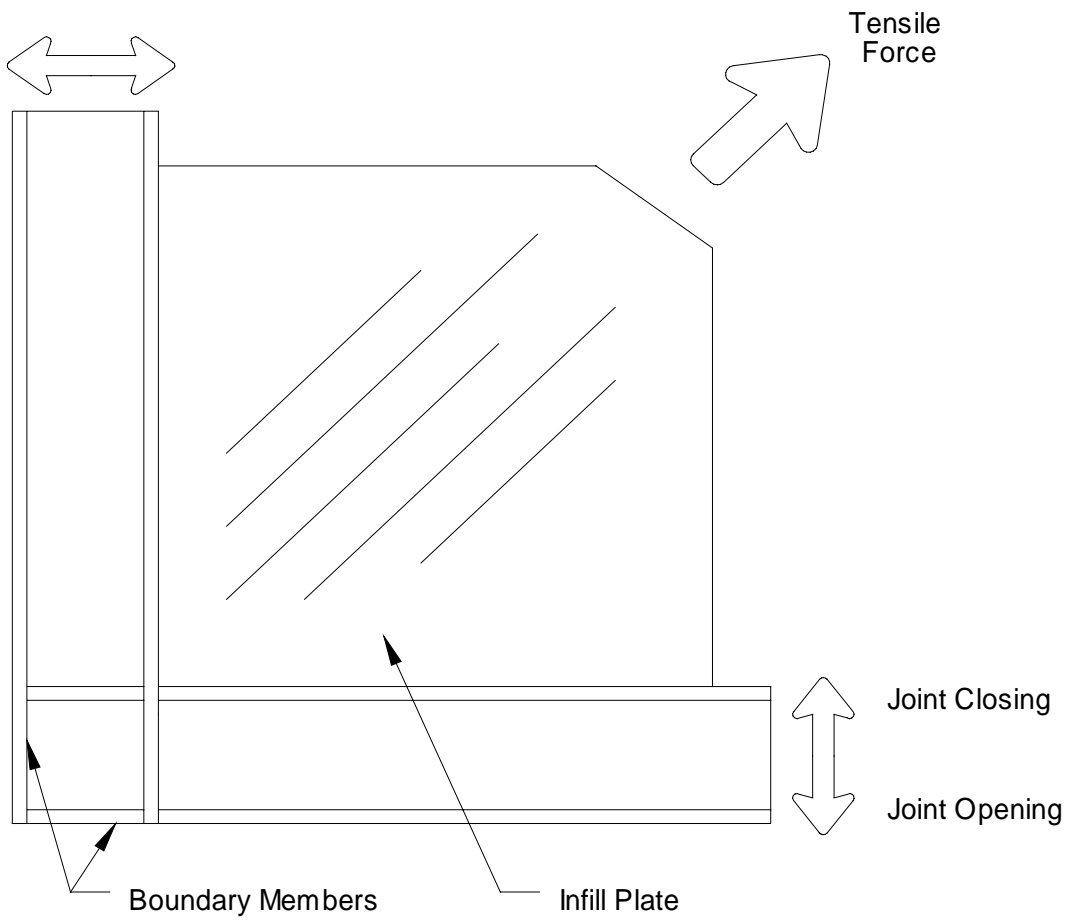


Figure 3.3 Loading Concept for Infill Plate Connection Tests

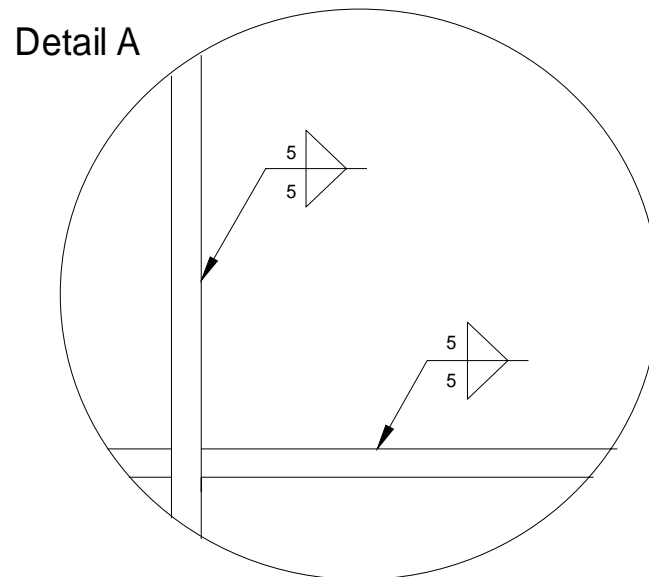
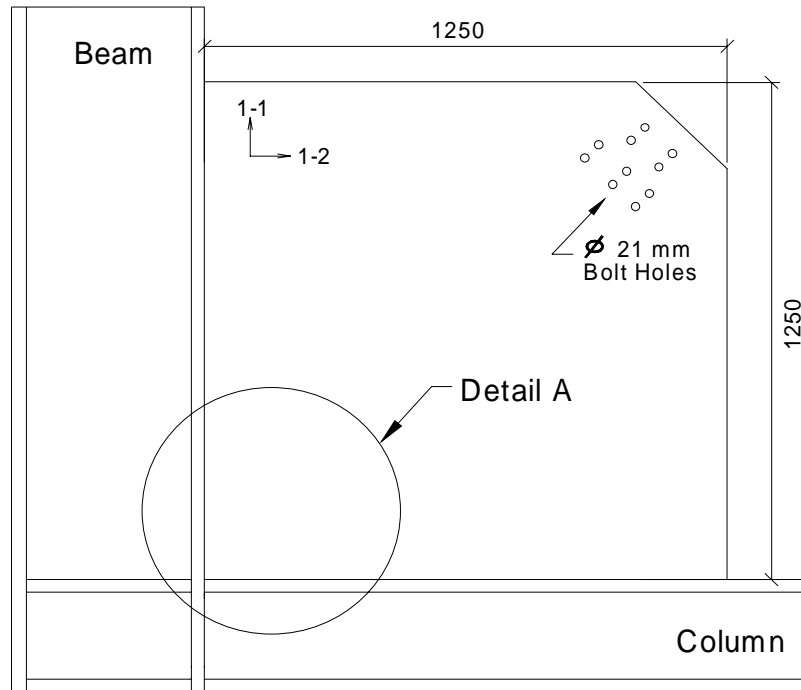


Figure 3.4 Infill Plate Connections Specimen 1

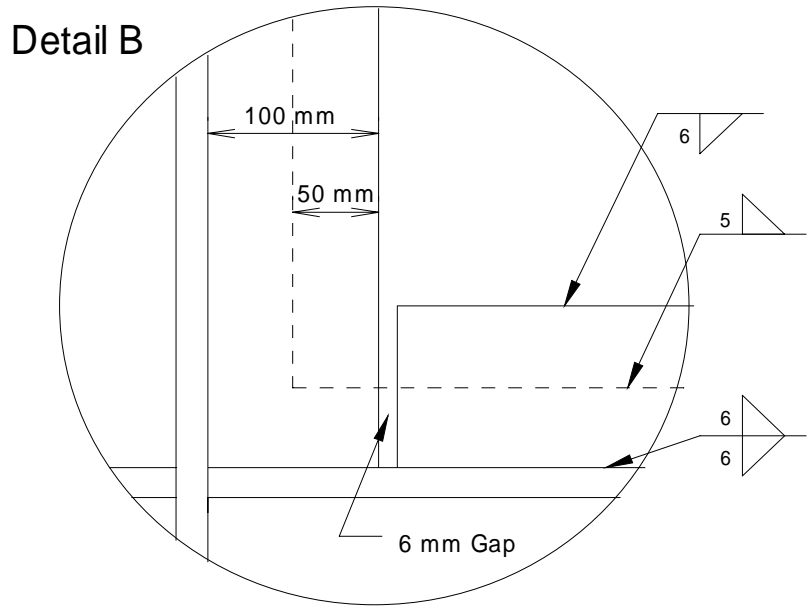
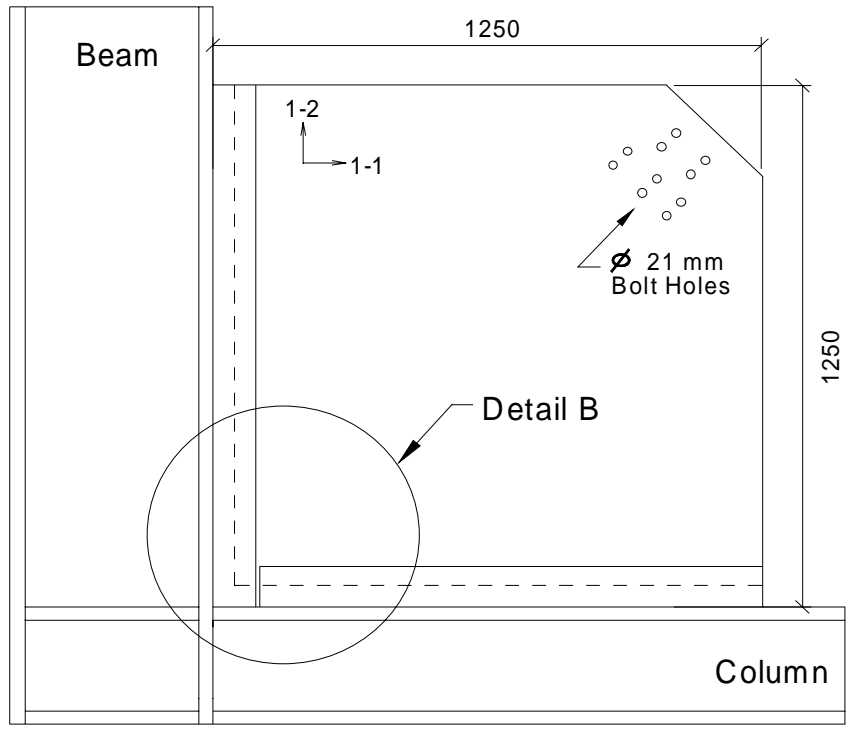


Figure 3.5 Infill Plate Connection Specimen 2

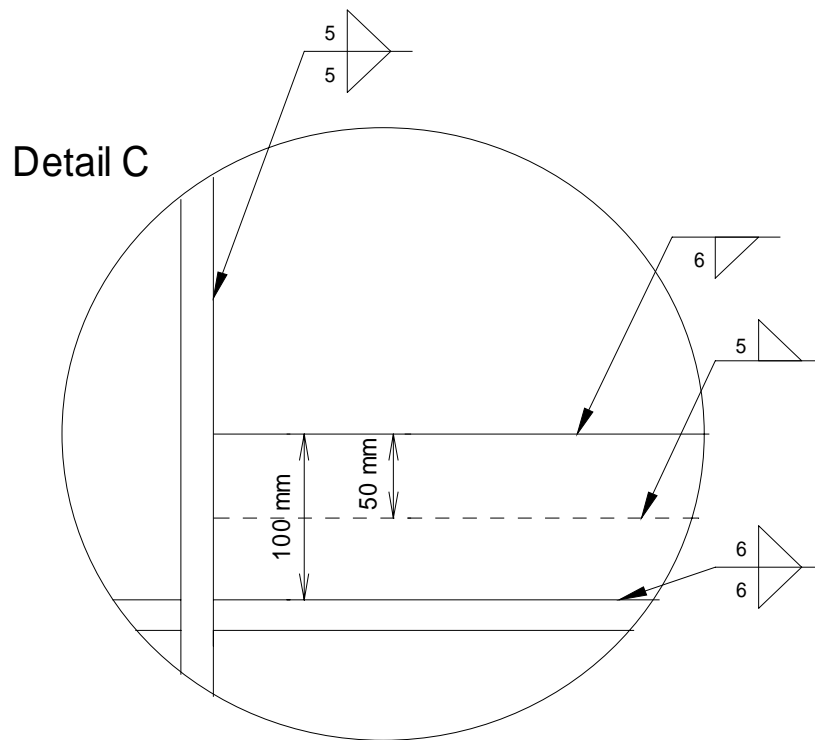
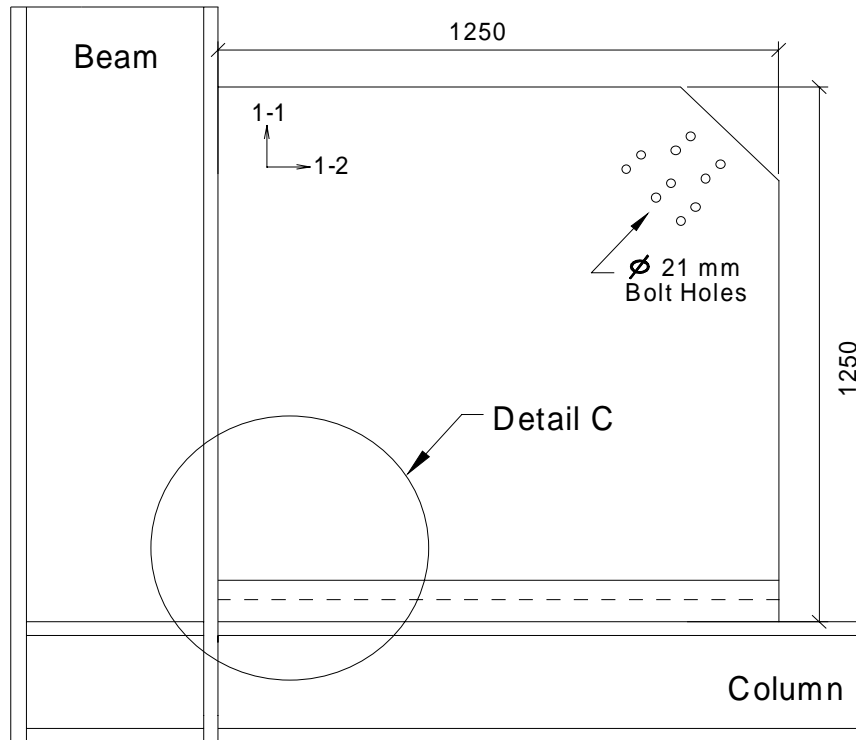


Figure 3.6 Infill Plate Connection Specimen 3

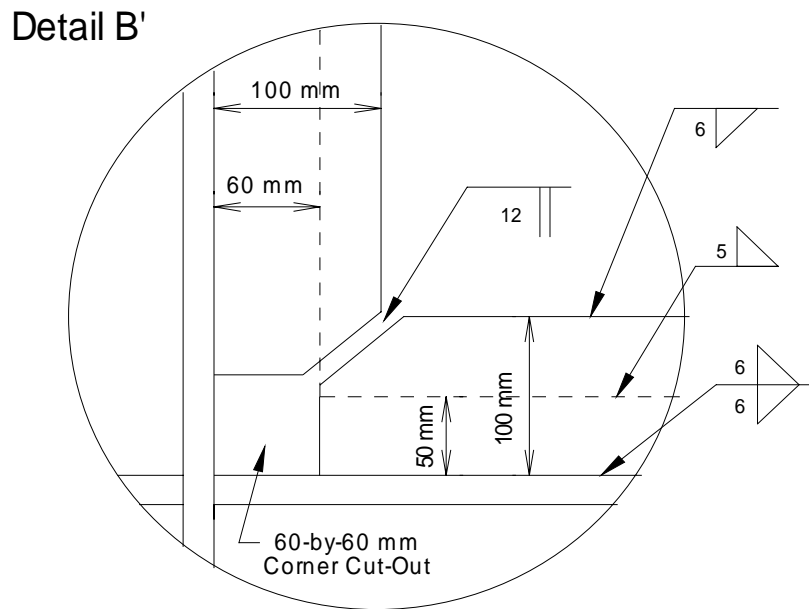
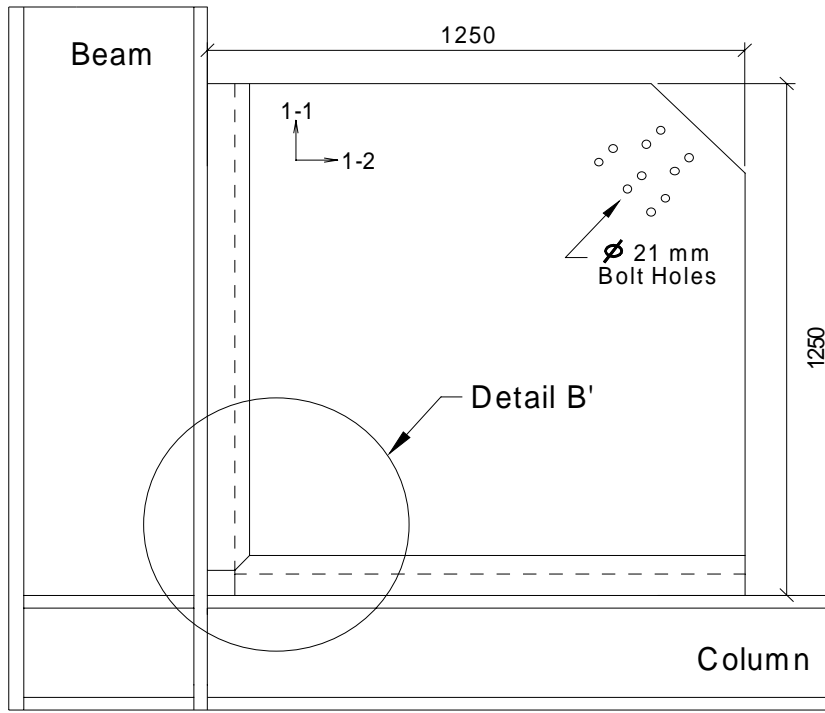


Figure 3.7 Infill Plate Connection Specimen 4

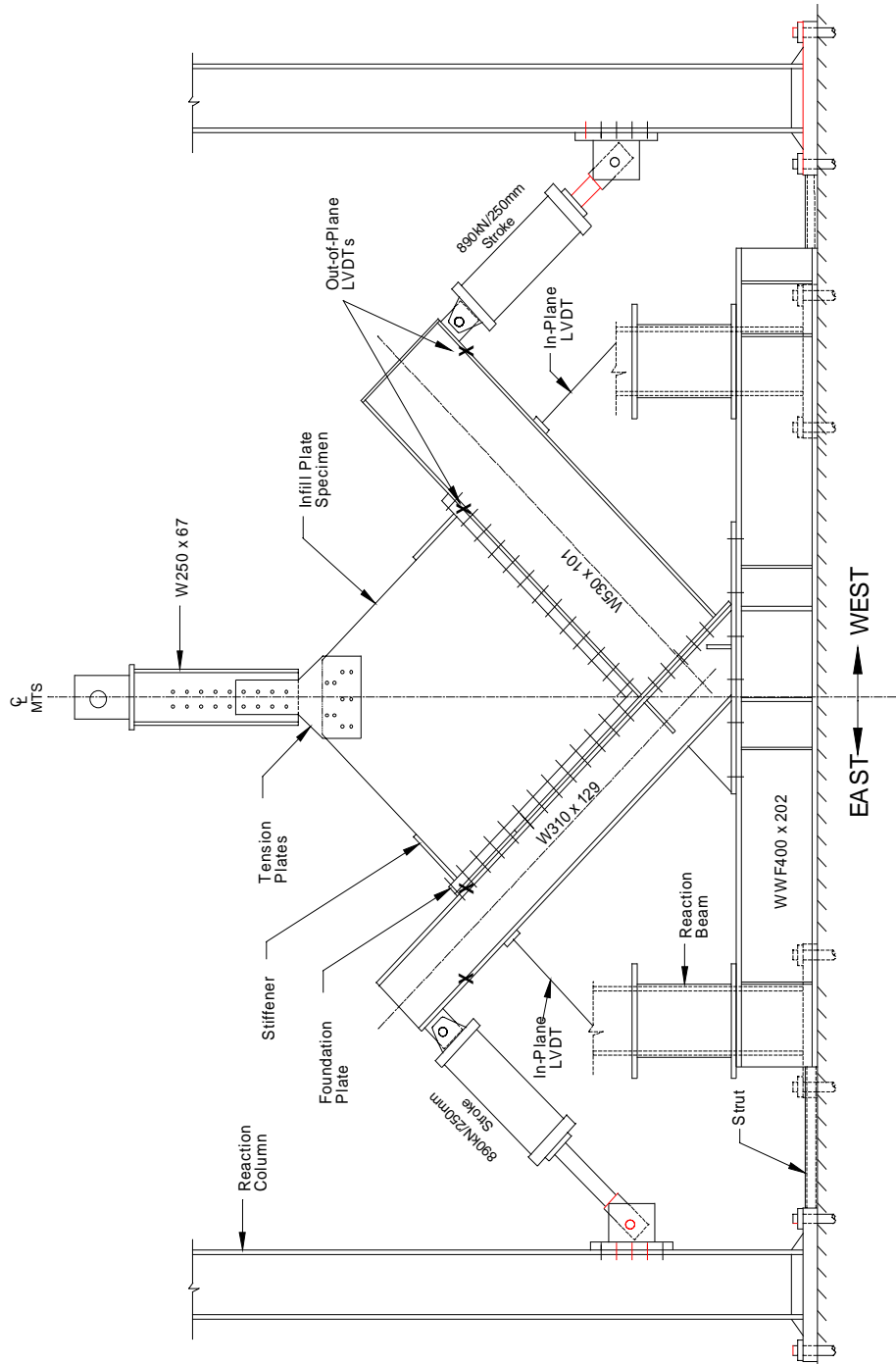


Figure 3.8 Test Set-Up

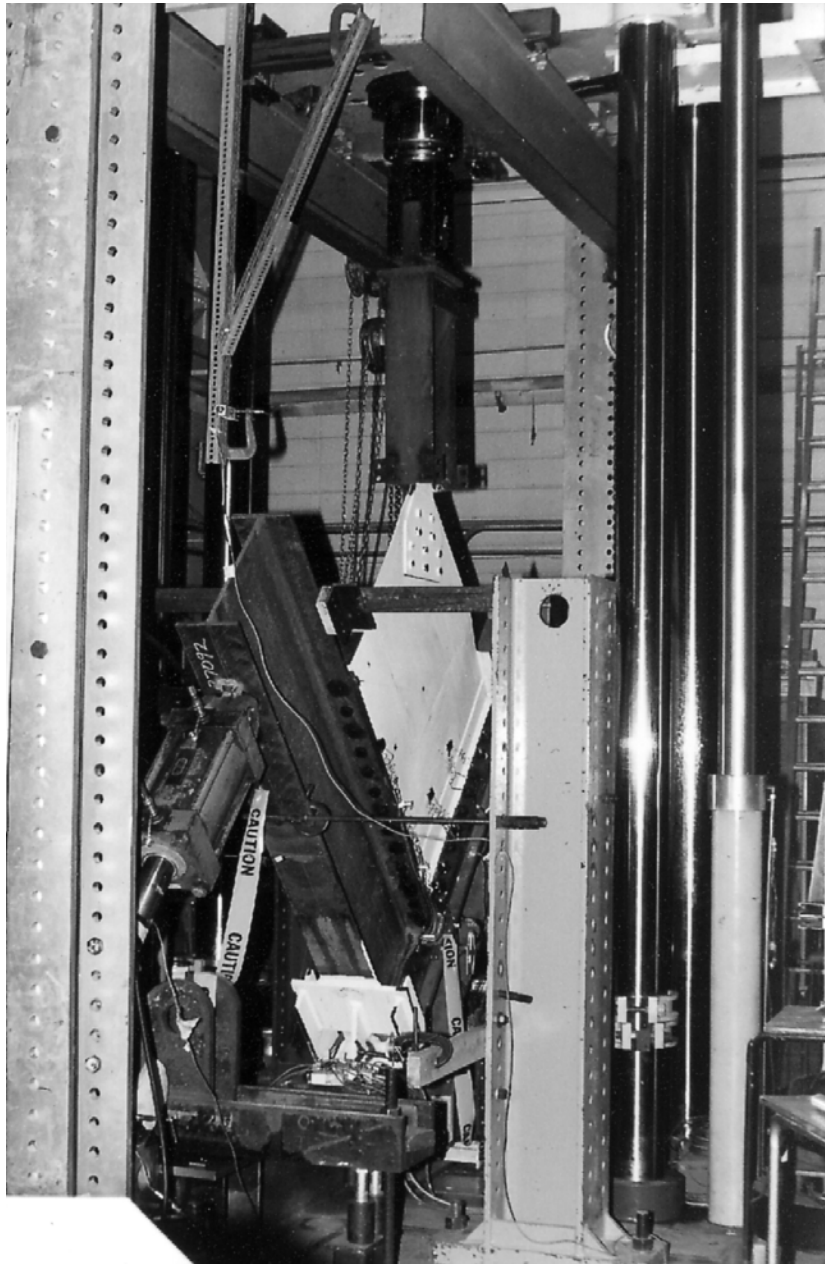
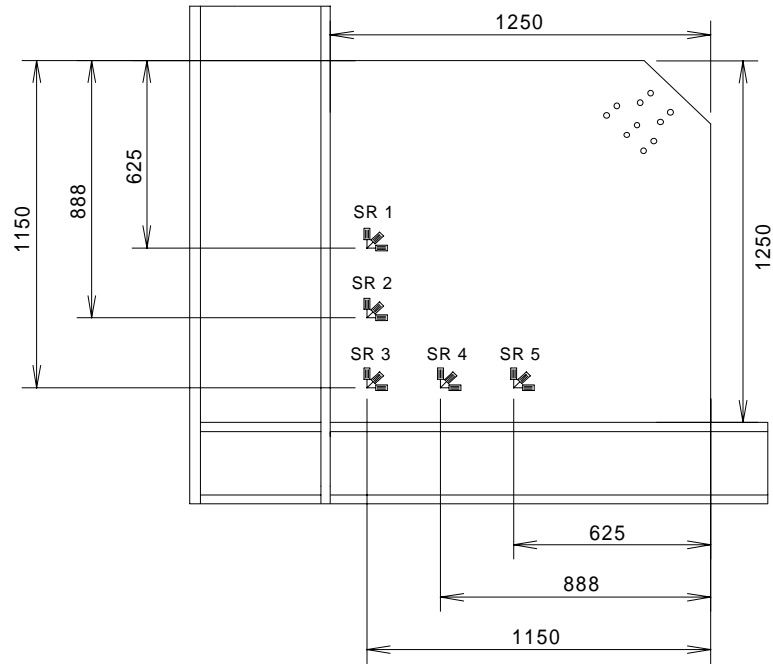


Figure 3.9 South Side of Test Set-Up — Looking Eastward



Figure 3.10 South Side of Test Set-Up — Looking Westward

Location of Strain Rosettes (SR) on Specimen 1



Location of Strain Rosettes (SR) on Specimens* 2, 3, and 4

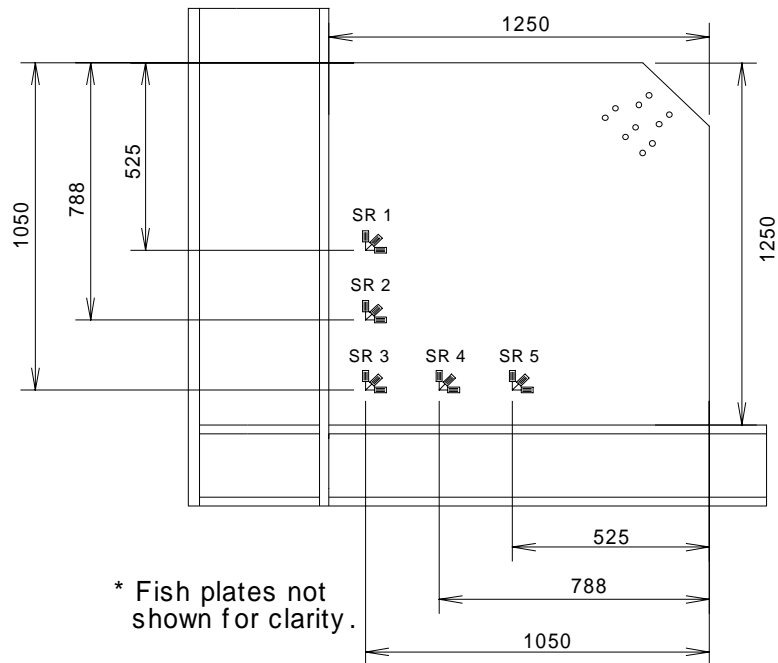


Figure 3.11 Strain Rosette Locations

4. Experimental Results

4.1 General

Quasi-static tests were performed on a total of four infill plate connection specimens. In this chapter, the numerical data that were collected and the observations that were made during the tests are described.

Chapter 3 described the test set-up and loading procedure that were used to test the infill plate connection specimens. Four test specimens, each 1250 mm by 1250 mm, were fabricated and tested under cyclic loading. Observations made during the testing of Specimen 1 helped to establish limits and general guidelines that were subsequently followed during the next three tests. For example, because of a limit on the jack capacity, a displacement restriction of about 2.5 mm was reached in the opening mode of a cycle (Part B). Similarly, a tensile load limit of 800 kN was reached that reflected the strength of the tension plates needed to transfer the load from the MTS machine to the infill plate.

During Test 1, a gradual softening was noticed in the response of the test set-up as loads were increased. It was observed that the difference in the load required to increase the inward displacement of the V-frame members became smaller with successive loading blocks. This was the result of a large crack that was detected in a fillet weld connecting the beam flange to the column during the last (sixth) cycle of loading block 8. Repairs were made to the V-frame connection, and a maximum inward displacement of approximately 17 mm during the first part of a loading cycle (Part A) was established for subsequent tests (refer to Table 3.2).

Experience gained in Test 1 developed the loading limitations outlined above. However, it was possible to test the four specimens as had generally been intended at the outset of the program. Infill plate connection specimens were subjected to the two major load effects present in an actual steel plate shear wall—repeated opening and closing of the corner detail, and tensile loading simulating the formation of a tension field in the infill plate.

4.2 Material Properties

Table 4.1 presents the material properties obtained from tension coupons taken

from three individual source pieces of steel plate. Elastic modulus, static yield stress and static ultimate stress values are given in the table. The modulus of elasticity for Infill Plate 1, Infill Plate 2, and the Fish Plate material is 189 500 MPa, 198 200 MPa, and 221 200 MPa, respectively. The values reported in Table 4.1 are the mean value of three coupons cut in each of two orthogonal directions from each plate. The coupon tests of the material confirmed that the plates were made of hot-rolled steel and could therefore be used for the preparation of the test specimens. Appendix A shows values obtained from individual coupon tests.

4.3 Test Data and Observations

The information collected during the infill plate connection tests is described in this section. In addition to giving a measure of the individual performance of the infill specimens, the data and observations presented below provide the necessary information with which to compare the various corner details tested. Comparisons between specimens are discussed in Chapter 6.

4.3.1 Out-of-Plane Measurements

Linear variable displacement transformers (LVDTs) were used to monitor the out-of-plane deflection of the beam and the column during cyclic loading. Their location is shown in Figure 3.8. Although some deflection was expected, measurements from the LVDTs show that out-of-plane movement of the beam and column was largely prevented by bracing placed at the ends of the V-frame members.

Displacements of the infill plate in the out-of-plane direction were monitored using a theodolite and a set of Demec points mounted on one side of the test specimen. The data collected from the Demec point readings for Specimen 2 are used in the finite element analysis presented in Chapter 5. Demec point data taken for all of the specimens are summarized in Appendix B.

4.3.2 Deterioration of the Infill Plate Connection Specimens

4.3.2.1 Specimen Buckling

As was described earlier (Section 3.6), the first part of a loading cycle (Part A)

involved the displacement of the boundary members so as to decrease the 90 degree angle between the beam and the column. Simultaneously, a tensile force was applied to the infill plate by the MTS machine. In all of the tests, buckles in the infill plate could be detected by the time of the second loading block. In the later loading blocks, the buckle amplitudes increased as the displacements of the boundary members were increased. This can be seen in Figure 4.1, which shows the buckled shape of Specimen 1. Loud sounds were emitted from the specimens as buckles formed and then straightened during a loading cycle. Increasing buckle amplitudes created significant bending strains on the surface of the infill plate, and this caused certain areas of the specimens to yield.

Yielding due to plate buckling was detected by the flaking of the whitewash coating on the specimen surface. At the end of each test, yielding was noted on at least one side of the infill plate, and along a band approximately 40 mm wide and 300 to 400 mm long. The bands were oriented at about 45 degrees from either member of the V-frame. This can be seen on the south side of Specimen 4 in Figure 4.2. (Forty-five degrees from the V-frame member means that the direction is vertical in the photograph.) Figure 4.2 also shows the corner region of the north side of Specimen 4 at the end of the test. In this case, the horizontal yield band was the result of a buckle that had formed locally within the crest of a larger buckle. This localized buckle was observed only in Specimens 2 and 4.

4.3.2.2 Hysteresis Behaviour

In-plane displacements of the V-frame members were monitored using two LVDTs—one attached to the free end of the beam and one attached to the free end of the column. Load cells mounted on the ends of the jacks were used to record the jack loads. The location and orientation of the LVDTs and load cells are shown in Figure 3.8. As explained in Chapter 3, loads and displacements were measured and recorded for both members. The line of action of the loads and displacements was oriented at 45 degrees to the horizontal, that is, in a direction perpendicular to either V-frame member. To simplify the presentation of data, the horizontal component of the beam displacement was added to the horizontal component of the column displacement. This identifies the total inward or outward horizontal displacement of the V-frame. Similarly, the horizontal

component of the beam jack load was added to the horizontal component of the column jack load. Hysteresis curves were obtained by plotting the total displacement versus the total jack load. Figures 4.3 to 4.6 show hysteresis curves for Specimens 1 to 4, respectively.

An adjustment necessary during testing accounted for the vertical movement of the V-frame, as recorded at the beam-to-column joint. An uplift in the V-frame took place because of the tensile load applied to the infill plate and the vertical component of the jack loads that were applied to the beam and column. LVDTs attached to the beam and column measured the total movement of the V-frame members—displacement due to the beam and the column deflections plus the displacement due to the vertical uplift of the entire V-frame. A correction was made to isolate the deflections of the beam and the column by subtracting the vertical V-frame uplift from the vertical component of the total movement of the V-frame members.

The characteristic “waves” seen in all of the hysteresis curves are a result of the procedure that was followed during testing. The greater stiffness of the beam as compared with the column meant that larger loads had to be applied to the beam than to the column. The necessity for unequal jack loads in order to maintain equal beam and column displacements made it difficult to control the exact displacement of the V-frame members. Frequent adjustments had to be made to the jack loads, while, at the same time, the test data were collected continuously. This resulted in the wavy appearance of the load versus deflection plots.

Hysteresis curves for Specimens 2 to 4 (Figures 4.4 to 4.6) show a series of eight individual loops. These represent the data recorded during the last cycle in each of the eight loading blocks. During testing of Specimen 1 (Figure 4.3), load cells were attached to the jacks only after the completion of loading block 3. Therefore, the hysteresis curve for Specimen 1 shows data loops only for loading blocks 4 to 8.

The parts of the hysteresis curves plotted in the negative quadrant of the graphs indicate the load and deflection response during the inward displacement of the V-frame members (Part A). The lopsided data distribution seen in all of the hysteresis curves is a result of the displacement limit in opening. As described above, this was the consequence of reaching the limit in the beam jack capacity.

At the end of Test 4, the infill connection specimen was removed from the test frame. The beam and column were then loaded one at a time. Each member was displaced, first inward and then outward, while the other member was held at zero displacement. Figure 4.7 shows these loading curves. In this case, the individual jack load versus the displacement of either V-frame member is seen in the figure. The plotted loads and displacements are those measured perpendicular to the beam and column. The slope of the curves give the stiffness values for the beam and the column. These are used later for the finite element model described in Chapter 5.

4.3.2.3 Specimen Tearing

The most severe sign of deterioration during the course of cyclic loading was the formation of tears in the specimen. To clarify the following descriptions, line drawing diagrams of the specimens (Figures 4.8, 4.10, 4.12, and 4.14) show a 200-by-200 mm close-up of the corner detail. The diagrams show numbered tears in the order that they are referred to below, and the length of tears at the end of testing. “East” and “West” labels on the diagrams refer to the orientation of the specimens as placed in the test frame (refer to Figure 3.8).

Testing of Specimen 1 produced a small amount of yielding above the infill plate-to-foundation plate welds. This yielding began on both sides of the specimen during the fourth cycle of loading block 3 (block 3-4). No tears were observed at any time during the testing of Specimen 1. Figure 4.8 shows the yielding that was observed on Specimen 1: yielding above the welds due to the transfer of forces from the infill plate to the frame, and yielding due to buckling (as described above). The photograph in Figure 4.9 taken at the end of block 6-3 shows yielding due to buckling on the north side of the specimen.

Testing of Specimen 2 resulted in a significant amount of tearing and yielding as compared with Specimen 1. The location of the tears is presented in Figure 4.10. (The tears are numbered in Figure 4.10 so that they can be referred to in the text that follows.) Both Figures 4.10 and 4.11 show Specimen 2 at completion of testing.

- The first tear in Specimen 2, Tear 1 (2 mm long), was noted during block 3-1 on the south side. It was located in the weld and was at the intersection between the two

infill plate-to-fish plate welds. During this cycle, a small band of yielding was noted on the south side between the two fish plates.

- A second tear, Tear 2 (45 mm long), was noted during block 6-3 on the north side. It was in the west fish plate, above the toe of the fish plate-to-foundation plate weld. By the time of this cycle, Tear 1 had propagated through the infill plate-to-fish plate weld (6 mm) and into the infill plate in the westward direction (7 mm).
- By the time of application of loading block 7-1, Tear 2 had propagated to the south side (11 mm long). Tear 1 had continued to propagate and had grown to a length of 16 mm.
- A third tear, Tear 3 (24 mm long), was noted by the end of the test. It was on the south side, in the east fish plate and above the toe of the fish plate-to-foundation plate weld. It was propagating eastward. Tear 1 had stopped propagating in length, but had moved through the thickness of the infill plate and was visible on the north side (14 mm long). Tear 2 had grown to a length of 63 mm on the north side and 41 mm on the south side. A band of heavy yielding was noted on the south side between the two fish plates. See Figure 4.11.

Testing of Specimen 3 also resulted in a significant amount of tearing and yielding as compared with Specimen 1. The location of the tears is referred to by number in Figure 4.12. Both Figures 4.12 and 4.13 show Specimen 3 at completion of testing.

- The first tear of Specimen 3, Tear 1 (6 mm long), was noted during block 5-3. It was on the south side and was in the toe of the fish plate-to-infill plate weld.
- A second tear, Tear 2 (21 mm long), was observed during block 6-3. It was on the south side, in the east fish plate, above the specimen-to-foundation plate weld. Tear 2 appears to have been a continuation of Tear 1, which had propagated across the width of the weld (8 mm long). During the same cycle, it was also noted that Tear 2 had moved through the plate and was visible on the north side (6 mm long).
- A third tear, Tear 3 (5 mm long), was seen during block 6-6 on the south side. It was in the infill plate, above the specimen-to-foundation plate weld. It propagated westward. Tear 3 appears to have started at the head of Tear 1. Tear 2 on the north side had grown to a length of 20 mm.
- A fourth tear, Tear 4 (13 mm long), was also noticed during block 6-6. It was on the

north side, in the infill plate. Tear 4 appears to have been caused by Tear 3 propagating through the plate from the south side.

- A fifth tear, Tear 5 (68 mm long), was seen during block 7-6. It was on the south side, in the infill plate, at the toe of the infill plate-to-fish plate weld. It propagated eastward. Tear 5 appears to have also started at the head of Tear 1.
- By the end of the test, Tear 1 had grown to a width of 3 mm, and Tears 2 and 3 on the south side had propagated to lengths of 70 mm and 21 mm, respectively. Tears 2 and 4 on the north side had propagated to lengths of 52 mm and 33 mm, respectively. A band of heavy yielding was noted on the north side. See Figure 4.13.

The testing of Specimen 4 produced a significant amount of tearing and yielding. The location of the tears is presented in Figure 4.14. Both Figures 4.14 and 4.15 show Specimen 4 at completion of testing.

- The first tear, Tear 1 (2 mm long), was noted during loading block 7-2. It was on the south side, in the east fish plate and at the toe of the fish plate-to-foundation plate weld. It propagated eastward.
- A second, third, and fourth tear, Tear 2 (18 mm long), Tear 3 (11 mm long), and Tear 4 (10 mm long), were also seen during block 7-2. They were on the south side, in the heat-affected zone of the weld between the two fish plates.
- By the time of block 8-1, a fifth tear, Tear 5 (10 mm long) had formed due to Tear 3 propagating through the thickness of the plate from the south side to the north side.
- A sixth tear, Tear 6 (18 mm long), was noted at the end of the test. It was on the south side, in the west fish plate, and at the toe of the fish plate-to-foundation plate weld. It had propagated westward. Tears 2 and 3 had joined to form a 1.5 mm wide crack. Tear 5 on the north side had propagated to a length of 16 mm. Tears 1 and 4 on the south side had propagated to lengths of 25 mm and 27 mm, respectively. Figure 4.15 shows the yielding in the Specimen 4 observed at the end of testing.

In summary, tears developed in three of the four infill plate connection specimens (Specimen 2, 3, and 4). The details of specimen tearing will be used both in the comparison between individual specimens and between an actual specimen and a corresponding finite element model.

4.4 Strain Gauge Data

Strain rosettes were mounted on the infill connection specimens. Five rosettes, located in close proximity to the boundary between the specimen and the V-frame members, were applied on each face of the test specimens. Strain readings taken from opposing rosettes were averaged. By averaging the rosette data, strains induced by plate bending were algebraically removed. The mean values are then considered as constant strains across the through-thickness of the plate.

Table 4.2 gives strain results for Specimen 2. Values of the normal strains and shear strain are given at two load levels. The loading block, cycle, and total horizontal V-frame displacement at which the strains occurred are indicated for each load level. Tables giving strain results for all four specimens are shown in Appendix C. The line drawing in Figure 4.16 depicts the orientation of the x- and y-axis along which the normal and shear strains are plotted in Figure 4.17. The normal strains that are shown in Figure 4.17, also for Specimen 2, were measured perpendicular to the axes along which the strain rosettes were located. For Rosette 3, the normal strain plotted was measured along the bisector of the x- and y-axes. The values along the X-Y axis in Figure 4.17 are the distances (in millimetres) between the strain rosettes relative to Rosette 3, which is located at the origin. Strain gauge results from Specimen 2 will be discussed and compared with the analytical results in Chapter 6.

Table 4.1 Material Properties

Specimen	Direction*	Modulus of Elasticity (MPa)	Static Yield Strength (MPa)	Static Ultimate Strength (MPa)
Infill Plate 1	1-1	191800	346	424
	1-2	187200	351	431
Infill Plate 2	1-1	203200	353	430
	1-2	193200	331	420
Fish Plate	1-1	234900	399	488
	1-2	207400	403	491

* Directions 1-1 and 1-2 are shown in Figures 3.4 to 3.7.

Table 4.2 Measured Strains from Specimen 2

		Rosette:				
		1	2	3	4	5
Part A	Block-Cycle: 5-6	-530.75	-71.9	-2234.2	282.2	203.5
	Total Jack Load (kN): -708	91.8	3713.7	2760.6	-27.3	-294.2
	Total Displ. (mm): -12.8	983.1	1886.0	2835.2	979.3	583.8
	Block-Cycle: 8-6	-565.7	159.7	-1455.4	577.2	-55.35
	Total Jack Load (kN): -885	82.3	5716.8	5355.4	414.4	-176.8
	Total Displ. (mm): -23.6	1268.8	1024.5	1688.2	2510.9	865.7
		ϵ_x				
		ϵ_y (MPa)				
		γ_{xy}				
		ϵ_x				
	ϵ_y (MPa)					
	γ_{xy}					
Part B	Block-Cycle: 5-6	365.7	498.3	-1272.6	288.2	158.9
	Total Jack Load (kN): 1029	208.8	692.6	2228.2	496.3	428.2
	Total Displ. (mm): 4.0	-1696.7	-28.1	-555.3	-1385.3	-1733.7
	Block-Cycle: 8-6	342.65	711.5	1047.8	164.5	-75.65
	Total Jack Load (kN): 1086	386.3	3884.4	4677.1	577.0	532.0
	Total Displ. (mm): 3.4	-1919.0	-5778.0	-7905.9	-2089.2	-1811.7
		ϵ_x				
		ϵ_y (MPa)				
		γ_{xy}				
		ϵ_x				
	ϵ_y (MPa)					
	γ_{xy}					

Note: Negative values indicate compressive loads and strains, and inward displacements.

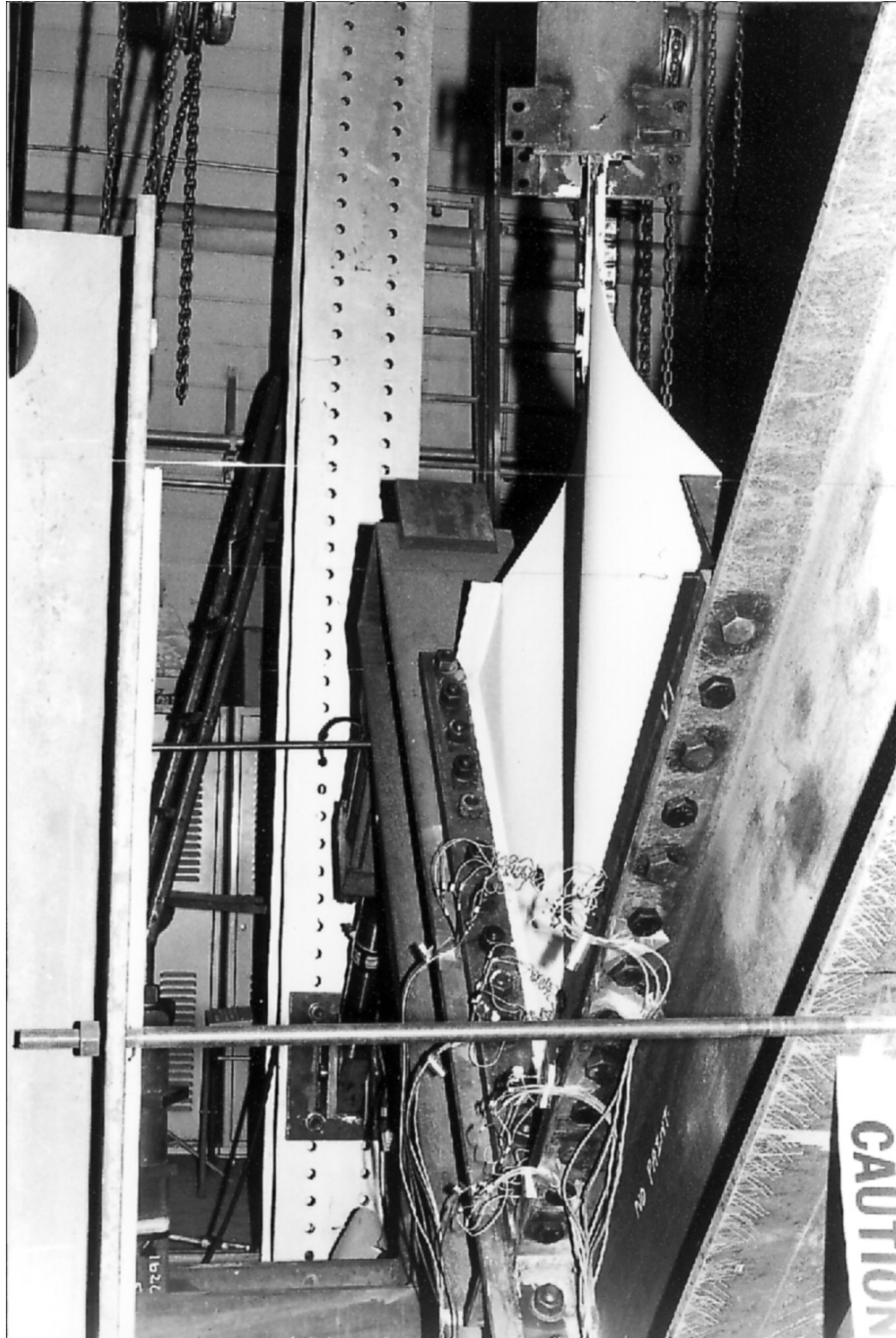


Figure 4.1 Buckling of Infill Plate

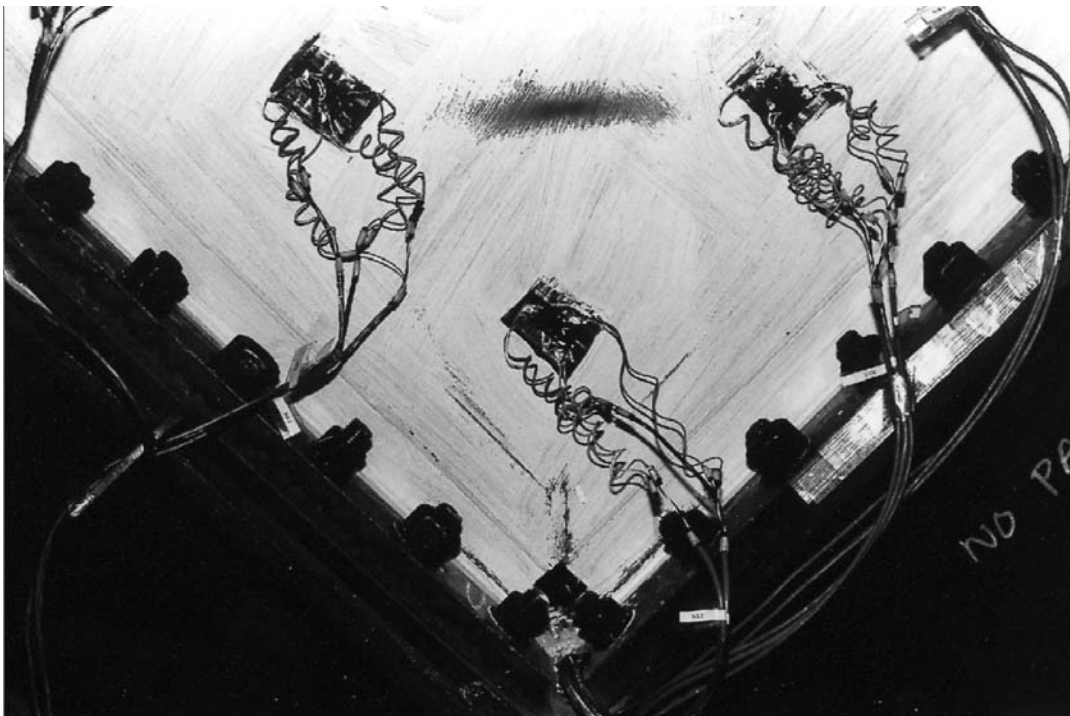
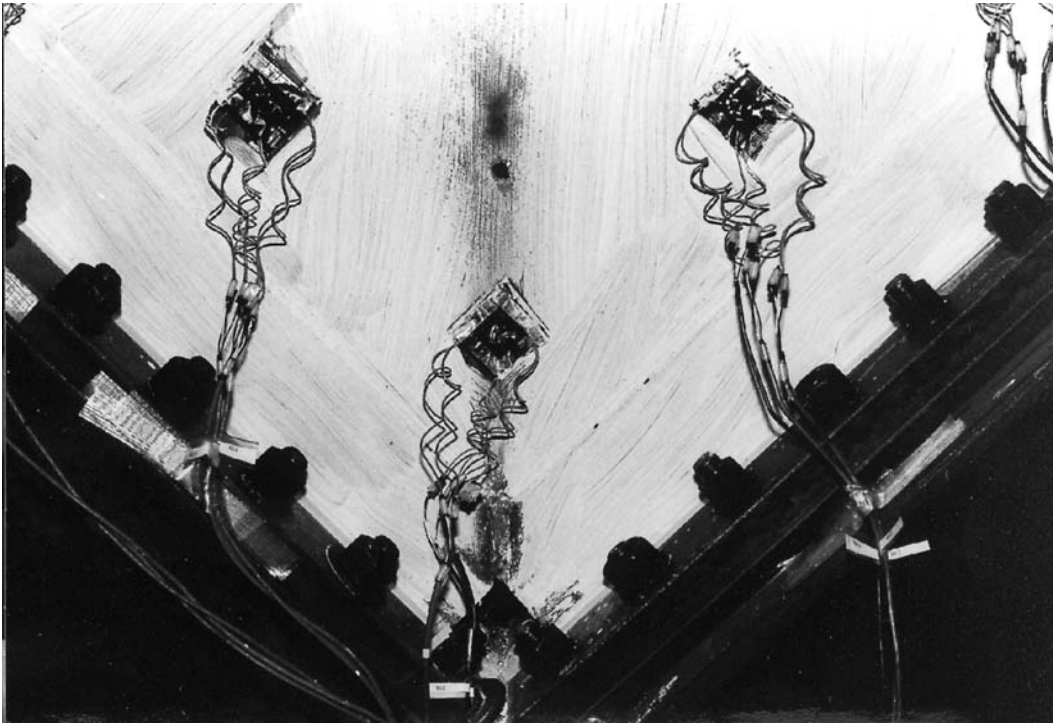


Figure 4.2 Yielding of Specimen 4 Due to Buckling

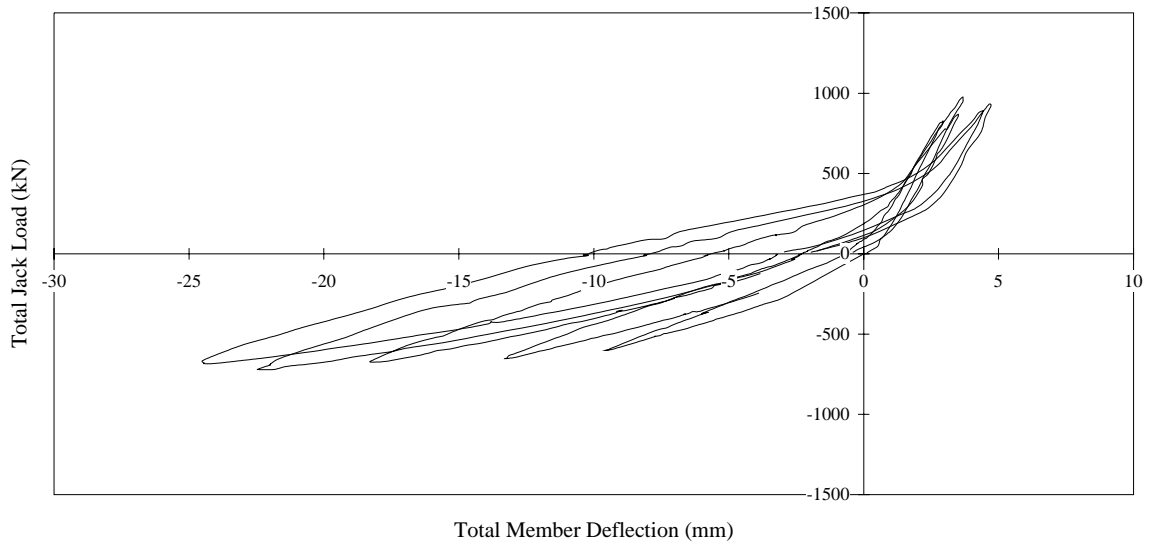


Figure 4.3 Hysteresis Curves for Specimen 1

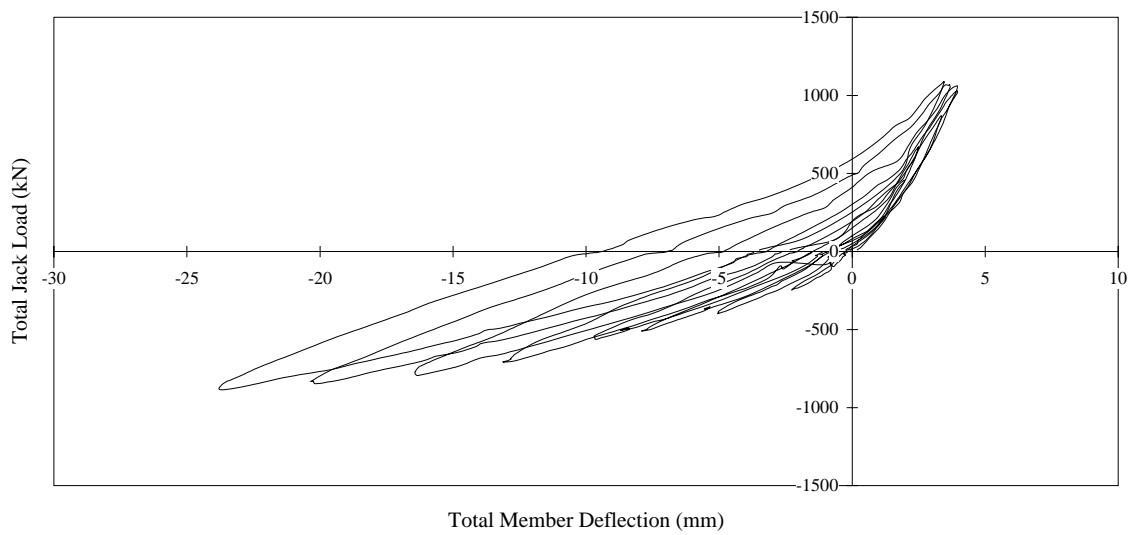


Figure 4.4 Hysteresis Curves for Specimen 2

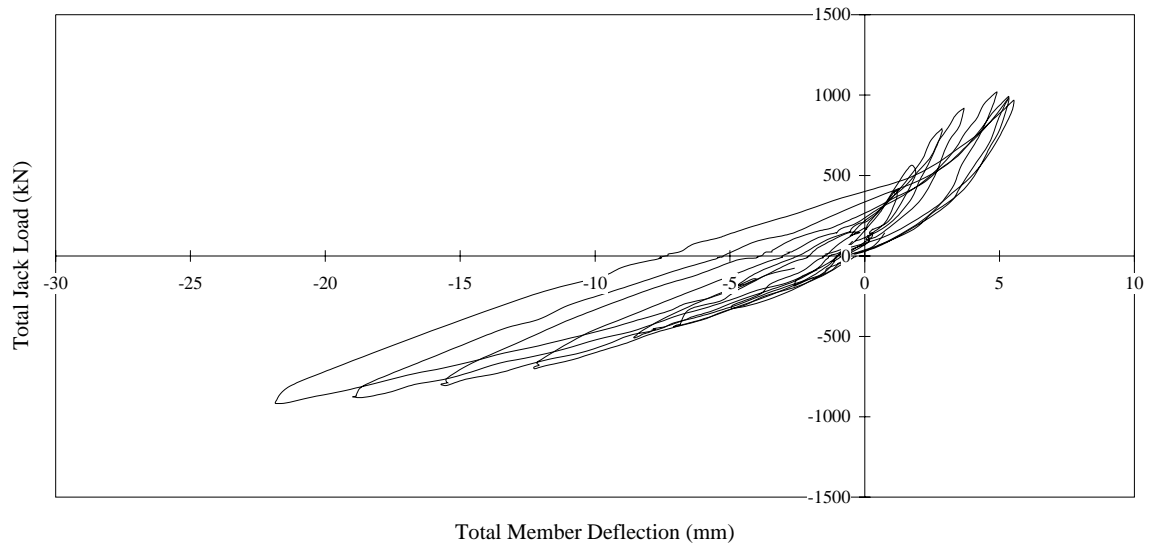


Figure 4.5 Hysteresis Curves for Specimen 3

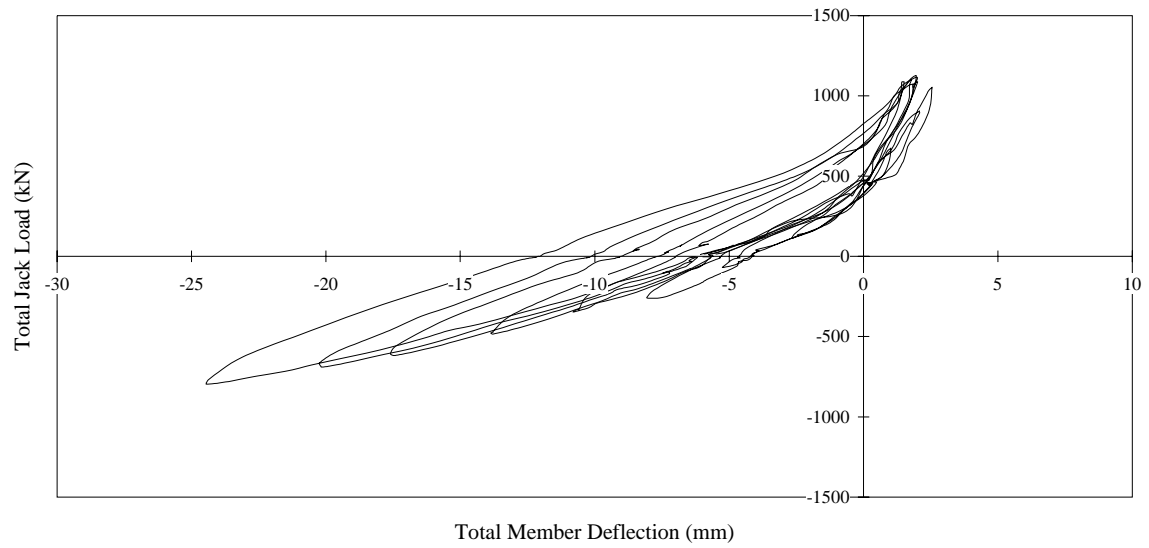


Figure 4.6 Hysteresis Curves for Specimen 4

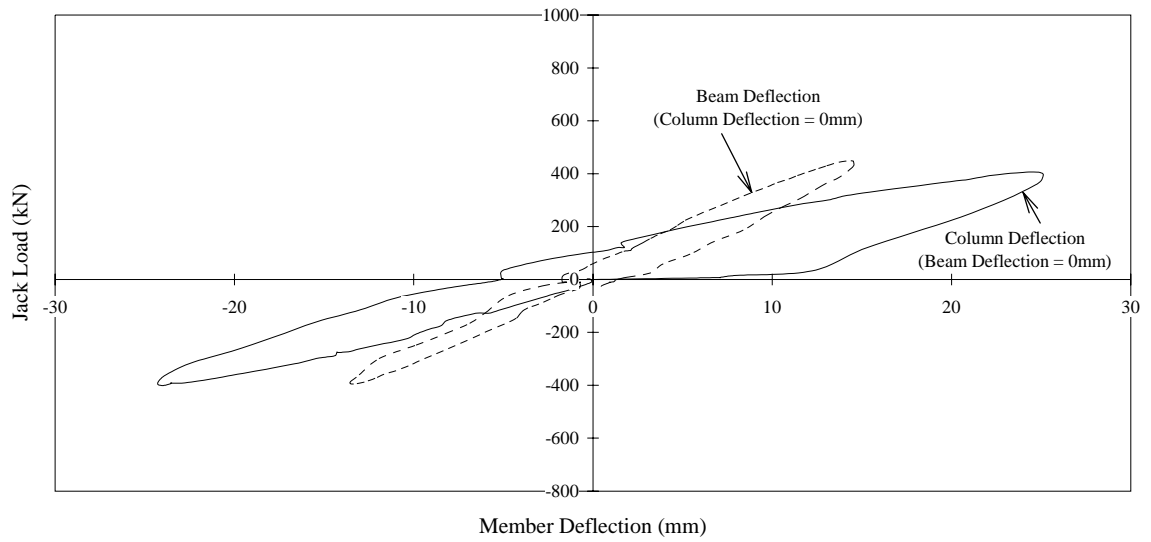


Figure 4.7 V-Frame Load Versus Displacement Response

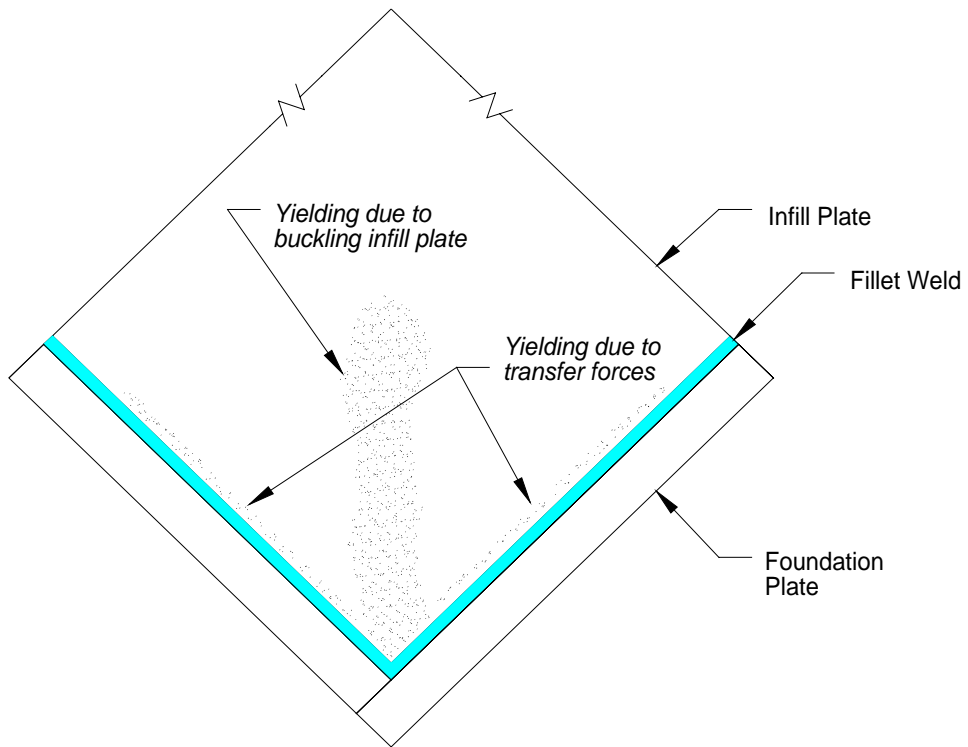


Figure 4.8 Yielding Observed on North and South Sides of Specimen 1

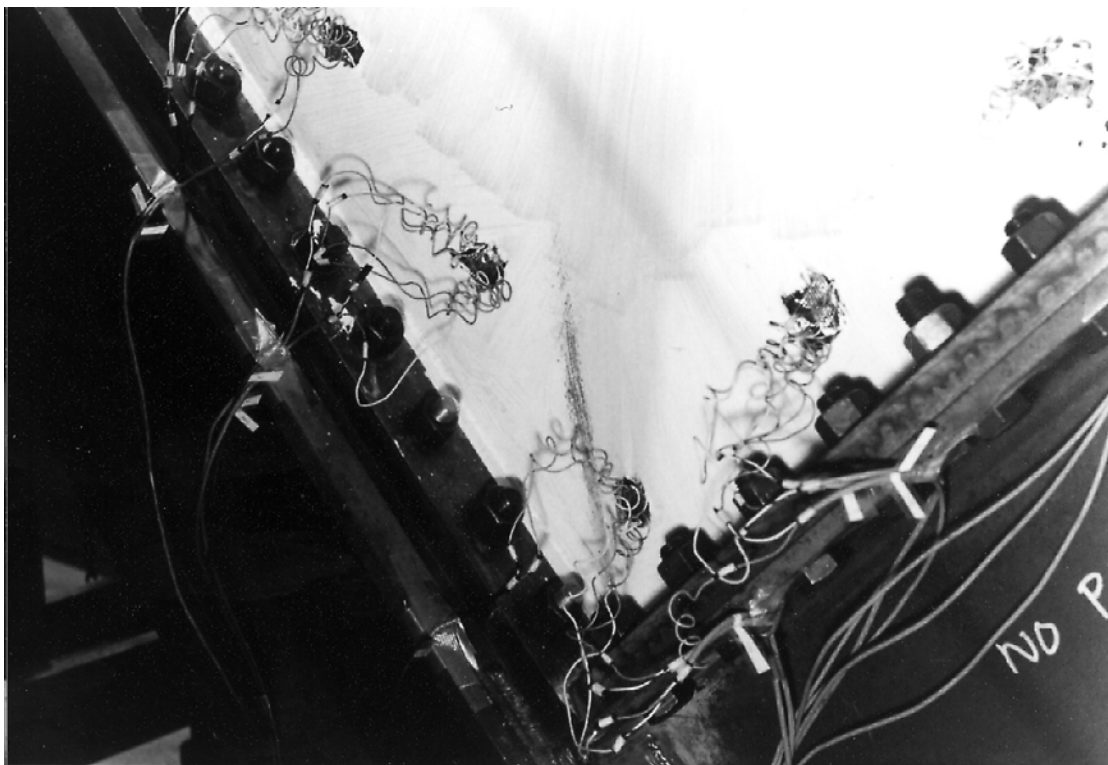


Figure 4.9 Yielding Observed on North Side of Specimen 1

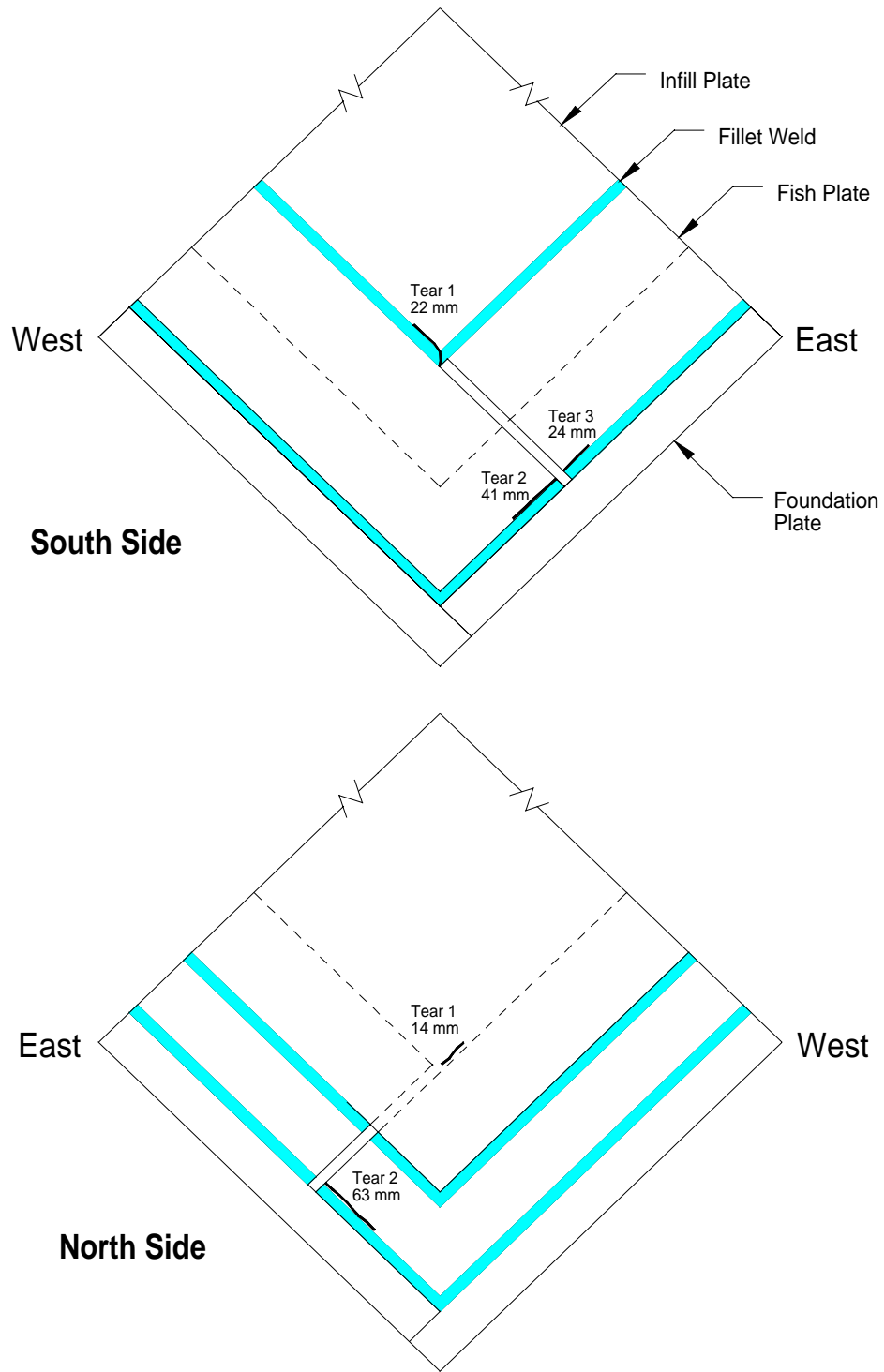


Figure 4.10 Tears Noted on Specimen 2

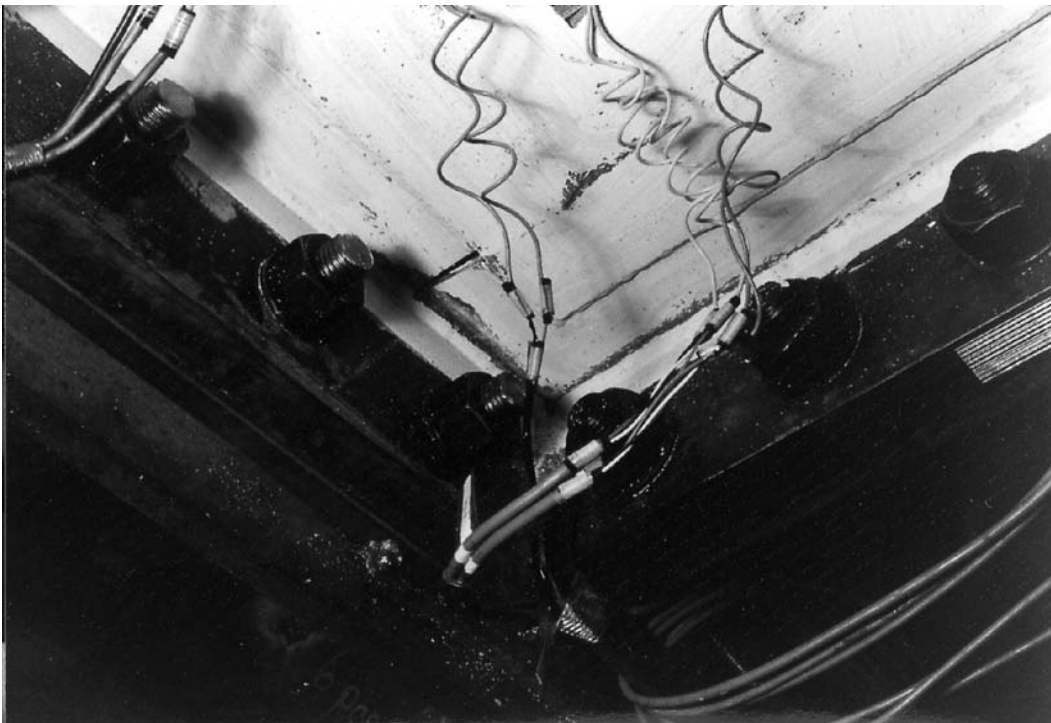
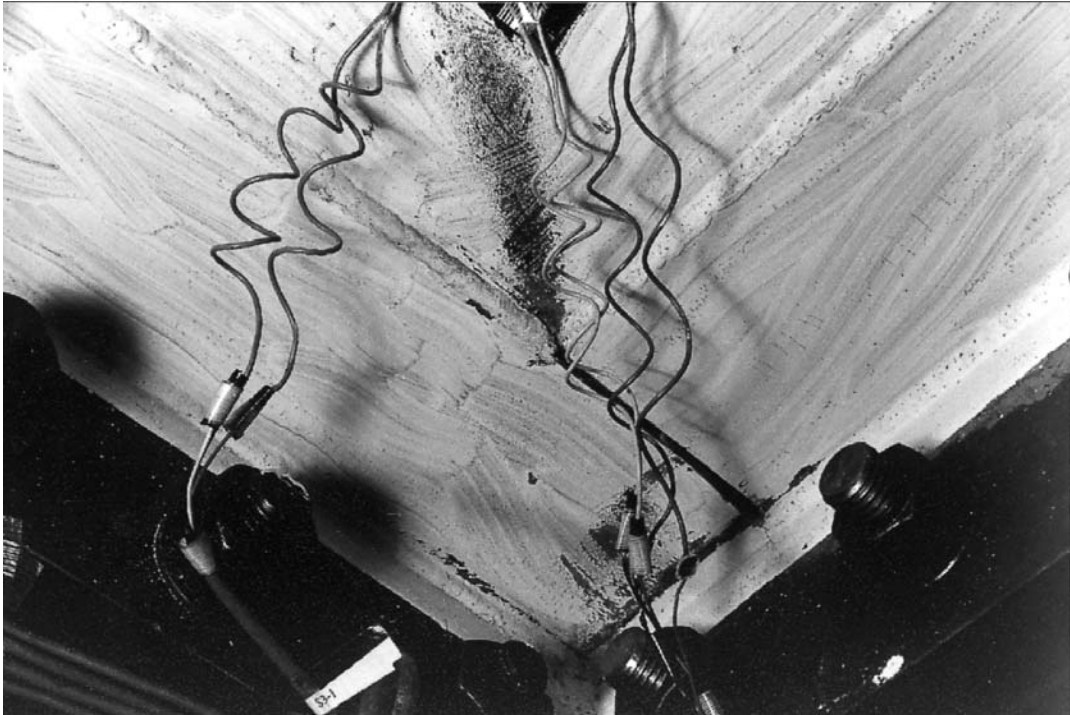


Figure 4.11 Specimen 2 Corner Detail at End of Testing

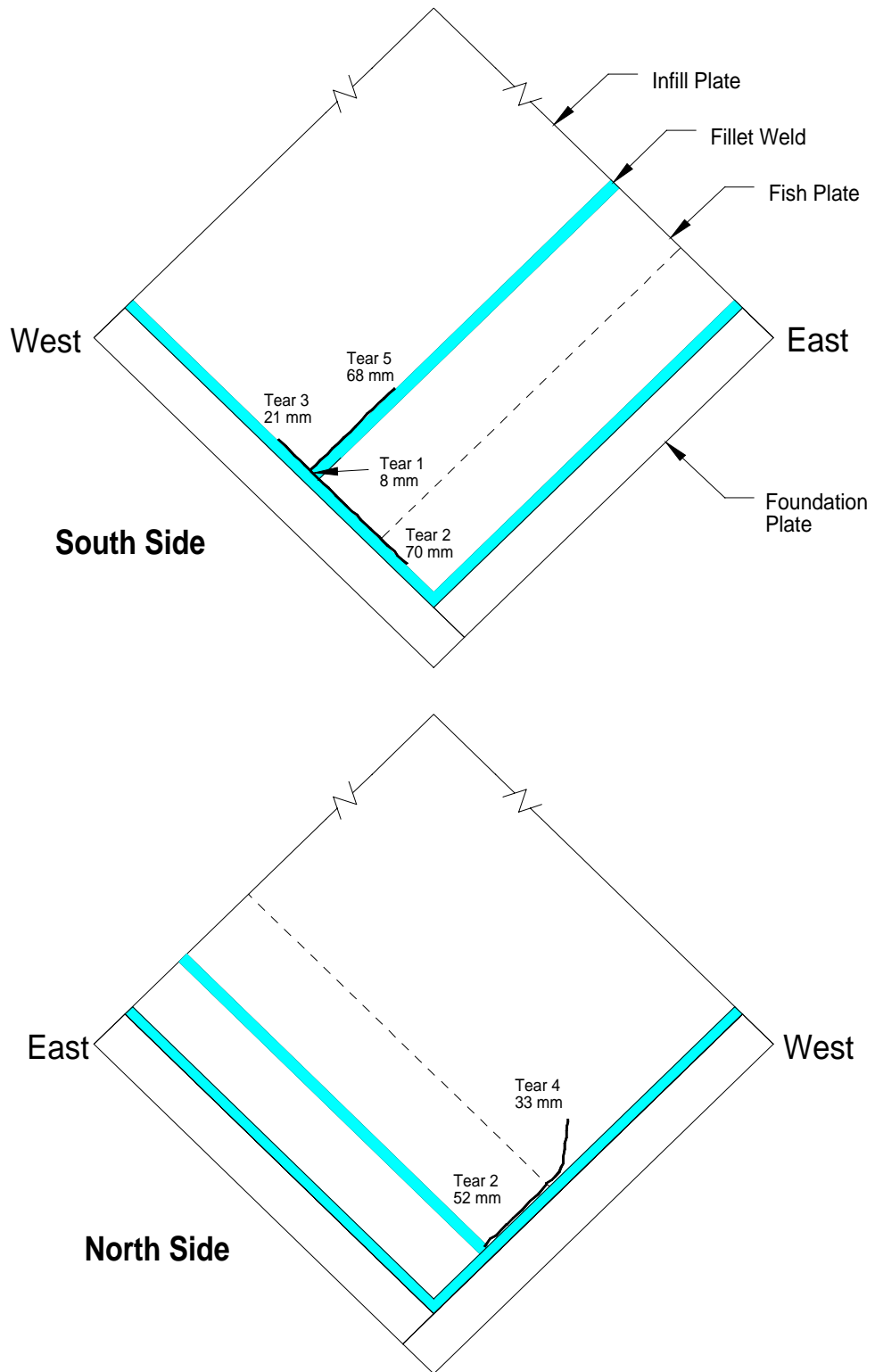


Figure 4.12 Tears Noted on Specimen 3

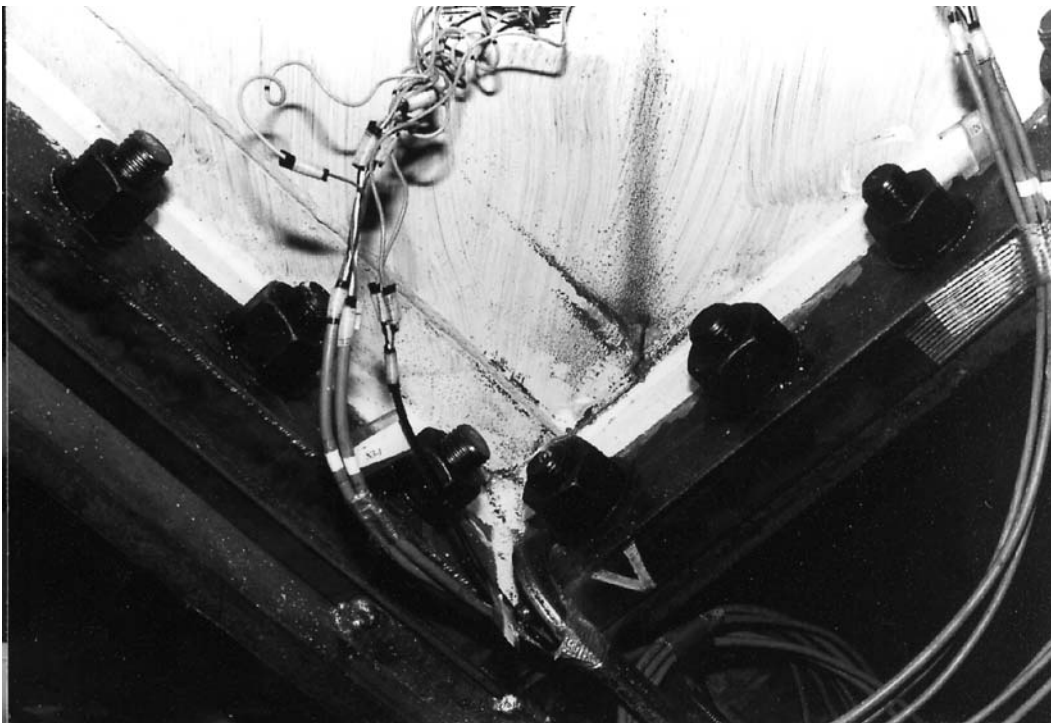
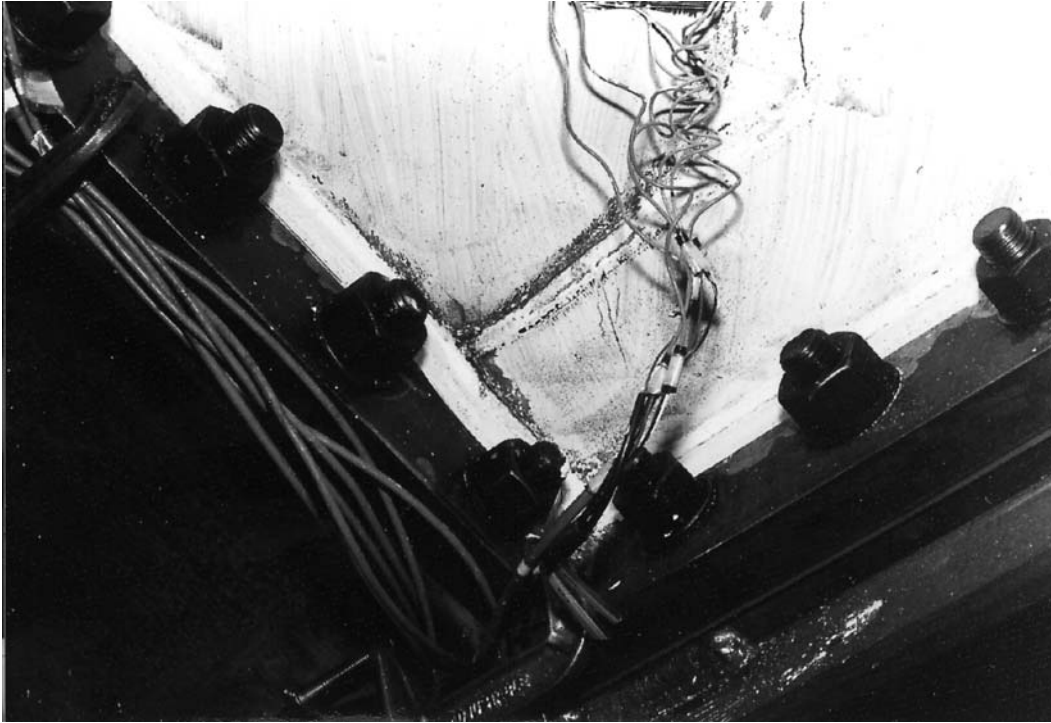


Figure 4.13 Specimen 3 Corner Detail at End of Testing

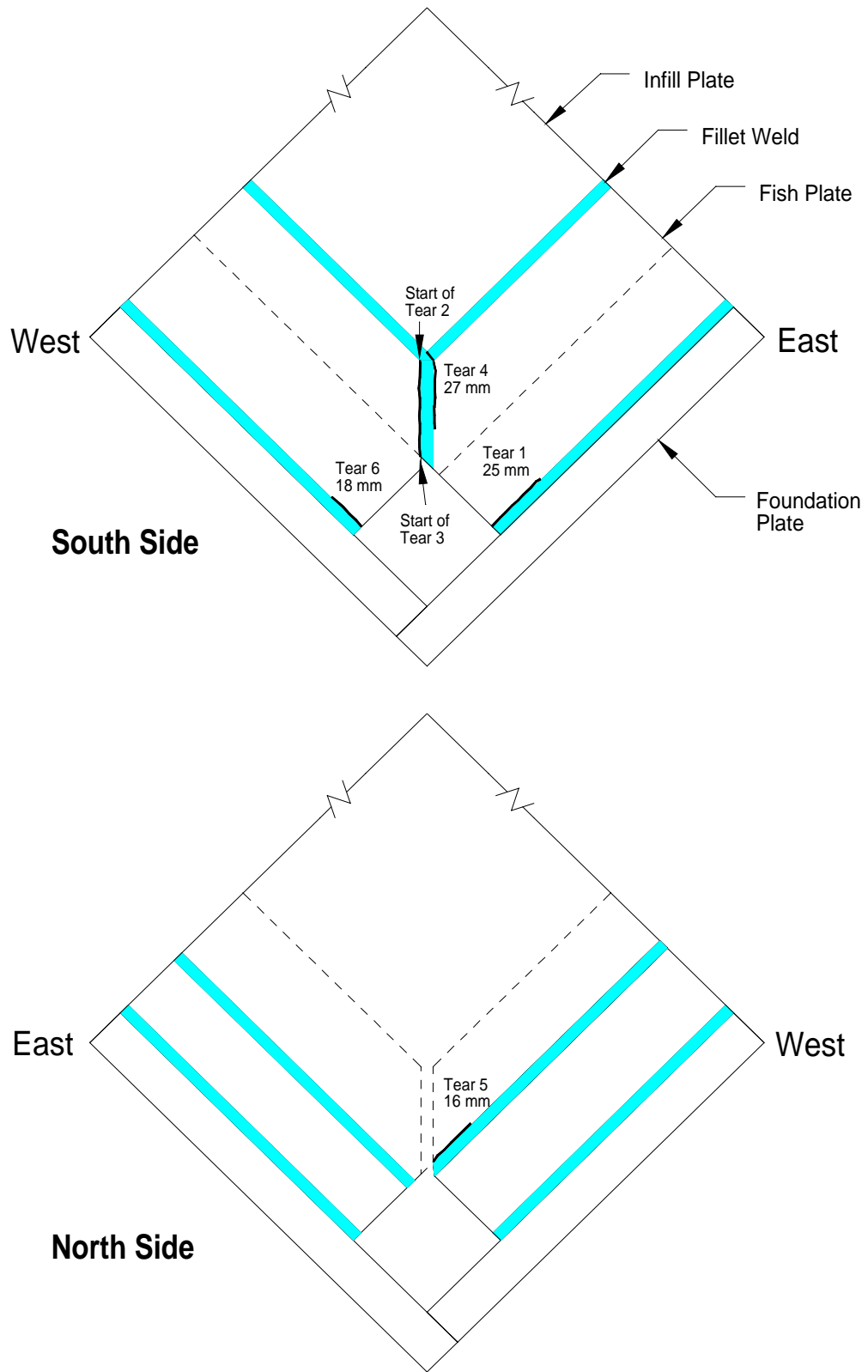


Figure 4.14 Tears Noted on Specimen 4

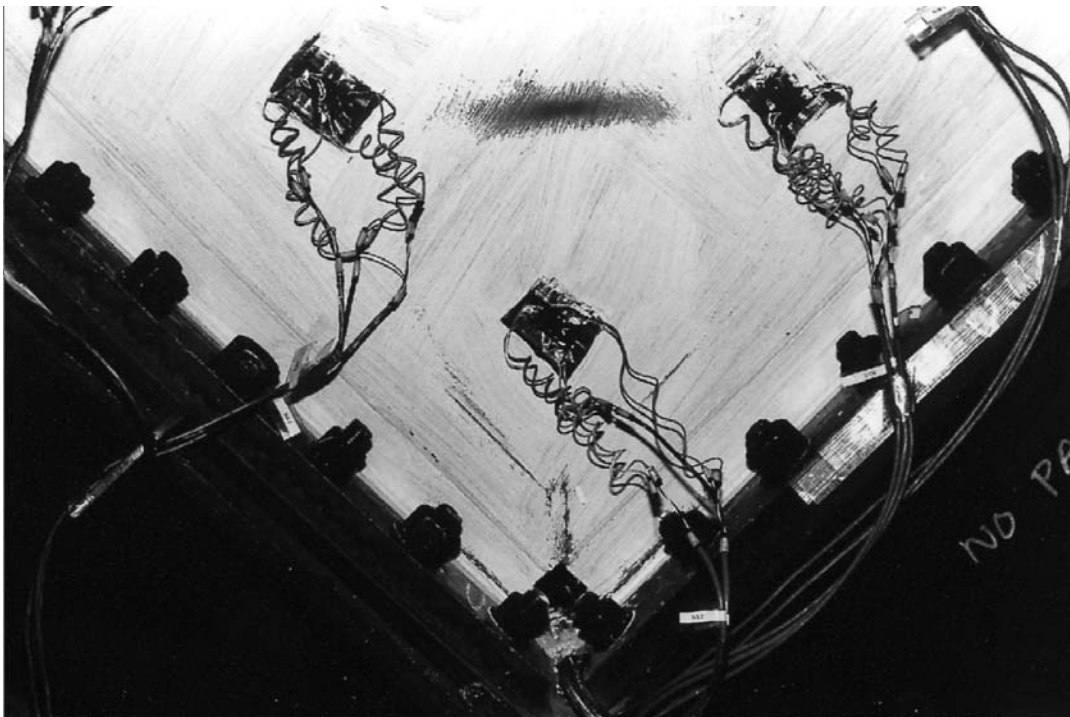
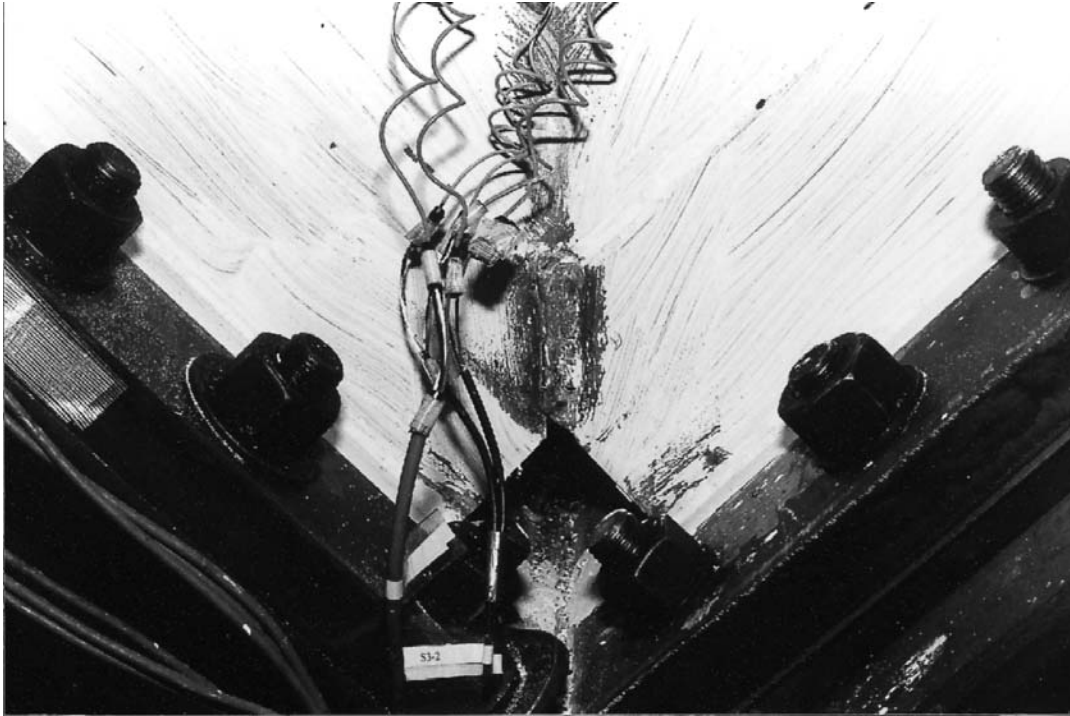


Figure 4.15 Specimen 4 Corner Detail at End of Testing

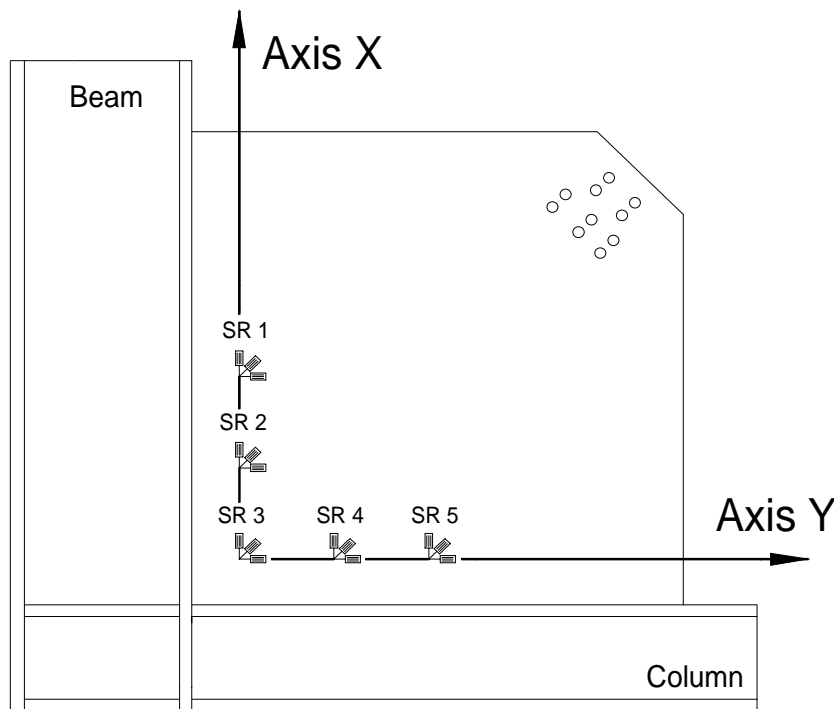


Figure 4.16 Axes for Strain Orientation

Total Inward Displacement (Part A) = 12.8 mm
 Total Outward Displacement (Part B) = 4.0 mm

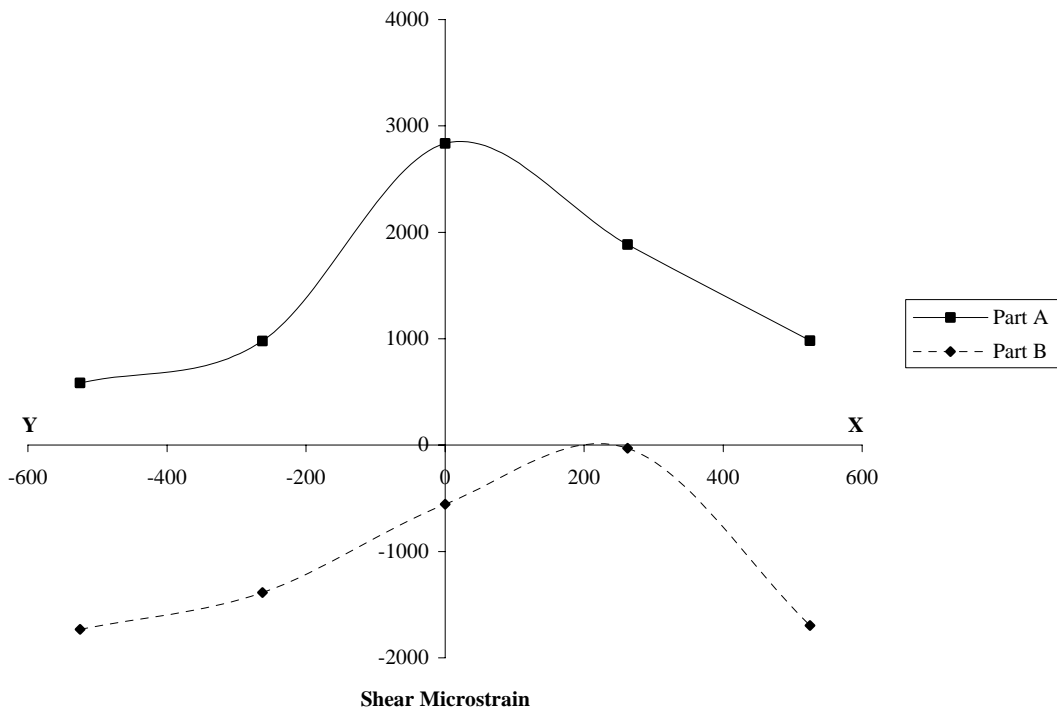
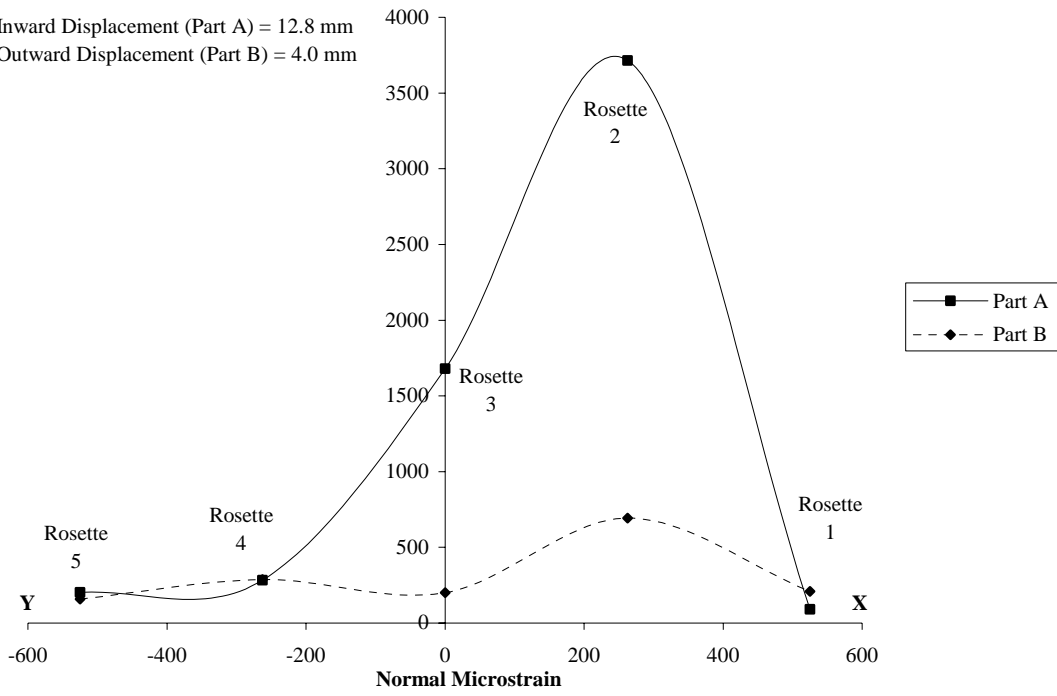


Figure 4.17 Measured Normal and Shear Strains

5. Finite Element Analysis

5.1 General

The goal of the finite element analysis was to develop a model that would predict the behaviour of Specimen 2. The primary test of the model will be to compare the predicted load versus displacement response against the response observed during testing. A comparison between the strains measured in the test specimen and the strains obtained from the analysis will be used to validate further the finite element model. Another objective of the finite element study is to determine whether the location of the tears observed in the test specimen can be correlated with the strain distribution in the finite element model. A validated finite element model will provide a useful tool for evaluating the effect of parameters that were not specifically investigated in the test program. A parametric study, however, is beyond the scope of the work presented here.

Specimen 2 was modelled using the commercial finite element code ABAQUS [Hibbitt *et al.* 1996]. Analysis of the model was conducted on a SUN SPARC workstation.

5.2 Description of the Model

The finite element model was built in two phases. First, the V-frame, consisting of the beam, column, and foundation plates, was analyzed in order to match the stiffness of the V-frame model to the stiffness of the test V-frame. In the second phase, the infill plate and fish plates were added to the V-frame. Two infill plate meshes, that is, a fine mesh and a coarse mesh, were analyzed to investigate convergence of the analysis. Only one V-frame mesh was used for the analysis of both the coarse and the fine mesh models.

5.2.1 Elements and Mesh

The ABAQUS element S4R was used to model both the V-frame and the infill plate connection specimen. The S4R element is a four node, doubly curved shell element that accounts for finite membrane strains and allows for a change in element thickness [Hibbitt *et al.* 1996]. This element has six degrees of freedom at its nodes: three displacement components and three in-surface rotation components. S4R is a reduced

integration element with only one integration point at the centroid of the element. The cross-sectional behaviour of the S4R element is integrated at five points across the thickness of the element. This allows for an accurate representation of material behaviour for non-linear problems.

The V-frame was modelled using 2252 shell elements. Figure 5.1 shows the mesh used to model the V-frame. The co-ordinate system shown in Figure 5.1 is the reference system that will be used for the descriptions that follow. The finite element model was oriented with the beam parallel to the x- or 1-axis and the column parallel to the y- or 2-axis. The beam and column were modelled with separate element arrays that formed the flanges and the webs. The flange plate element arrays were tied to the web element arrays using the “tie” multi-point constraint option of ABAQUS. Similarly, the beam and column were joined by tying beam nodes to column nodes. Loads were applied to beam and column nodes as point loads and, in order to prevent the possibility of a premature local failure in the web of either the beam or column, stiffeners were included in the finite element model. However, stiffeners were not needed in the actual test specimen because the jack loads were distributed into the V-frame members through tongue attachments (shown in Figure 3.8).

In order to model the bolted connection between the foundation plates and the beam and the column of the V-frame, nodes in the foundation plate mesh were tied to nodes in the mesh of the beam and column flanges. Locations of the tied foundation plate and flange nodes corresponded to the bolt locations in the actual test specimen. The beam and column stiffener elements referred to above were also joined to the beam and column mesh using the tie multi-point constraint.

The entire V-frame model was restrained at the lower end of the column by setting all degrees of freedom of the reaction nodes to zero. The restrained column nodes are highlighted in Figure 5.1. In order to model the stiffness of the actual V-frame, material properties for the beam and the column were adjusted to obtain a good prediction of the V-frame behaviour observed during testing of the V-frame without the infill plate. Further discussion of the V-frame model material properties is presented below.

The infill plate specimen and the fish plates were modelled using both a coarse mesh and a fine mesh. Figures 5.2 and 5.3 show the coarse and fine meshes, respectively. The coarser mesh used 50 mm square shell elements, for a total of 671 elements, and the fine mesh used 25 mm square shell elements, for a total of 2688 elements. The fish plates (oriented in the 1- and 2-directions) were modelled using rectangular element arrays that were lapped by the square array of infill plate elements. The 6 mm gap between the two fish plates in the actual specimen (refer to Figure 3.5) was included in the model. The infill plate stiffeners used in the test specimen to prevent premature tearing of the plate at its free edges were also incorporated in the model. Fish plate-to-foundation plate, fish plate-to-infill plate, and stiffener-to-infill plate fillet weld connections were modelled by tying the appropriate nodes. Ten spring elements (seen in Figures 5.2 and 5.3) were included in the models at the location where a tensile force was applied to the actual infill specimens. This tensile force, which was applied to the test specimen through a tension connection with ten bolts (refer to Figure 3.8), was applied to the finite element model at the nodes that corresponded to the location of the bolts. The spring elements were used to simulate the out-of-plane restraint of the infill plate that was provided by the tension plates and the tension member (also seen in Figure 3.8) in the actual test set-up.

5.2.2 Initial Conditions

Out-of-plane imperfections can play an important role in the behaviour of a thin plate in compression. Initial imperfections induce bending of the plate, thereby setting up secondary stresses. This causes an apparent reduction of the in-plane plate stiffness and, possibly, a decrease in the load level at which a plate will buckle under compression. More importantly, in a non-linear load-displacement analysis such as the one performed here, initial imperfections are essential for the analysis to converge to a low energy buckling mode.

As was described in Chapter 3, the out-of-plane initial imperfections in the infill plate were measured at Demec points mounted on one side of the specimen. Some of the effects that contributed to the out-of-flatness measured in all four specimens included handling prior to testing and distortion due to welding. Both the coarse and fine infill plate meshes for the finite element model of Specimen 2 were given a maximum initial

imperfection of 22 mm. This value was calculated by averaging the two maximum Demec point readings taken at two of the seven Demec locations on Specimen 2 prior to testing. In the model, the out-of-plane displacements were described as a parabola across the infill plate, both in the 1- and the 2-directions. A maximum displacement of 22 mm was established at the centre of the infill plate model and there was zero displacement at the corners.

No attempt was made to model the residual stresses in the finite element model. However, residual stresses are likely to play an important role in the load response of the plate and can be expected to have significant localized effects in areas of the plate near welds.

5.2.3 Material Model

The V-frame was modelled using an isotropic, elastic-plastic material. The elastic modulus selected for the V-frame model was 180 000 MPa. The yield strength of the beam, column, and column panel zone was taken as 350 MPa, 450 MPa and 400 MPa, respectively. It should be noted that the material properties selected for the analysis are those that predicted well the results of the test on the V-frame and may not be exactly representative of the beam and column material. The material model used for the beam and column does not only reflect the material in the beam and the column, but also reflects to some extent the support condition provided to the V-frame. The reader may recall that the test V-frame was mounted on a distributing beam which may have provided a more flexible support to the V-frame than assumed in the finite element model. The infill plate specimen was modelled using an isotropic, elastic-plastic material. The constitutive model incorporated a von Mises yield surface and an isotropic strain hardening flow rule. True stress versus strain curves, derived from material tests, were used to define the material response, which was taken to be identical in tension and in compression. The material response input for the numerical analysis of the infill plate used a mean stress versus strain curve recorded for tension coupon testing of Specimen 2. Figure 5.4 shows the stress versus strain curve used in the finite element model.

5.3 Analysis

The analysis performed with the finite element model of Specimen 2 was a static load versus displacement response analysis that included the nonlinear effects of geometry and material response. In a case where there is a possibility of unstable behaviour—for example, a thin plate in compression—the modified Riks solution strategy implemented in ABAQUS [Hibbitt *et al.* 1996] is recommended. The modified Riks, also known as the arc length method, uses the load magnitude and the displacements as unknowns, and controls the increments (arc lengths) taken along the load versus displacement response curve. Since the Riks algorithm treats both loads and displacements as unknowns, termination of a Riks loading step will not occur at a predetermined load or displacement. Instead, the Riks step will end at the first solution that satisfies the user-defined step termination criterion. This criterion can be a maximum load, a maximum displacement at a given degree of freedom, or a maximum number of increments within a load step.

The exact boundary conditions at the beam-to-column joint in the test set-up were not known. This was because of the modifications that were made to the joint subsequent to testing of Specimen 1 (Section 4.1) when weld tearing occurred at the joint. Therefore, the V-frame model was analyzed first in order to determine whether the perfect boundary conditions assumed in the model (the beam was “tied” to the column) simulated the actual stiffness of the frame. Chapter 4 described how the actual V-frame stiffness was measured by displacing each member, first inward and then outward, while the other member was held at zero displacement. A similar loading approach was taken for the V-frame model. The beam was loaded at its free end, first in the positive 2-direction (refer to Figure 5.1) and then in the negative 2-direction, while the column was pinned at its free end in the 1, 2, and 3-directions. Likewise, the column was loaded at its free end in the positive and negative 1-direction while displacements at the free end of the beam were kept at zero by using a pin restraint in that location.

As explained above, the material properties for the beam and column were adjusted to obtain a good correlation between the test results and the numerical model. In Figure 5.5, a comparison between the test results and the finite element results indicates that the stiffness of the actual V-frame members is similar to the stiffness of the

modelled V-frame. Once the stiffness of the V-frame had been adjusted to match that of the test frame, it was possible to introduce the infill plate into the model.

Loading of the entire test set-up model—the infill plate, the fish plates and the V-frame—proceeded in four steps. The loading applied to the finite element model is equivalent to the last loading block that was applied to Specimen 2. In the first load step, the beam and column were loaded at their free ends in the positive 2- and 1-direction, respectively. This caused the beam and column to move inward, thereby compressing the infill plate. Simultaneously, a tensile load simulating the tension force applied to the test specimen by the MTS testing machine was applied to the free corner of the infill plate portion of the model. A maximum tensile load of 800 kN was reached at the same time as the maximum beam and column loads were reached. For the second load step, the model was unloaded in a proportional way.

In the third load step, the V-frame members were loaded at their free ends in a manner to cause the beam and column to displace outwards. As was the case in the actual test, there was no load applied directly to the infill plate during this step. Loading of the finite element model was terminated during the third step when the loads applied to the beam and column reached the maximum value applied during the physical testing. In the fourth load step, the loads applied to the beam and column were released. The four load steps described above were applied to both the model with the coarse infill plate mesh and to the model with the fine infill plate mesh.

5.4 Results of the Analysis

In order to compare the results of the finite element models to that of the test specimen, the load and displacement values from the analysis were obtained and plotted. Figure 5.6 shows the load versus displacement curves for both the coarse mesh and fine mesh. As described in Section 4.3.2.2, the hysteresis data collected for the four experimental specimens was presented as the total horizontal jack load versus the total horizontal V-frame displacement. Therefore, the displacements recorded at the free end of the beam and column of the finite element model were also combined to obtain the total V-frame displacement. The same was done with the loads applied to the beam and column of the model, thereby giving a total load value.

For a conforming finite element solution the refinement of a model will result in an increase in the strain energy of the overall structure. Put another way, a finite element model will soften its load versus displacement behaviour with the increase of elements in the mesh. However, a finite element model will generally be stiffer than the actual structure. Figure 5.6 shows that the load versus displacement behaviour of the coarse mesh and fine mesh are similar. This indicates that the analysis is converging to an exact solution. Since there is only a very small difference in response between the coarse mesh and the fine mesh, it can be concluded that the size of the coarse mesh is adequate to model this detail. Comparisons between the finite element solution and the actual experimental results from Specimen 2 are presented in Chapter 6.

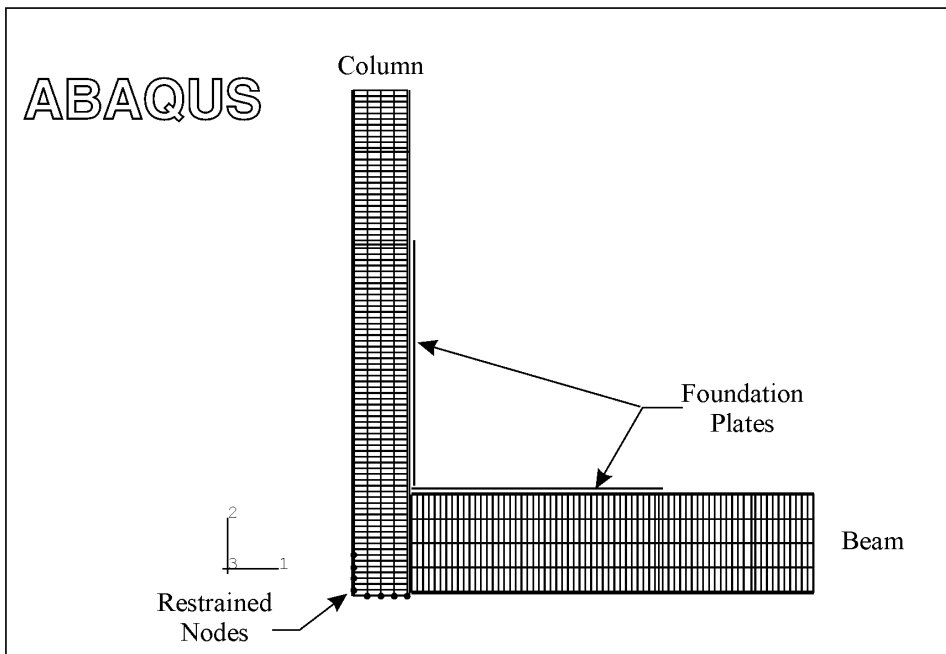
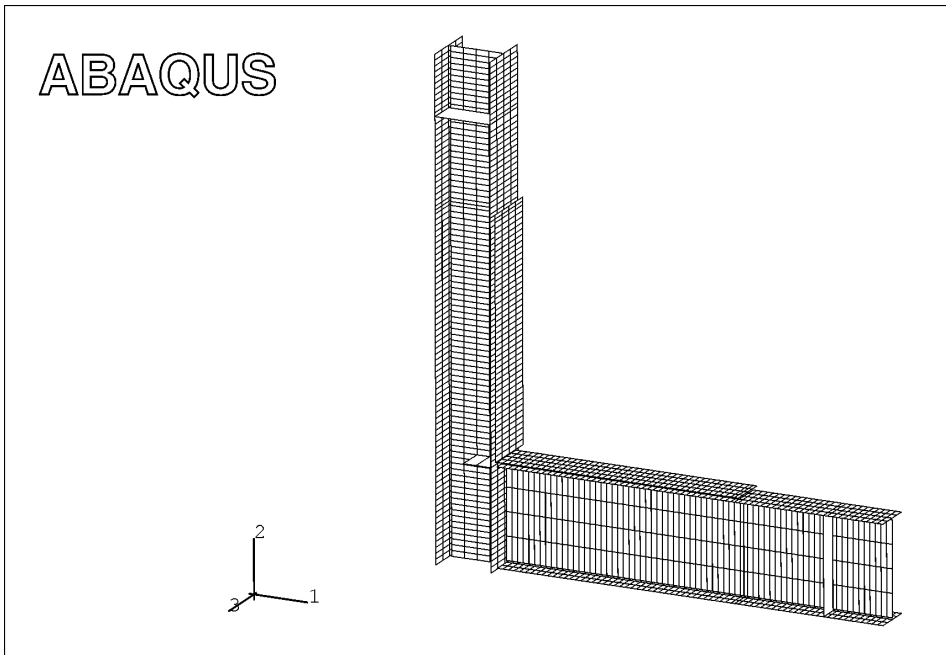


Figure 5.1 V-Frame Finite Element Model

ABAQUS

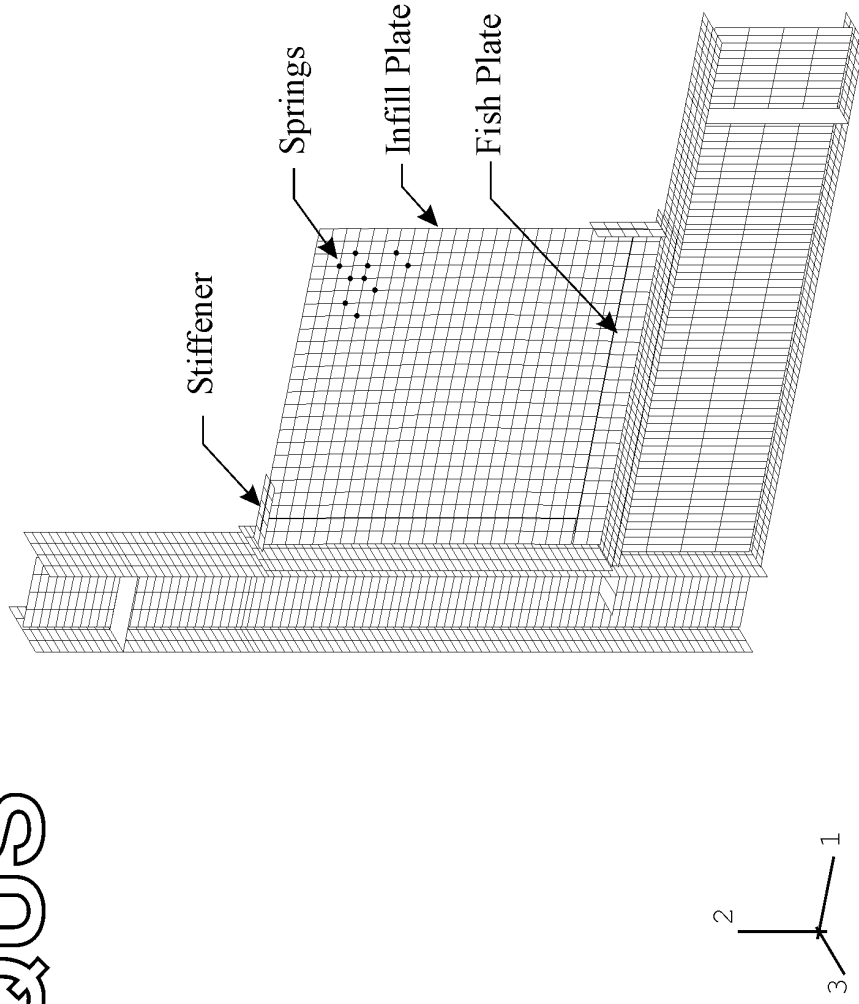


Figure 5.2 Coarse Finite Element Mesh

ABAQUS

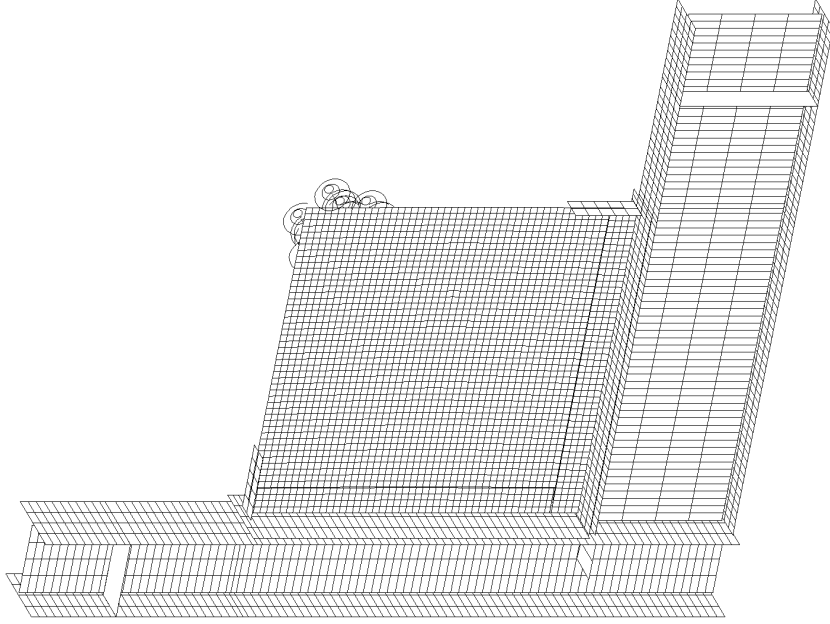


Figure 5.3 Fine Finite Element Mesh

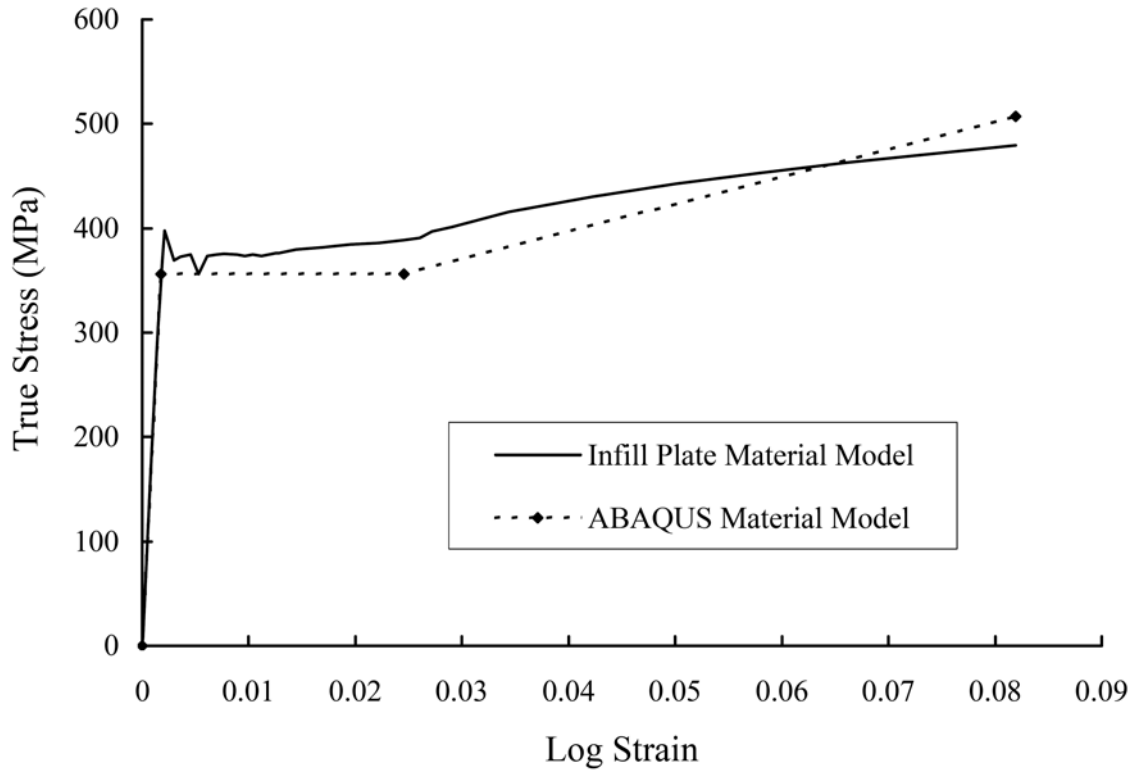


Figure 5.4 Material Model

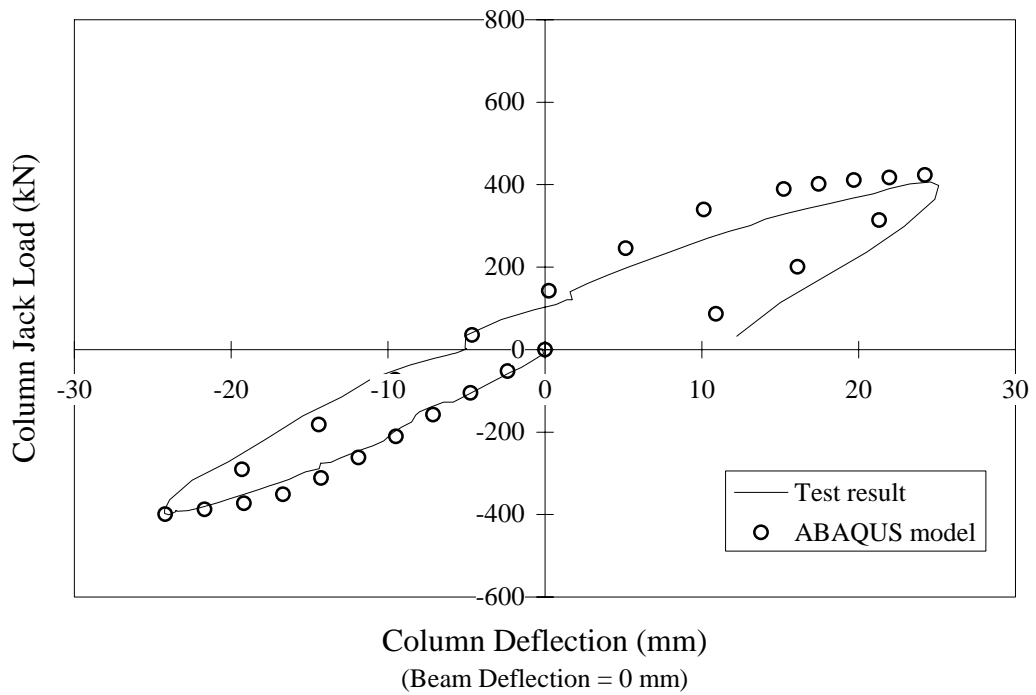
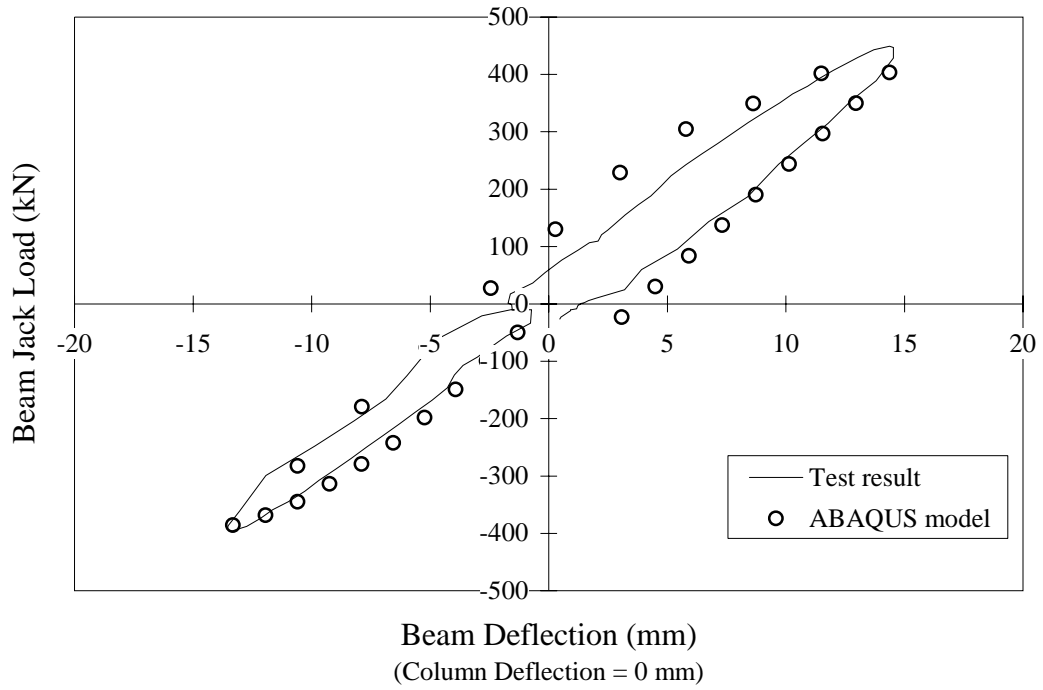


Figure 5.5 V-Frame Stiffness — Experimental Versus Analytical

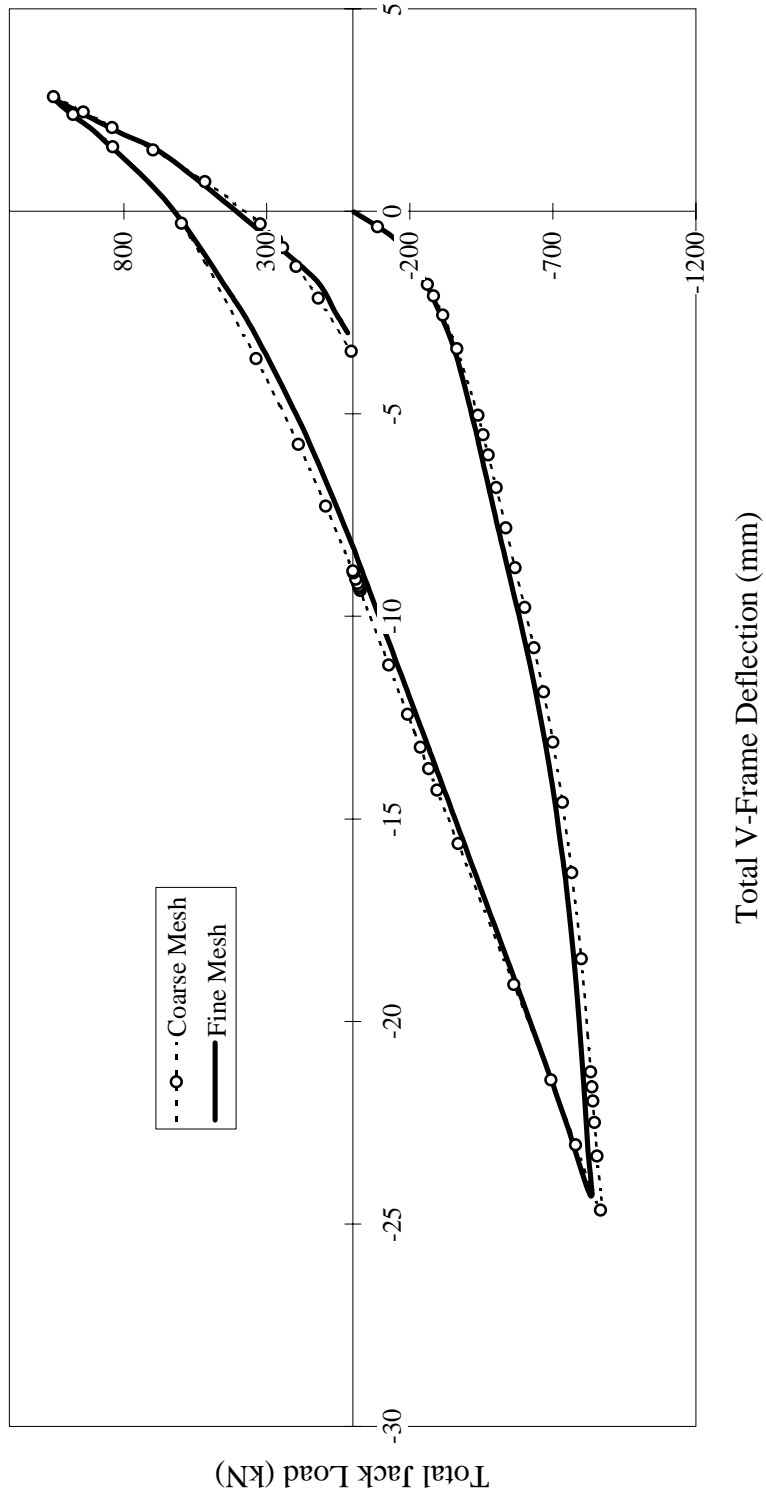


Figure 5.6 Finite Element Analysis Results for Coarse and Fine Meshes

6. Discussion

6.1 Experimental Results of Infill Plate Connection Specimens

6.1.1 Buckling of Specimens

Buckling of the infill plate was noted in the specimens by the time of the second loading block, at a total inward V-frame displacement of 5 mm. In all specimens, the post-buckling deformations of the plate during the higher loading blocks produced some yielding of the infill plate portion of the specimen. The buckling configuration and the post-buckling deformations were similar in all four specimens tested. Both Specimens 2 and 4 showed a localized buckle (seen in Figure 4.2) in proximity to the intersection of the orthogonal fish plates. It is likely that this buckle is a result of the stiff boundary provided by the fish plates. The transition from a 5 mm infill plate to a 6 mm fish plate, which included an area of plate overlap that resulted in a total plate thickness of 11 mm, affected the formation of a buckle in that area. Specimens 1 and 3, which did not have two orthogonally oriented fish plates, did not display the localized buckle.

Observations from this experimental program suggest that a specimen with a corner detail using two fish plates is susceptible to the formation of buckles in the beam-to-column joint area. However, the buckle configuration observed in a shear panel is dependent on the boundary conditions of the infill plate. The infill plate connection specimens were welded along two edges and were free along the two other edges, whereas in a steel plate shear wall the infill panel is attached on all four sides. Therefore, the buckle configurations observed in the infill plate connection tests are not necessarily representative of behaviour in an actual steel plate shear wall. This conclusion is supported by observations made during the four-storey unstiffened steel plate shear wall test performed by Driver *et al.* [1997]. Driver used fish plates along all four edges of each shear panel (Figure 3.1). In the bottom panel of Driver's shear wall, a series of large buckles and smaller localized buckles had formed throughout the plate by the end of the test. In contrast, only one major buckle in the direction orthogonal to the tension field and a localized buckle (in Specimens 2 and 4) were observed in the infill plate connection tests reported herein.

6.1.2 Load Versus Displacement Response

The load versus displacement response of the test specimens was used to monitor and compare the overall behaviour of the specimens during testing. The data collected during loading and unloading of the test specimens were described in Section 4.3.2.2 and presented in Figures 4.3 to 4.6. In all cases, increased hysteresis was observed in the load versus displacement curves during the higher loading blocks, which reflected a gradual increase in the amount of plastic deformation. This plastic deformation was due, in part, to the large buckles that formed in the infill plate connection specimens during the inward displacement of the beam and the column. The buckles caused plastic deformations in the specimen and prevented the beam and column from returning to their initial displacement at the end of a load cycle. The non-zero displacements at zero load is characterized by the leftward migration of the hysteresis loops seen in Figures 4.3 to 4.6.

The entire series of hysteresis loops for Test 4, shown in Figure 4.6, is shifted away from the point of zero load. This was caused by the cumulative inward displacement of the V-frame members that occurred as the four specimens were tested. In fact, by the time of Test 4, jack loads were required to open the beam-to-column joint in order to allow for placement of the new specimen in the V-frame. This resulted in an initial non-zero jack load reading at the start of the test and a leftward shift of all the load versus displacements curves.

In order to facilitate the comparison of Specimens 1 to 4, the envelope of each hysteresis curve is plotted in Figure 6.1. Loading envelopes were obtained by plotting the maximum total jack load versus the maximum total deflection recorded during the last cycle in each loading block. (Because load cells were attached to the jacks only after the completion of loading block 3 in Test 1, the initial portion of the loading envelope for Specimen 1 was obtained by converting manually-recorded jack pressures at maximum displacements.)

The non-linear response of the test specimens observed at higher load levels is a result of two effects, namely, yielding of the test frame and buckling of the infill plate. Although it was clear that there was yielding in the infill plate, the lower loads and flatter envelope observed for Specimen 1 (Figure 6.1) can be attributed mostly to the weld tear propagation at the beam-to-column joint (Section 4.1). Notwithstanding the shift in its

load versus displacement curve (explained above), it can be seen that the response for Specimen 4 (Figure 6.1) is very similar to the response of Specimens 1 to 3. This is because the load versus displacement envelope for Specimen 4 runs parallel to the other three curves, with the exception of the behaviour of Specimen 1 at the higher negative jack loads.

A comparison between the test specimens was also made within a particular loading block. Table 4.2 presents the maximum load and deflection values for the first and last cycles in loading blocks 2, 5, and 8 for Specimen 2. Similar tables for Specimens 1, 3, and 4 are shown in Appendix D. The data given in the tables shows that there was stable behaviour within a load block, since the data show no significant changes in the required jack load for a specified deflection within each block. It can be concluded that specimen deterioration occurred because of the increase in load between successive loading blocks, and not because of repeated loading within the same loading block.

In summary, the load versus displacement behaviour of the infill connection specimens shows a similar response for all four details. The loading envelopes that are plotted in Figure 6.1 show gradual and stable deterioration of the load versus displacement response for the specimens at higher compressive jack loads.

6.1.3 Tearing of Specimens

Tearing occurred in Specimens 2, 3, and 4, and it was concentrated within an area approximately 200 mm-by-200 mm around the corner detail region of the infill plate specimen. Testing of Specimen 1 produced only a small amount of yielding in the infill plate. The load versus displacement plot given in Figure 6.1 shows that Specimen 1 was subjected to the same magnitude of displacement as the other three specimens. However, at the completion of testing there was no tearing observed in Specimen 1, whereas in Specimens 2 to 4 there were tears in the welds or in the heat-affected zones around the welds.

The absence of tears in Specimen 1 can be attributed to the connection detail used in the first test—the infill plate was welded directly to the boundary members. Connecting the infill plate directly to the boundary members excludes the use of fish

plates and, thereby reduces the amount of welding required for the shear panel. Furthermore, the incorporation of fish plates in the shear panel (Specimens 2 to 4) requires a weld between the fish plate and the infill plate that is located further into the steel panel. This results in the presence of a weld and a related heat-affected zone with reduced ductility in an area of increased bending strains as compared with the bending strains found at the infill panel-to-boundary member welds. In other words, out-of-plane bending of the plate acting upon these less ductile zones (and acting in conjunction with the in-plane stresses), is more likely to create tears in this arrangement than in a directly-connected infill plate.

It is likely that the initiation of plate tearing occurred in the closing portion of a loading cycle, Part A. The buckles that form in the infill specimens during closing of the joint can be expected to produce large bending strains in the corner area of the infill plate. Once a tear had formed in a specimen, propagation of the tear was aided by the cyclic action of loading, that is, by the action of low cycle fatigue. During the opening portion of a loading cycle, Part B, the boundary members were displaced outwards. This caused the buckles that had formed in Part A to straighten, thereby producing a reversed straining effect concentrated at the corner of the infill plate.

The formation of the first tear in the specimens was detected as early as the first cycle in the third loading block for Specimen 2 and as late as the second cycle of the seventh loading block for Specimen 4. However, considering that tears were detected by visual inspection of the specimens during testing, it is likely that many of the tears were not observed until they had grown to a substantial length.

The tears in Specimens 2, 3, and 4 initiated either in the weld or in the base material adjacent to the weld. For example, all of the tearing observed in Specimen 3 was a result of Tear 1 (Figure 4.12), which was located in the weld material at the intersection of the fish plate-to-infill plate weld. From the tearing observed in Specimens 2 and 4, it is evident that a corner detail with discontinuous boundaries is particularly susceptible to tearing. The 6 mm gap between the fish plates in Specimen 2 and the corner cut-out, or chamfer, in Specimen 4 (seen in Figures 4.10 and 4.14, respectively) create stress raisers as a result of an interruption in the specimen-to-boundary member weld. Both of these specimens developed tears in the fish plates that propagated from these areas.

Upon close examination of the tearing observed in Specimen 4 (Figure 4.14), it was noted that more tearing had occurred in the fish plate attached to the column (Tears 2, 3, 5 and 6) than in the fish plate attached to the beam (Tears 1 and 4). It is believed that the geometric asymmetry in that detail (refer to Figure 3.7) may have contributed to unequal load transfer from the infill plate to the fish plates. In addition, the groove weld joining the two fish plates in Specimen 4 produced a large heat-affected zone in the parent material, thereby making it more susceptible to tearing.

6.1.4 Summary of Specimen Behaviour and Response

The examination of the buckling and hysteresis behaviour outlined above revealed no major differences in the response of the four specimens. The most significant sign of specimen deterioration was the formation of tears. When summarizing the tearing observed for each specimen it is necessary to reiterate the considerations that led to the selection of the four corner details. Section 3.1 described a steel plate shear wall panel that uses fish plates along two adjacent panel sides (Figure 3.2). With this infill plate connection scheme there is a possibility of no fewer than three different corner details. These three infill connection details were selected for the present experimental program (Specimens 1 to 3), in addition to a fourth detail (Specimen 4), which was an alternative to Specimen 2.

Considering a shear panel that has fish plates at two of its boundaries, it can be seen that Specimens 1 to 3 form a group of related corner details. Since one or more of the details will be found in a shear wall panel, such as the one shown in Figure 3.2, it is appropriate to compare these details. This can be done on the basis of their strength and integrity. In the case of the detail used for Specimen 4, the most logical comparison is against Specimen 2, because the former was developed as an alternative to the latter. At the completion of testing, there were more tears in Specimen 4 as compared with Specimen 2 (Figure 4.10 and 4.14). However, the tears in Specimen 4 were not observed until loading block 7, whereas tears in Specimen 2 were observed as early as loading block 3. Thus, in terms of physical damage, there is not enough evidence to be able to distinguish between these two details. Most important, the load versus deformation

behaviour of both Specimen 2 and 4 was not significantly different from that of the other two specimens.

When discussing the results of all of the tests, it is important to appreciate the magnitude of the deterioration that was observed relative to the size of the entire specimen. Figure 6.2 shows Specimen 2 and Specimen 4 removed from the test frame after completion of testing. In this figure, it is evident that the tears described above are very small relative to the size of the entire 1250 mm square specimen. Although tearing was observed, there is no evidence that the formation of tears resulted in a loss of load-carrying capacity during testing.

In comparison to the large-scale four-storey steel plate shear wall tested by Driver *et al.* [1997], the infill plate corner connections were not subjected to the same severe level of loading. In fact, the deformations that were seen in the Driver test were more demanding than the deformations that would be expected during most earthquake events. Even at high loads the entire steel plate shear wall system, which of course included Driver's infill plate connection detail (similar to Specimen 2 in this study), exhibited stable behaviour and a high degree of ductility.

The most significant limitation of the infill plate connection tests was the tensile load limit reached due to the strength of the tension connection—the maximum tensile load of 800 kN was not sufficient to yield the infill connection specimens. In contrast, one of the most prominent characteristics seen in the bottom panel of the Driver shear wall was yielding due to the tension field action in the thin steel plate. At lower load levels, however, the behaviour of the infill panel connections in the large-scale Driver test was similar to the behaviour of the infill connection details presented herein. By extrapolating this observation, it can be judged that any of the four details, Specimens 1 to 4, will perform adequately under conditions of severe loads and deformations.

6.2 Comparison with the Results of Earlier Studies

In Chapter 2, a presentation of previous work using welded infill plate connections highlighted three experimental programs carried out at the University of Alberta. In the first two test programs [Timler and Kulak 1983, and Tromposch and Kulak 1987], double-panel, unstiffened steel plate shear wall specimens with pin-

connected and bearing-type boundary member connections were subjected to reversed loading. The welded fish plate details used for the infill panel-to-boundary member connections in both tests were similar to that used in Specimen 2 of the current program. A third test, performed by Driver *et al.* [1997], specifically investigated the adequacy of a selected infill plate corner connection.

Results from the three tests outlined above showed generally good behaviour of the infill connection details. Testing of the Timler and Kulak [1983] specimen resulted in a weld tear in an infill plate-to-fish plate connection (shown in Figure 2.4). A tear at this location was not observed in Specimen 2. It is likely that the tear in the Timler specimen was initiated at the gap between the orthogonal fish plates, which had been filled with a groove weld. The 6 mm gap in Specimen 2 was not filled with a weld, and, consequently, there was no tearing observed in that area of the corner detail.

The Tromposch and Kulak [1987] and Driver *et al.* [1997] infill corner connections differed slightly from the Timler detail. In these tests, a strap plate was welded between the fish plates in order to provide some continuity. Results from both these tests showed that most of the tears seen in the infill plate were again along welds connecting the infill plate to the fish plate. There also were tears along welds connecting the strap plate to the fish plates. In comparison with the results from Specimen 2, the details using a welded strap plate are more susceptible to tearing. The improvement in detail behaviour seen in Specimen 2 can be attributed to the reduced amount of welding used for the infill plate corner connection.

6.3 Finite Element Analysis

The finite element model developed in order to predict the behaviour of Specimen 2 was described in Chapter 5. Two infill plate mesh—a coarse mesh and a fine mesh—were analyzed at a magnitude of loading equivalent to the loading applied to Specimen 2. Results of the analysis, shown in Figure 5.6, showed very similar load versus displacement behaviour between the coarse and the fine meshes. This indicates convergence of the finite element analysis towards an exact solution. In the following sections, a comparison is made between the results of the finite element analysis and the experimental observations made of Specimen 2. Although the adequacy of the coarse

mesh to model the corner detail was proven by the convergence of the finite element model, the comparison between measured and calculated strains uses results from the fine mesh analysis.

6.3.1 Load Versus Displacement Comparison

One of the goals of the finite element analysis was to obtain a load versus displacement response that is comparable to the hysteretic behaviour recorded for Specimen 2. The data plotted in Figure 6.3 shows the finite element results superimposed on the hysteresis curves obtained for Specimen 2. There is good agreement between the analytical and the experimental load versus displacement response.

Unloading of the finite element model from a maximum negative jack load followed a path very close to the unloading portion of the outermost hysteresis loop for Specimen 2. At zero load, the residual deformation predicted by the model is only slightly less than that observed in the test specimen. During the last two loading steps, shown as the positive load portion of the curves in Figure 6.3, the finite element model predicted a slightly stiffer response than the one observed in the test.

Good agreement between the numerical model and the experimental data is also observed in a comparison between the observed and predicted deformed shape of the specimen at maximum inward V-frame displacement (see Figure 6.4).

6.3.2 Strains in the Infill Plate

6.3.2.1 Comparison with Strain Gauge Data

Another method of verifying the finite element model is to compare the strains measured during actual testing and the strains obtained from the analysis. Measured strains from Specimen 2 were shown in Figure 4.17. The strains obtained from the finite element model were calculated by averaging strains at integration points located on the two surfaces of a particular element. The analytical strain results were restricted to a single strain reading per element, at the centroid of that element. Therefore, it was necessary to interpolate linearly between two or more adjacent elements in order to obtain strain data for specific points that corresponded to strain rosette locations on

Specimen 2. A source of error was introduced because of this need for data manipulation, since it is unlikely that the calculated strains varied linearly between the elements.

In Figs. 6.5 and 6.6, a comparison is made between analytical and recorded strains for Specimen 2. The comparison is for cycle 6, loading block 5 and is taken at maximum loads during the opening and closing portions. The data from the numerical analysis are taken at total V-frame displacements that are comparable to the displacement recorded during block 5-6 of the actual test. The normal and shear strain plots given in Figures 6.5 and 6.6 do not show a good correlation between the recorded and the predicted strains.

The strains at two points in close proximity can vary substantially in an area with a high strain gradient, thus resulting in a significant difference between the measured and calculated strains. This is seen Figures 6.5 and 6.6 where the strain gradient—represented by the slope of the curves—accounts for the major difference seen between the experimental and analytical strain data. For example, yielding of the material will give rise to large increases in strains. When comparing measured strains with predicted strains within a location that has yielded, it is possible to get a large discrepancy because of the high strain gradient. At strain rosette locations 1 and 5, the curves in Figures 6.5 and 6.6 indicate lower strain gradients, and this is reflected in better correlation between the actual and the predicted strains.

In modelling the V-frame, the beam stiffness and the column stiffness in the finite element model were selected to match the response measured in the actual V-frame (Section 5.2.4). The effect of possible beam-column joint rotation in the V-frame was not specifically included in the numerical model, since it was not measured during testing. This resulted in unequal displacements of the V-frame members in the analytical model, unlike the beam and column displacements of the actual specimen. As described earlier, equal displacements were maintained during testing. The difference between the analytical model displacements and the test specimen displacements did not noticeably affect the load versus displacement comparison. However, the discrepancy between the calculated and measured member displacements may have contributed to the lack of correlation between the observed and calculated strain distributions.

6.3.2.2 Correlation of Strains with Specimen Tearing

It is clear that the formation of tears in the infill plate connection specimens was the most manifest indicator of specimen response to the imposed quasi-static cyclic loading. Thus, it is desirable to obtain a finite element model that can predict the regions of a given infill corner detail that are most susceptible to tearing. Accordingly, the predicted strain distribution in the finite element model of Specimen 2 was examined in order to evaluate the correlation between the analytical results and the tearing observed in the actual test.

The initiation and propagation of tearing in a thin plate subjected to cyclic loading will take place in areas of the plate that undergo repeated strain reversals. Examination of the magnitude and direction of principal maximum strains in the corner region of the finite element model should make it possible to determine the locations where tearing is most likely to occur. Figures 6.7 and 6.9 show contour plots of major principal strain on a 300-by-400 mm close-up on the side of the infill plate where the tears were observed on Specimen 2. Vector plots of the major principal strains in the same regions are given in Figures 6.8 and 6.10. Data that is presented in both the contour and vector plots gives the surface strains, as opposed to an average strain through the thickness of the plate.

Figures 6.7 and 6.8 show contour and vector plots, respectively, at a maximum total inward V-frame displacement of 23.8 mm. The darker regions shown in Figure 6.7 indicate areas of large principal strains. The area around the mid-length of the 6 mm gap between the two orthogonal fish plates shows a concentration of tensile strains. Although there were no tears observed at this location in the actual specimen, it is plausible that this area could become critical at higher loads or during further cyclic loading. The concentration of strains shown in the contour plot was caused by the infill plate-to-fish plate connection made at this location. As was the case in the physical specimen, there was no direct connection between the two fish plates in the finite element model.

The vectors plotted in Figure 6.8 show the directions of the strains that were presented in the contour plot (Figure 6.7). The length of the vectors depicts the relative magnitude of the strain. Two vectors at the same location are seen where the fish plates are lapped by the infill plate.

The strain vectors in Figure 6.8 show a tension field oriented at 45 degrees from the horizontal. This is a result of the tensile force applied to the free corner of the infill plate model (Section 5.2.4). A band of tensile strains oriented approximately perpendicular to the tension field strains (Figure 6.8) is indicative of a buckle in this direction, that is, orthogonal to the tension field.

In Specimen 2, tearing took place at either end of the 6 mm gap. The same regions on the finite element model vector plot (Figure 6.8) show strains that are oriented approximately perpendicular to the direction of tearing seen in Specimen 2. This is the direction of straining that would cause tearing to occur. When comparing the observed tears to the finite element model described herein, consideration must be given to the fact that the model did not take into account the welds *per se* and the heat-affected zones found adjacent to welds. These are important factors that are likely to affect the location and orientation of tearing.

The maximum principal strain contour plot seen in Figure 6.9 shows the corner of the infill plate connection specimen model at a total maximum outward V-frame displacement of 3.1 mm. A strain concentration similar to the one in Figure 6.7 is seen at the mid-length of the 6 mm gap. Again, these strains are due to the infill plate-to-fish plate connection in this area. A corresponding vector plot of the maximum principal strains is given in Figure 6.10. The strain vectors at each end of the gap are oriented in a direction approximately perpendicular to the tears observed in Specimen 2.

It is interesting to note that the vector pattern on the infill plate in Figure 6.10 shows an arched band of compressive principal strains intersecting an area of tensile principal strains. This strain pattern is due to a localized buckle similar to those seen in Specimens 2 and 4 (Figure 4.2). Compressive strains at this location also provide an explanation for the shape of the normal strain distribution plotted in Figure 6.6 for the results of the numerical analysis. The minimum principal strains corresponding to the maximum principal compressive strains in Figure 6.10 occur at about 45 degrees from the horizontal fish plate. This is the direction in which normal strains were measured at the location of Strain Rosette 3 for both the test specimen and the finite element model. Therefore, the compressive strains seen in Figure 6.10 provide an explanation for the negative strain value plotted at location zero along the Axis X-Y for the “ABAQUS”

curve in Figure 6.6. Additionally, the strain gradients depicted in Figures 6.7 to 6.10 illustrate the problem that may arise when comparing measured with calculated strains if the location of the strain gauges is not exactly known or if the strain is averaged over a finite surface of the test specimen (as is the case with strain rosettes).

Overall, the results of the numerical analysis shown in Figures 6.7 to 6.10 show reasonable correlation between the predicted strains and the locations of tearing observed in Specimen 2. It is judged that the finite element method can be used as a reliable tool to determine the adequacy of an infill plate connection detail.

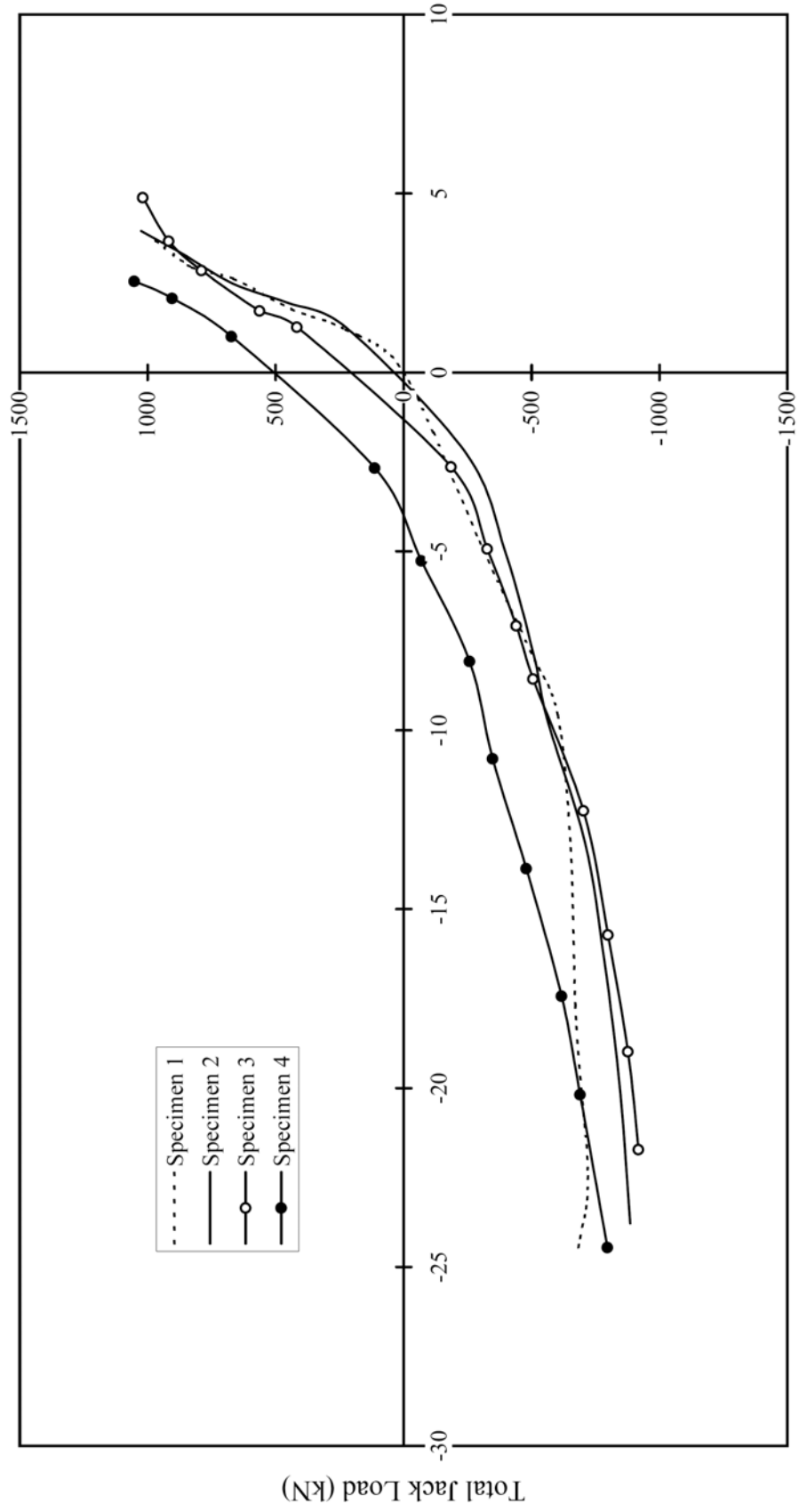
Table 6.1 Comparison of Loading Blocks for Specimen 2

Part A

Loading Block:	2		5		8	
	1	3	1	6	1	6
Total Inward V-Frame Deflection (mm)	-5.4	-5.0	-13.3	-12.8	-23.5	-23.6
Total Jack Load (kN)	-415	-391	-667	-685	-896	-842

Part B

Loading Block:	2		5		8	
	1	3	1	6	1	6
Total Outward V-Frame Deflection (mm)	1.8	2.0	3.6	4.2	3.6	3.4
Total Jack Load (kN)	431	451	950	978	1093	1089



Total Member Deflection (mm)

Figure 6.1 Load Versus Displacement Envelopes

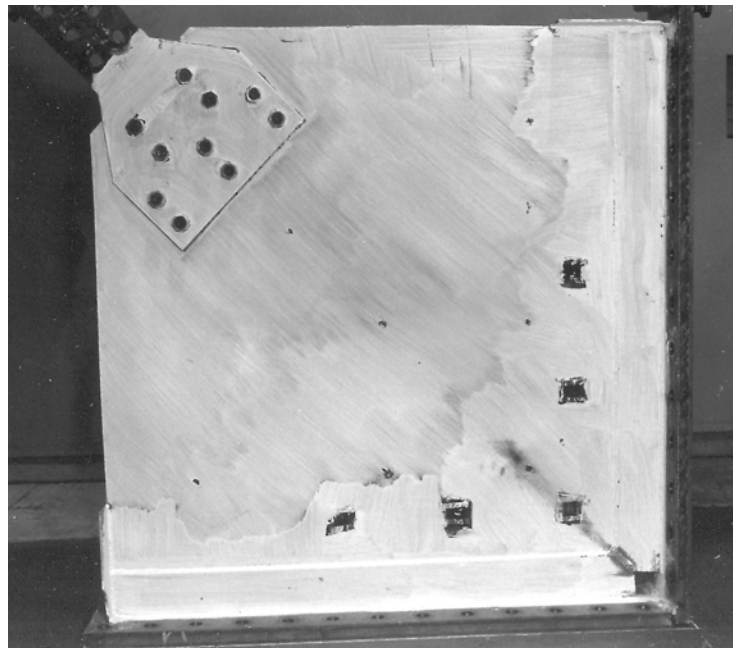
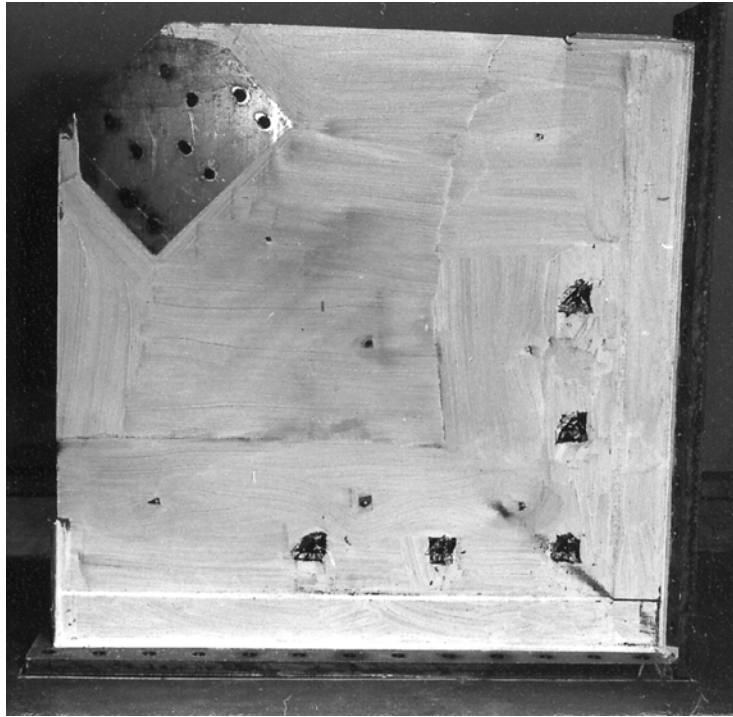


Figure 6.2 Specimen 2 and Specimen 4 at End of Testing

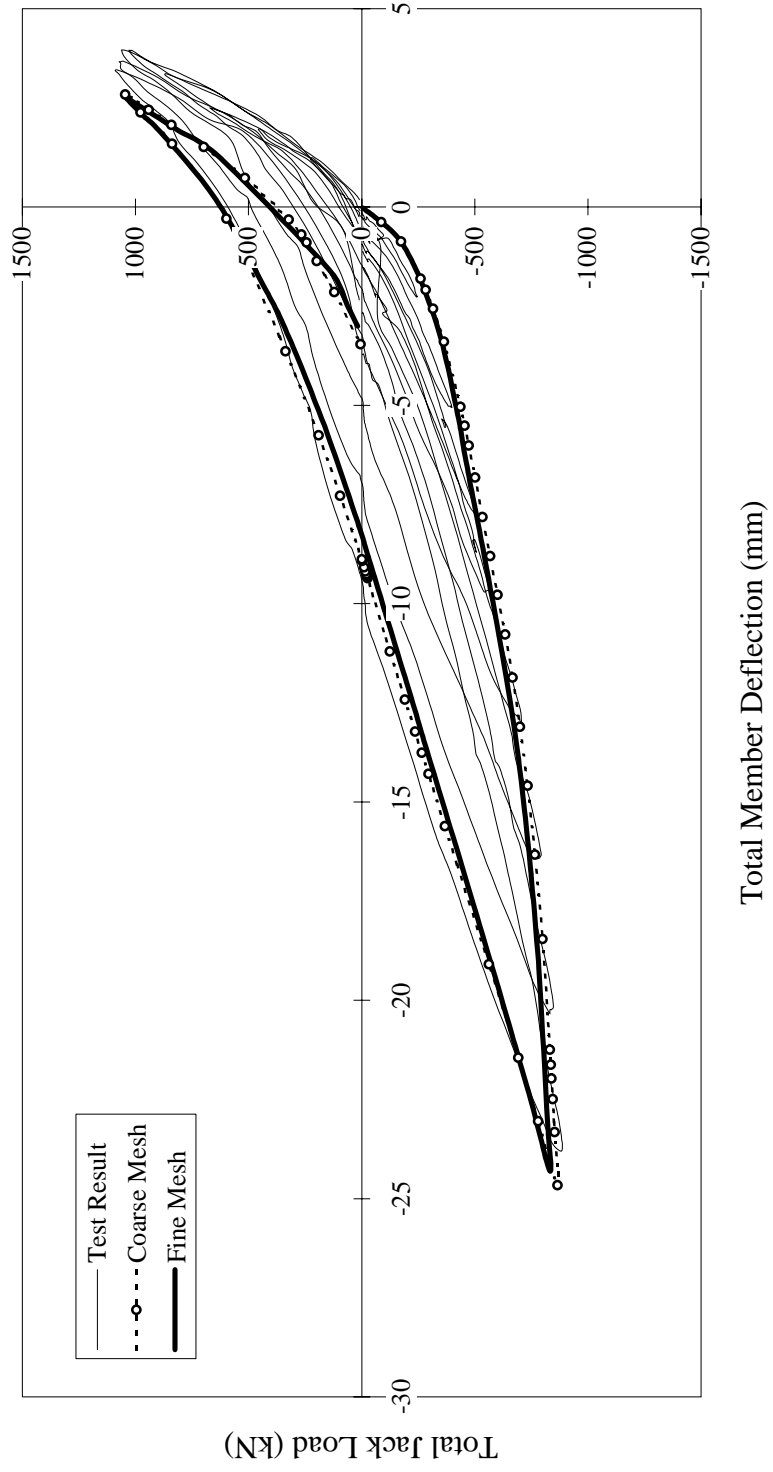


Figure 6.3 Specimen 2 Response Compared to Analysis Results

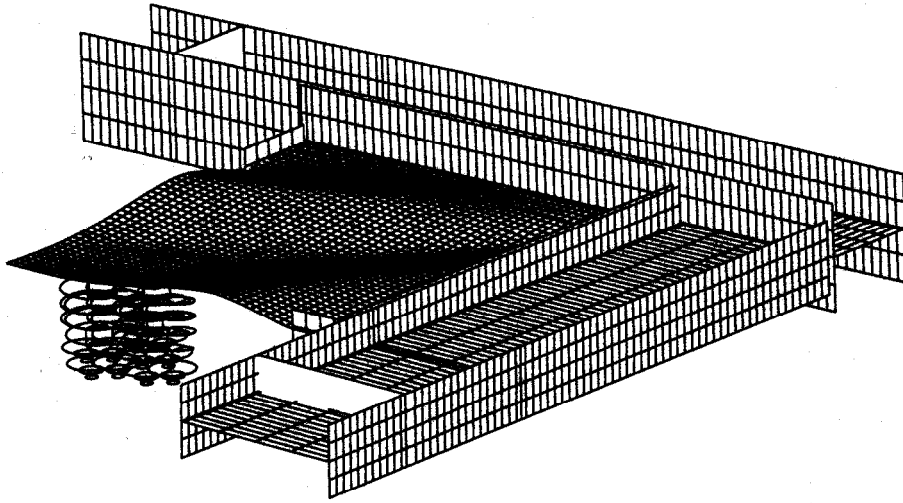
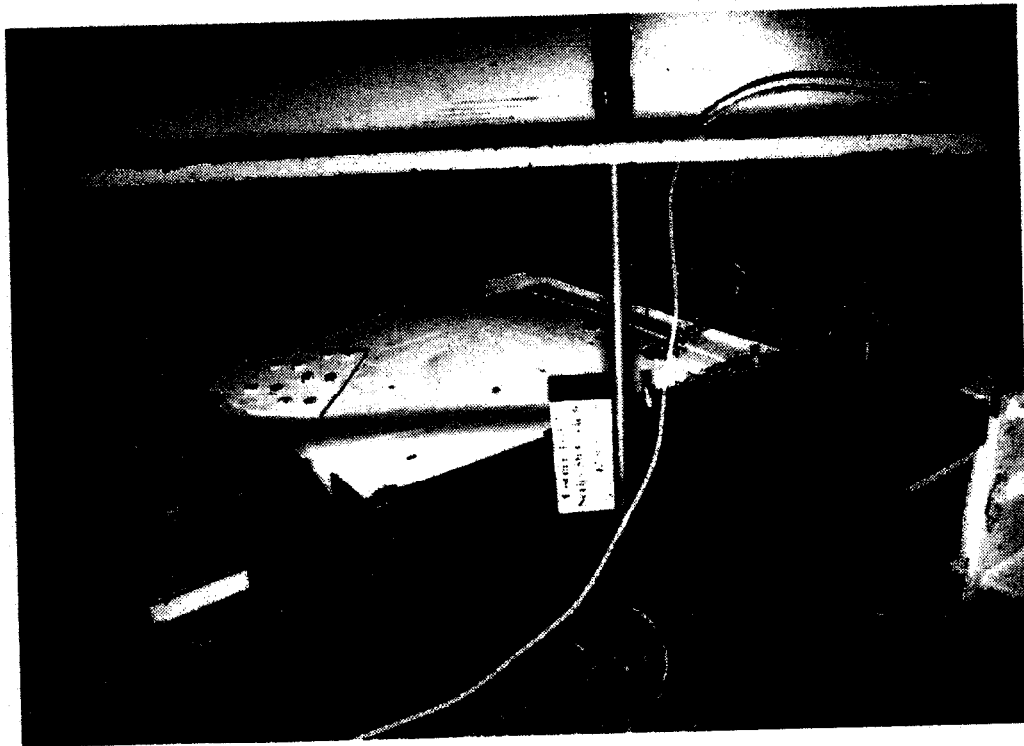


Figure 6.4 Test Specimen 2 – Comparison of the Observed Deformed Shape with the Predicted Deformed Shape

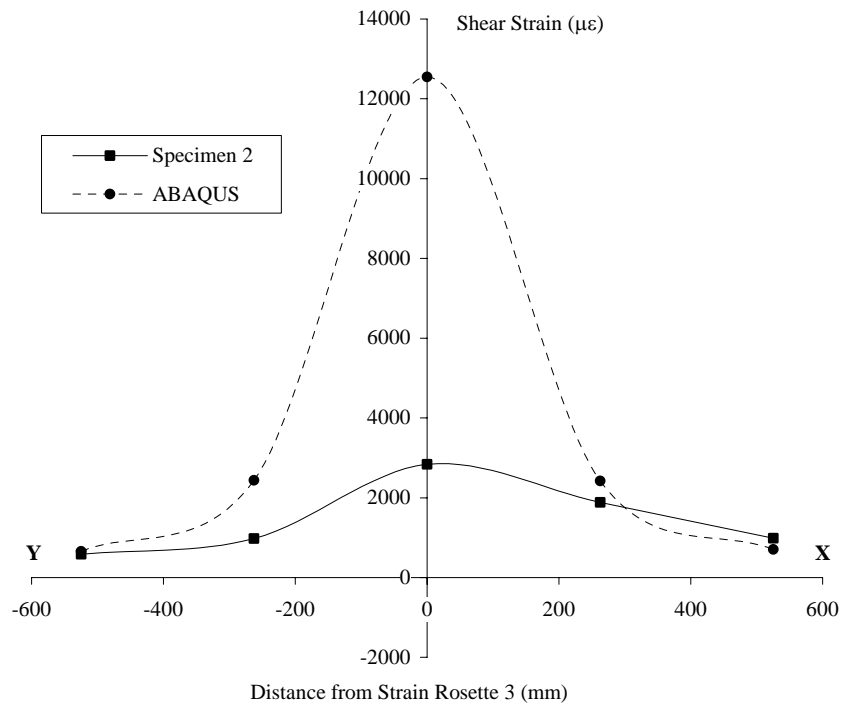
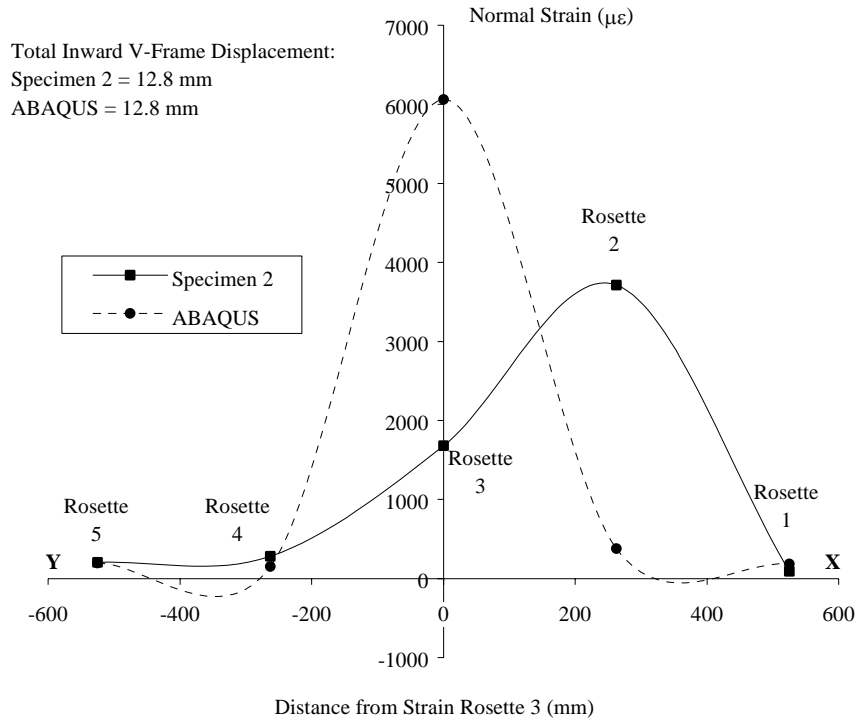


Figure 6.5 Strain Comparison at Inward V-Frame Displacement

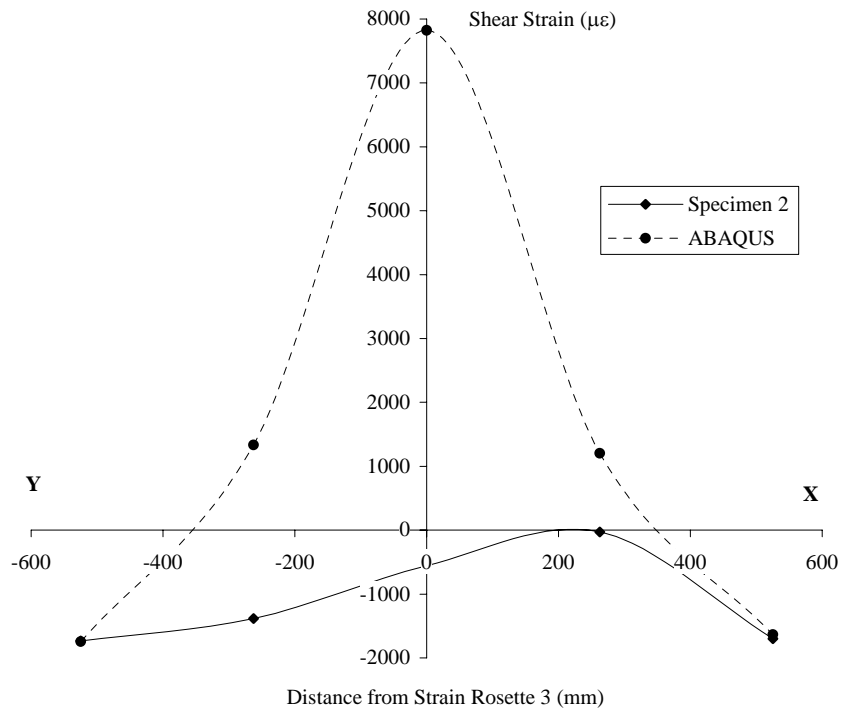
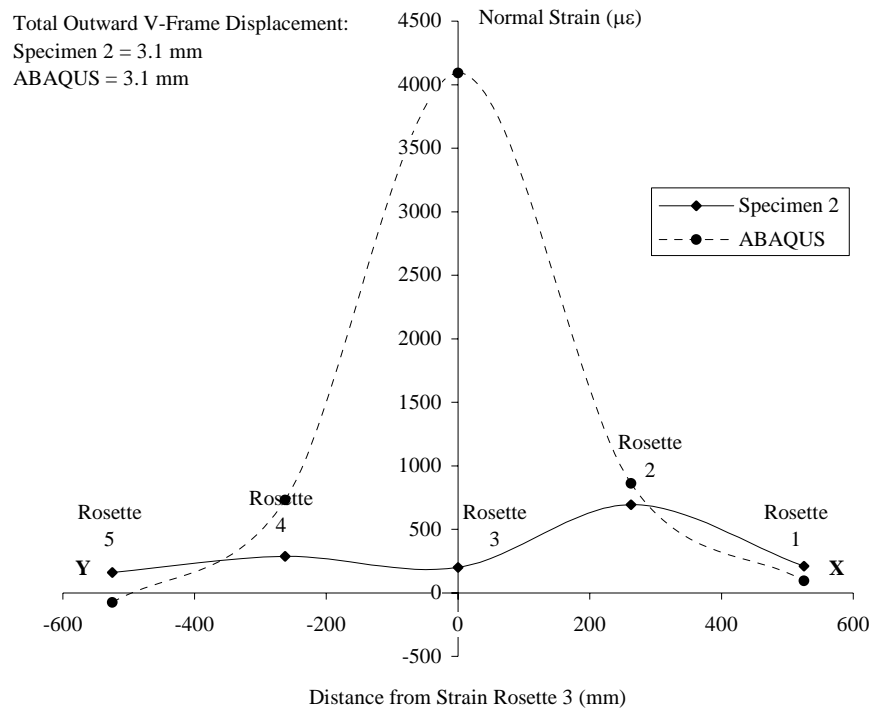


Figure 6.6 Strain Comparison at Outward V-Frame Displacement

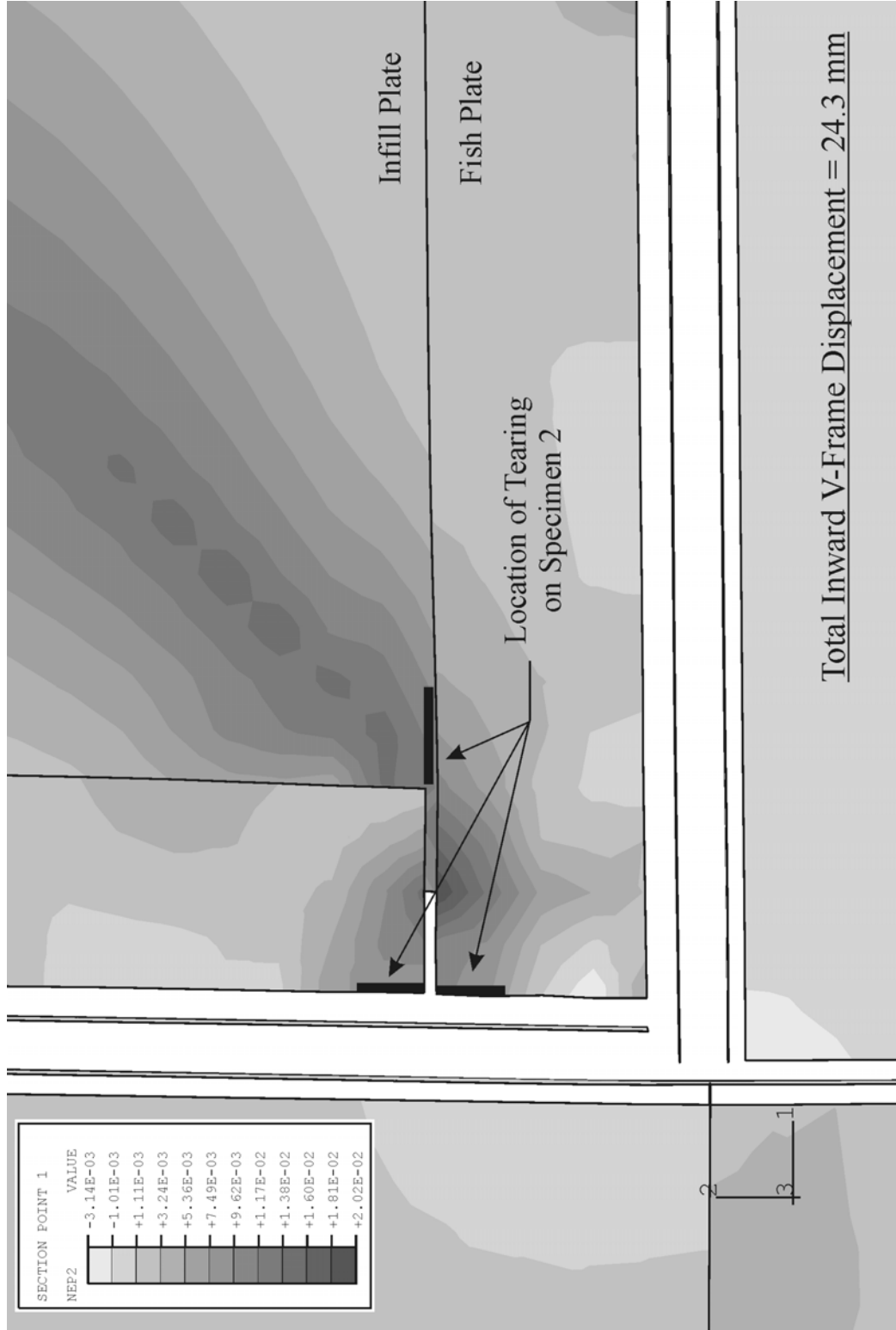


Figure 6.7 Major Principal Strain Vector Plot at Maximum Inward V-Frame Displacement

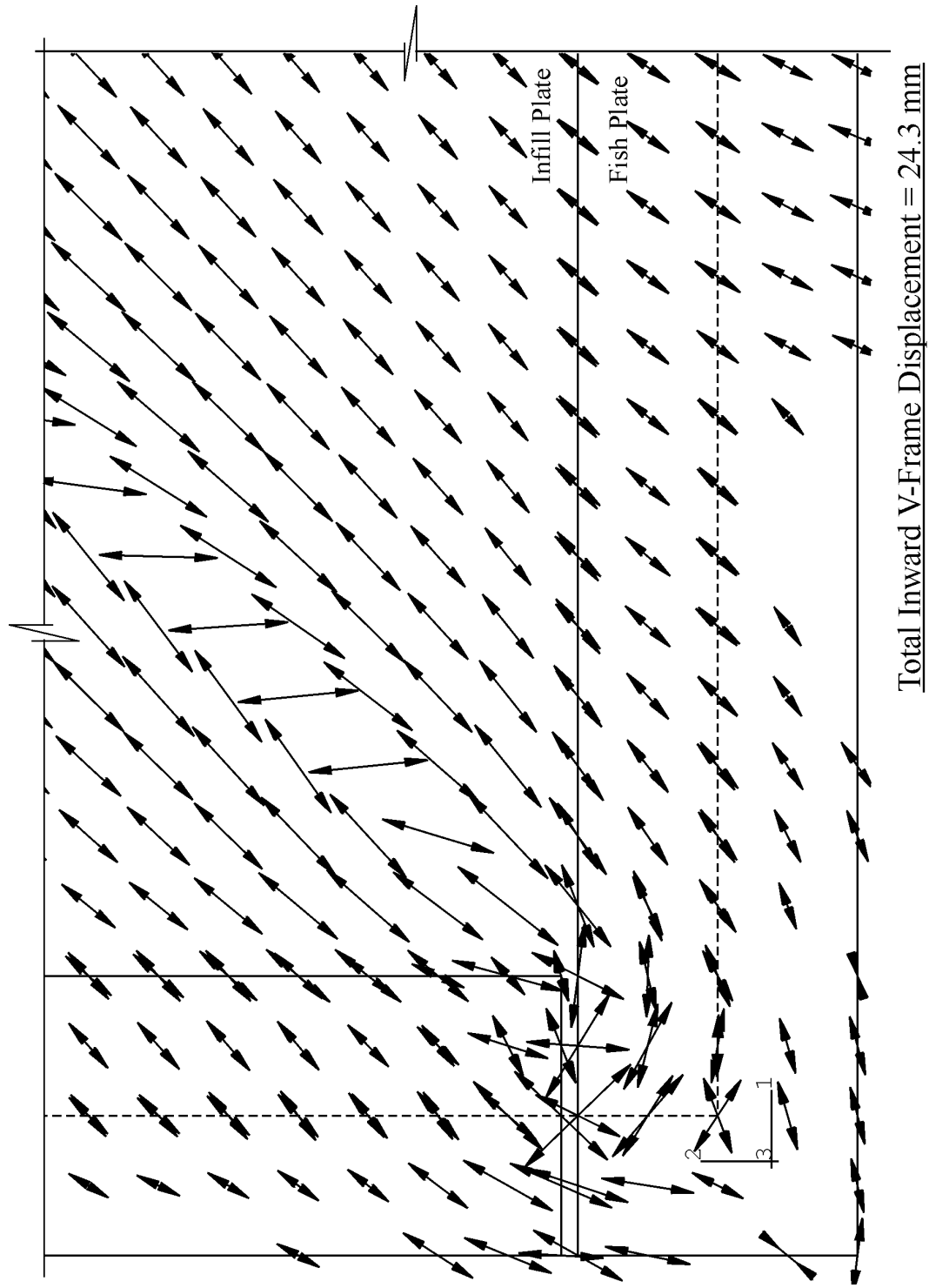


Figure 6.8 Major Principal Strain Vector Plot at Maximum Inward V-Frame Displacement

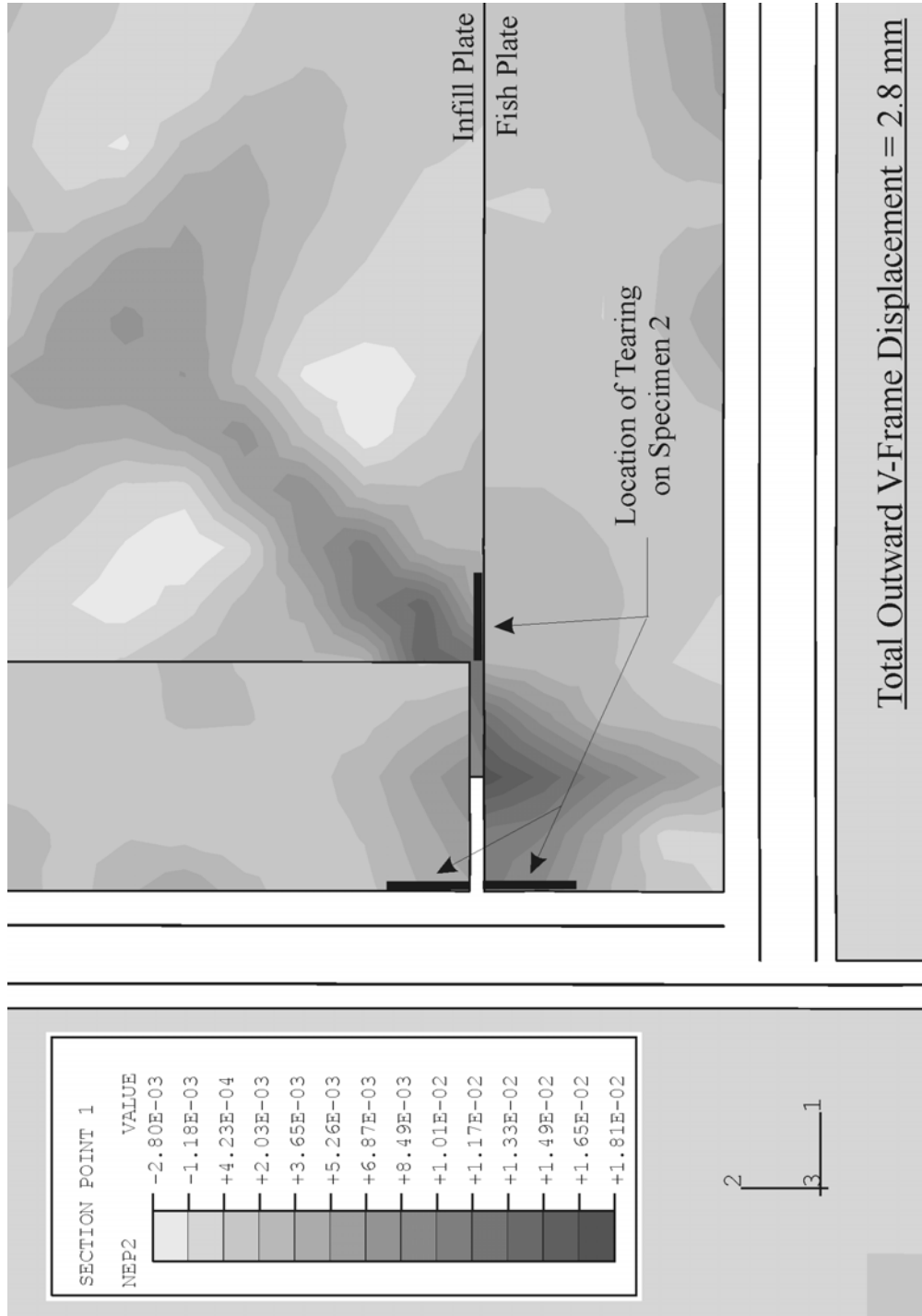


Figure 6.9 Major Principal Strain Distribution at Maximum Outward V-Frame Displacement

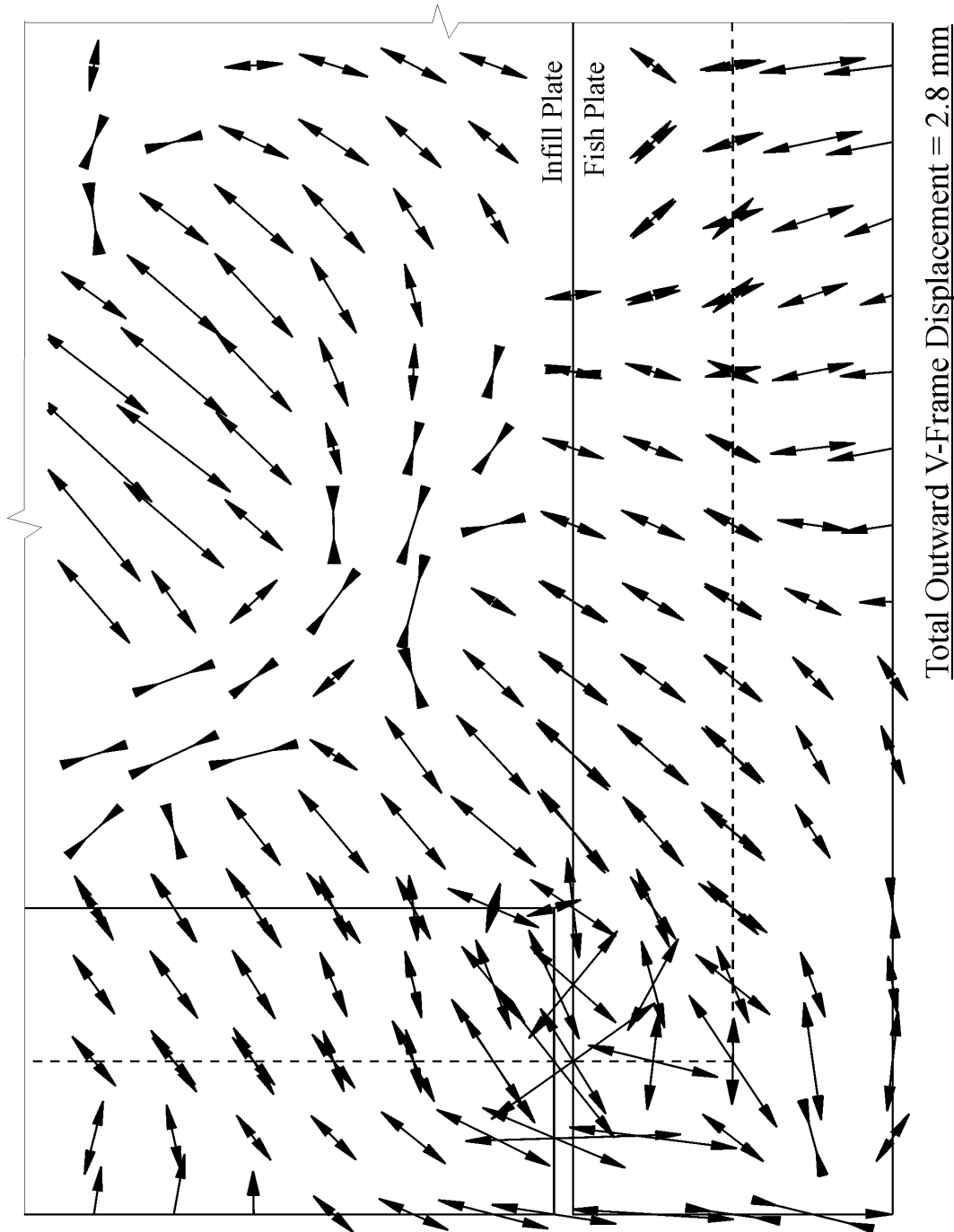


Figure 6.10 Major Principal Strain Vector Plot at Maximum Outward V-Frame Displacement

7. Summary, Conclusions and Recommendations

7.1 Summary and Conclusions

Testing has shown that unstiffened steel plate shear walls are an extremely ductile and stable lateral force-resisting system [Driver *et al.* 1997]. The ability of a steel plate shear wall to resist effectively lateral loads on a structure—such as wind loading and earthquake loading—depends in part on the transfer of forces from the infill panel to the stiff boundary members. The infill plate-to-boundary member connection is especially critical where the infill plate connects into the beam-to-column joint. This is an area of stress concentrations and large reversing strains.

This study was undertaken to investigate the behaviour of welded infill plate connection details. Each detail consisted of an infill panel welded to boundary members—a beam and a column connected at right angles. Four corner specimens were selected for the experimental program: 1) an infill plate welded directly to the boundary members; 2) fish plates welded to each of the boundary members and the infill plate then lapped over the fish plates and welded; 3) a fish plate welded to only one boundary member, the infill plate welded directly to the other boundary member, and lapped and welded onto the fish plate ; 4) two fish plates with a 60 mm square corner cut-out welded to boundary members and the infill plate lapped asymmetrically over the fish plates and welded.

In the physical tests, the specimens were subjected to the two major effects relevant to corner details in an unstiffened steel plate shear wall. The first is the effect of the repeated opening and closing action of the beam-to-column joint that results when lateral loads act cyclically on a structure. The second effect is the development of the tension field that forms diagonally in a panel after the thin plate buckles in shear.

Quasi-static cyclic testing of the four infill plate connection details produced data that were used for the evaluation and comparison of the specimens. The load versus displacement response of the specimens showed similar behaviour for all four details. Tears, concentrated in the corner region of the infill panel, were observed during the testing of Specimens 2, 3 and 4.

In addition to the experimental program, a finite element model was developed to

predict the behaviour of one of the infill plate corner connection specimens. The numerical model was verified by comparing the predicted load versus displacement response against the response observed during testing. Calculated strains from the model were also correlated to tearing observed in the test specimen.

The following conclusions can be drawn from the results of the work described above:

1. Each of the four infill plate corner connection details responded in a totally satisfactory way to the quasi-static cyclic loading;
2. The load versus displacement response of the details showed gradual and stable deterioration at higher loads;
3. The formation of tears in the connection details did not result in a loss of load-carrying capacity;
4. The infill plate connection detail welded directly to the boundary members was less susceptible to tearing than were the details that used fish plates. On its own, the former detail does not represent a practical connection scheme, however, since it would require precise fitting of the infill plate into the rectangle formed by the beams and the columns in a given bay and storey;
5. The connection detail incorporating a 60 mm square corner cut-out, which was an attempt to reduce an area of high stresses, did not noticeably improve the load versus displacement behaviour of the detail as compared with the detail with two orthogonally oriented fish plates (no corner cut-out);
6. The finite element method can be used to predict reliably the load versus displacement behaviour of infill plate corner connection details;
7. Good correlation exists between tears observed on a tested corner connection detail and the strain distribution obtained from a finite element model of the same detail.

7.2 Recommendations

In order to produce economical designs, designers and fabricators should have

access to different infill plate connections details for the construction of steel plate shear walls. This allows the selection of the most economical scheme for the erectors at any particular time and in any given region of the country. Although the four specimens tested in the experimental program represent a practical solution, other details could still be investigated. The numerical model developed in Chapter 5 proved that there is good potential for using the finite element method as a tool to evaluate the effects of parameters that were not specifically investigated in the test program. For example, the finite element method could be used to explore the effects of the following parameters on the performance of an infill panel-to-boundary member arrangement:

1. The width of the fish plates used in the panel-to-boundary member connection;
2. The size of the infill panel corner cut-out in the beam-to-column joint region;
3. The thickness of the infill plate and the fish plates;
4. The type of connection between the beams and the columns (rigid, semi-rigid, or simple connections).

Additional testing of infill plate connection details would probably be necessary in order to validate some of the results obtained from the study proposed above. Further analytical work is also required in order to predict more precisely the occurrence of tears in an infill panel corner detail. In particular, the location of the tears and the load levels at which these tears will occur is of interest.

List of References

- Anon. 1978. Patent problems, challenge spawn steel seismic walls. *Engineering News Record*, January 26.
- Applied Technology Council 1992. Guidelines for cyclic seismic testing of components of steel structures. Report No. 24, Applied Technology Council, Redwood City, CA.
- ASTM 1992. A370-92, Standard test methods and definitions for mechanical testing of steel products. American Society for Testing and Materials, Philadelphia, PA.
- Caccese, V., Elgaaly, M., and Chen, R. 1993. Experimental study of thin steel-plate shear walls under cyclic load. *Journal of Structural Engineering, ASCE*, 119(2): 573-587.
- Driver, R.G., Kulak, G.L., Kennedy, D.J.L., and Elwi, A.E. 1997. Seismic behaviour of steel plate shear walls. Structural Engineering Report No. 215, Department of Civil Engineering, University of Alberta, Edmonton, AB.
- Hibbit, Karlsson, and Sorenson 1996. ABAQUS. Hibbit, Karlsson, and Sorenson, Inc., Pawtucket, RI.
- Nakashima, M., Iwai, S., Iwata, M., Takeuchi, T., Konomi, S, Akazawa, T., and Saburi, K. 1994. Energy dissipation behaviour of shear panels made of low yield steel. *Earthquake Engineering and Structural Dynamics*, 13: 1299-1313.
- Takahashi, Y., Takeda, T., Takemoto, Y., Takagi, M. 1973. Experimental study on thin steel shear walls and particular bracings under alternative horizontal load. Preliminary Report, IABSE Symposium on Resistance and Ultimate Deformability of Structures Acted on by Well-defined Repeated Loads, Lisbon, Portugal, pp. 185-191.
- Thorburn, L.J., Kulak G.L., and Montgomery, C.J. 1983. Analysis of steel plate shear walls. Structural Engineering Report No. 107, Department of Civil Engineering, University of Alberta, Edmonton, AB.

Timler, P.A. and Kulak, G.L. 1983. Experimental study of steel plate shear walls. Structural Engineering Report No. 114, Department of Civil Engineering, University of Alberta, Edmonton, AB.

Tromposch, E.W. and Kulak, G.L. 1987. Cyclic and static behaviour of thin panel steel plate shear walls. Structural Engineering Report No. 145, Department of Civil Engineering, University of Alberta, Edmonton, AB.

Troy, R.G. and Richard, R.M. 1988. Steel plate shear wall designs. Structural Engineering Review, 1: 35-39.

Appendix A

Results of Tension Coupon Tests

Table A.1 Coupon Test Results

Specimen	Direction*	Modulus of Elasticity (MPa)	Static Yield Strength (MPa)	Static Ultimate Strength (MPa)
Infill Plate 1	1-1a	185 100	352	435
	1-1b	194 400	344	419
	1-1c	196 000	343	418
	1-2a	200 900	345	419
	1-2b	172 400	343	426
	1-2c	188 200	364	447
Mean		189 500	348	427
Std. Dev.		10 096	8	12
Infill Plate 2	1-1a	203 700	353	430
	1-1b	207 300	352	430
	1-1c	198 700	353	431
	1-2a	193 000	325	416
	1-2b	189 800	333	420
	1-2c	196 900	335	423
Mean		198 233	342	425
Std. Dev.		6521	12	6
Fish Plate	1-1a	231 700	399	489
	1-1b	240 100	399	487
	1-1c	233 000	400	488
	1-2a	206 500	402	491
	1-2b	214 900	406	493
	1-2c	200 900	400	489
Mean		221 183	401	490
Std. Dev.		15 966	3	2

* Directions 1-1 and 1-2 are shown in Figures 3.4 to 3.7.

Appendix B
Demec Point Data

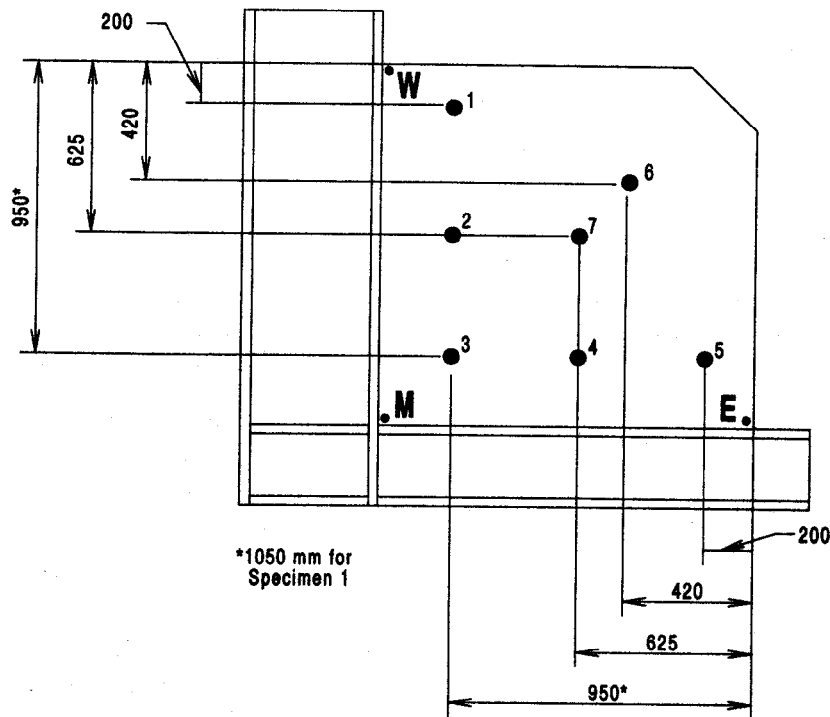


Figure B.1 Location of Demec Points on Specimens

The figure above shows the location of the Demec points that were used to monitor the movement of the infill plate connection specimens during testing (Chapter 3). Demec point data for all four specimens are given in Tables B.1 to B.4. All measurements in the tables are in millimetres and are relative to the measurements taken at three points on the panel-to-boundary member weld of the specimens (shown as 'W', 'M' and 'E' in Figure B.1, and referred to as West, Mid and East in the tables) prior to each test. The location of the panel-to-boundary member weld was considered to be at zero, that is, coincident with the centreline of the MTS machine, at the beginning of a test. Each set of readings in the tables is identified by a loading block, a cycle, and a "stage." The term stage refers to a particular point within a cycle: 1. Start of a cycle at zero load; 2. Maximum inward displacement of V-frame members; 3. Completion of Part A; 4. Maximum outward displacement of V-frame members; 5. Completion of Part B.

Table B.1 Demec Point Data for Specimen 1

Block	Cycle	Stage	Location of Measurement									
			West	Mid	East	1	2	3	4	5	6	7
2	3	1	0	0	0	11	5	0	-4	-11	2	2
	3	1	0	0	0	11	6	0	-7	-11	4	3
		2	-2	-1	3	16	19	5	-22	-19	10	8
		3	-2	0	3	11	8	1	-8	-12	4	4
		4	-4	0	4	4	2	-1	-5	-8	-3	-2
4	2	5	-2	0	2	10	6	-7	-11	4	2	
	1	1	-2	0	2	11	7	-7	-11	4	3	
	1	5	-1	0	3	11	7	-6	-11	5	4	
	1	1	1	3	14	10	3	-3	-7	9	7	
	2	1	-2	0	2	11	8	-8	-11	5	4	
	4	1	-3	-2	-1	9	6	-1	-12	-14	1	
	4	2	-2	-2	1	16	19	4	-25	-21	4	
	4	4	-3	-2	0	10	6	-2	-14	-16	4	
	4	4	-6	-3	-2	0	0	-4	-7	-12	-1	
	4	4	-4	-2	-2	9	5	-3	-12	-16	-1	
	10	5	-1	0	1	11	8	1	-8	-12	4	
	5	5	1	-1	0	3	9	1	-12	-13	2	2
		1	1	-1	1	1	12	13	-15	-15	-3	3
	6	6	1	-2	1	3	11	14	-15	-15	0	2
		6	2	1	2	4	18	32	-28	-18	8	8
6		3	-1	2	3	14	19	-18	-16	6	6	
6		5	-1	2	3	12	15	-15	-14	1	4	
3		2	2	1	4	19	35	-32	-20	9	9	
7	6	1	-1	1	2	11	17	-17	-15	3	4	
	6	2	2	2	3	18	35	-31	-19	8	9	
	6	3	0	2	3	16	24	-20	-16	9	9	
	6	5	-2	2	3	12	17	-16	-14	3	4	
	3	2	3	4	4	19	38	-32	-19	9	10	

Table B.2a Demec Point Data for Specimen 2

Block	Cycle	Stage	Location of Measurement									
			West	Mid	East	1	2	3	4	5	6	7
1	1	1	0	0	0	-4	4	0	-11	-33	-4	1
	3	1	0	2	2	-3	7	2	-12	-31	-2	3
		2	-4	2	2	-5	15	9	-21	-40	6	11
		3	0	2	2	-3	8	5	-13	-31	1	4
		5	0	2	3	-3	7	3	-12	-30	1	4
3	3	1	-1	2	3	-3	8	4	-15	-30	1	4
		2	-5	2	3	-3	17	10	-28	-44	5	10
		3	-1	2	3	-4	9	4	-18	-33	2	5
		5	-1	2	3	-5	7	3	-16	-31	1	1
		2	-7	0	1	-22	10	11	-29	-48	7	11
4	6	1	-1	0	2	-11	5	3	-16	-33	2	5
		2	-7	0	0	-28	8	11	-28	-48	7	12
		3	-2	1	1	-15	6	5	-18	-35	2	6
		5	-1	0	2	-10	6	3	-16	-32	1	5
		2	-5	0	-2	-35	2	14	-29	-52	9	15
5	6	1	-3	0	0	-28	-17	-7	-32	-40	-39	-42
		2	-5	1	-1	-36	2	16	-27	-52	10	17
		3	-2	2	1	-23	2	9	-16	-37	1	7
		5	-2	2	1	-26	-18	-5	-31	-38	-36	-42
		2	-5	1	-1	-40	-2	19	-27	-53	11	20
6	6	1	0	3	4	-30	-21	-4	-32	-37	-36	-47
		2	-3	3	1	-40	-2	23	-26	-53	13	19
		3	0	3	3	-27	0	13	-16	-38	-1	8
		5	0	3	4	-29	-21	-3	-31	-36	-37	-48
		2	0	3	4	-29	-21	-3	-31	-36	-37	-48

Table B.2b Demec Point Data for Specimen 2 (con't)

Block	Cycle	Stage	Location of Measurement									
			West	Mid	East	1	2	3	4	5	6	7
7	4	2	-4	3	1	-43	-3	23	-28	-55	14	23
	6	1	0	4	4	-24	1	1	-13	-34	1	9
	6	2	-3	4	2	-42	-3	23	-26	-54	15	25
	6	3	0	4	4	-31	-1	12	-17	-39	2	13
	6	5	0	4	4	-24	0	1	-12	-34	-1	9
	6	2	-3	5	2	-46	-4	25	-27	-56	18	27
8	6	1	1	4	5	-25	1	2	-12	-34	4	12
	6	2	-3	5	2	-46	-4	26	-26	-54	18	28
	6	3	1	4	4	-31	-1	13	-17	-41	3	14
	6	5	1	4	4	-24	1	0	-12	-34	4	13
	6	2	1	4	4	-24	1	0	-12	-34	4	13

Table B.3 Demec Point Data for Specimen 3

Block	Cycle	Stage	Location of Measurement									
			West	Mid	East	1	2	3	4	5	6	7
1	1	1	0	0	0	-3	2	0	12	12	14	14
	3	2	-1	-2	1	-14	-26	-11	22	26	-6	-9
	6	1	-1	-1	0	-7	-8	-4	12	13	10	7
	6	2	-1	-1	1	-15	-27	-11	22	25	-7	-9
	6	3	-1	-2	0	-8	-9	-4	14	15	9	6
4	6	5	-1	-2	-1	-7	-9	-3	14	15	12	8
	3	2	-1	1	2	-13	-28	-11	26	29	-4	-10
	6	2	0	-1	0	-15	-28	-10	25	26	-7	-10
	6	1	-2	-2	-1	1991	-11	-5	13	12	4	1
	6	2	-1	-1	1	-21	-33	-9	31	29	-8	-10
5	6	3	-1	-1	-1	-11	-12	-4	18	17	5	2
	6	5	-2	-1	-1	-13	-16	-4	16	14	1	0
	3	2	1	3	4	-23	-37	-7	42	37	-4	-7
	6	1	0	-1	1	-13	-16	-3	19	16	2	-1
	6	2	1	1	4	-24	-38	-6	42	37	-5	-7
6	6	3	0	0	1	-17	-22	-3	27	24	0	-1
	6	5	0	-1	1	-13	-16	-4	19	16	2	1
	3	2	0	1	4	-28	-42	-7	45	39	-5	-8
	6	1	0	0	1	-15	-19	-4	22	21	-30	-2
	6	2	0	1	4	-27	-42	-6	44	39	-5	-9
8	6	3	0	1	2	-18	-24	-4	30	27	-1	-3
	6	5	0	0	1	-15	-19	-5	22	19	1	-2

Table B.4 Demec Point Data for Specimen 4

Block	Cycle	Stage	Location of Measurement									
			West	Mid	East	1	2	3	4	5	6	7
1	1	1	0	0	0	-19	-1	0	-3	-23	-12	-2
	3	2	-3	0	0	-35	-3	19	-12	-42	15	21
		1	0	1	1	-21	-5	6	-7	-25	-14	-2
		2	-2	1	-1	-36	-4	20	-15	-43	15	22
		3	0	1	1	-20	-5	8	-8	-23	-10	2
		6	0	1	1	-22	-5	6	-7	-25	-14	-1
4	2	-3	1	-1	-39	-5	22	-14	-44	15	25	
5	6	2	-3	1	-1	-39	-5	23	-14	-43	15	24
	3	2	-4	-1	-2	-43	-7	25	-18	-49	18	27
	6	1	0	-1	-1	-29	1	18	-5	-33	17	23
	6	2	-3	-1	-2	-44	-7	25	-17	-48	17	28
	6	3	0	0	0	-33	-2	21	-8	-36	17	24
	6	5	0	0	-1	-30	1	19	-5	-34	17	22
6	3	2	-4	1	-2	-47	-8	29	-18	-52	20	31
	6	2	-4	-1	-2	-48	-8	29	-19	-52	18	30
	3	2	-3	1	0	-47	-7	33	-20	-52	21	34
7	6	1	1	1	2	-31	1	18	-8	-34	12	20
	6	2	-3	1	0	-48	-7	33	-21	-52	20	33
	6	3	2	3	2	-36	-2	26	-13	-41	15	27
	6	5	1	2	1	-31	1	19	-7	-34	11	19
	3	2	-3	2	0	-51	-8	37	-22	-56	22	36
	6	2	-3	2	0	-52	-9	37	-22	-56	23	37

Appendix C
Experimental Strain Results

Table C.1 Measured Strains from Specimen 1

	Rosette:	1	2	3	4	5
Part A	Block-Cycle: 5-6	-616	-362	-769	527	576
	Total Jack Load (kN): -649	615	487	-17	-339	-651
	Total Displ. (mm): -13.2	1366	1493	4205	2065	1141
	Block-Cycle: 8-6	-831	-	-474	711	601
	Total Jack Load (kN): -680	481	-	408	-221	-754
	Total Displ. (mm): -24.5	1078	-	4446	2448	1357
	ϵ_x					
	ϵ_y					
	γ_{xy}					
	ϵ_x					
	ϵ_y					
	γ_{xy}					
Part B	Block-Cycle: 5-6	161	355	939	247	225
	Total Jack Load (kN): 962	200	-257	-247	145	117
	Total Displ. (mm): 3.7	-1742	-1292	-693	-513	-1377
	Block-Cycle: 8-6	135	-	654	160	220
	Total Jack Load (kN): 890	162	-	-525	164	176
	Total Displ. (mm): 4.4	-1310	-	8	77	-863
	ϵ_x					
	ϵ_y					
	γ_{xy}					
	ϵ_x					
	ϵ_y					
	γ_{xy}					

Note: Negative values indicate compressive loads and strains, and inward displacements.
Rosette 2 not functioning properly.

Table C.2 Measured Strains from Specimen 2

		1	2	3	4	5
Rosette:						
Part A	Block-Cycle: 5-6	-530.75	-71.9	-2234.2	282.2	203.5
	Total Jack Load (kN): -708	91.8	3713.7	2760.6	-27.3	-294.2
	Total Displ. (mm): -12.8	983.1	1886.0	2835.2	979.3	583.8
	Block-Cycle: 8-6	-565.7	159.7	-1455.4	577.2	-55.35
	Total Jack Load (kN): -885	82.3	5716.8	5355.4	414.4	-176.8
	Total Displ. (mm): -23.6	1268.8	1024.5	1688.2	2510.9	865.7
	ϵ_x					
	ϵ_y					
	γ_{xy}					
	ϵ_x					
	ϵ_y					
	γ_{xy}					
Part B	Block-Cycle: 5-6	365.7	498.3	-1272.6	288.2	158.9
	Total Jack Load (kN): 1029	208.8	692.6	2228.2	496.3	428.2
	Total Displ. (mm): 4.0	-1696.7	-28.1	-555.3	-1385.3	-1733.7
	Block-Cycle: 8-6	342.65	711.5	1047.8	164.5	-75.65
	Total Jack Load (kN): 1086	386.3	3884.4	4677.1	577.0	532.0
	Total Displ. (mm): 3.4	-1919.0	-5778.0	-7905.9	-2089.2	-1811.7
	ϵ_x					
	ϵ_y					
	γ_{xy}					
	ϵ_x					
	ϵ_y					
	γ_{xy}					

Note: Negative values indicate compressive loads and strains, and inward displacements.

Table C.3 Measured Strains from Specimen 3

	Rosette:	1	2	3	4	5	
Part A	Block-Cycle: 5-6	-259.9	-157.5	379.3	632.6	22.65	
	Total Jack Load (kN): -702	334.8	866.8	688.7	54.1	-17.9	
	Total Displ. (mm): -12.2	1162.5	1835.9	1078.4	1078.0	1414.6	
	Block-Cycle: 8-6	-199.95	-12.9	800.1	694.7	-212.25	
	Total Jack Load (kN): -910	138.0	1177.8	1103.3	293.2	-19.0	
	Total Displ. (mm): -21.9	763.1	2076.2	998.5	1530.5	1429.2	
		ϵ_x					
		ϵ_y microstrain					
		γ_{xy}					
Part B	Block-Cycle: 5-6	290.7	390.2	292.5	300.4	-56.7	
	Total Jack Load (kN): 1017	244.6	-53.4	486.4	634.4	557.7	
	Total Displ. (mm): 4.9	-1616.7	-1401.7	-195.4	-1590.3	-1524.3	
	Block-Cycle: 8-6	333.3	436.1	458.7	351.8	-121.65	
	Total Jack Load (kN): 964	210.8	-192.1	154.3	573.5	497.5	
	Total Displ. (mm): 5.5	-1291.4	-928.5	-266.4	-1235.9	-1205.3	
		ϵ_x					
		ϵ_y microstrain					
		γ_{xy}					

Note: Negative values indicate compressive loads and strains, and inward displacements.

Table C.4 Measured Strains from Specimen 4

		1	2	3	4	5
Rosette:						
Part A	Block-Cycle: 5-6	-289.65	317.8	-	534.7	94.3
	Total Jack Load (kN): -479	198.6	6856.1	-	-331.1	-521.1
	Total Displ. (mm): -13.9	1155.7	-4055.7	-	1854.7	737.1
	Block-Cycle: 8-6	-186.7	793.4	-	1043.0	-22.25
	Total Jack Load (kN): -787	119.1	7471.8	-	-95.4	-457.2
	Total Displ. (mm): -24.4	2029.4	-2910.8	-	4311.7	824.5
	ϵ_x					
	ϵ_y microstrain					
	γ_{xy}					
	ϵ_x					
	ϵ_y microstrain					
	γ_{xy}					

Part B	Block-Cycle: 5-6	368.0	519.9	-	632.8	33.4
	Total Jack Load (kN): 1098	117.0	2130.8	-	432.9	327.5
	Total Displ. (mm): 1.8	-871.1	-2650.0	-	-1174.2	-967.75
	Block-Cycle: 8-6	464.15	369.4	-	859.7	-169.3
	Total Jack Load (kN): 1087	41.1	4507.7	-	526.7	402.8
	Total Displ. (mm): 2.0	-1384.3	-7470.1	-	-1459.7	-1476.0
	ϵ_x					
	ϵ_y microstrain					
	γ_{xy}					
	ϵ_x					
	ϵ_y microstrain					
	γ_{xy}					

Note: Negative values indicate compressive loads and strains, and inward displacements.
Rosette 3 not functioning properly.

Appendix D
Loading Block Data

Table D.1 Comparison of Loading Blocks for Specimen 1

Part A

Loading Block:	5		8	
Cycle:	1	6	1	6
Total Inward V-Frame Deflection (mm)	-13.0	-13.2	-25.9	-24.5
Total Jack Load (kN)	-655	-649	-725	-680

Part B

Loading Block:	5		8	
Cycle:	1	6	1	6
Total Outward V-Frame Deflection (mm)	3.6	3.7	3.4	4.4
Total Jack Load (kN)	989	962	920	890

Note: Part B, loading block 8 shows an increase in deflection within the block. This can be attributed to the weld tear in the V-frame joint (refer to Section 4.1).

* Data for loading block 2 not available since beam and column deflections only measured after loading block 3.

Table D.2 Comparison of Loading Blocks for Specimen 2

Part A

Loading Block:	2		5		8	
Cycle:	1	3	1	6	1	6
Total Inward V-Frame Deflection (mm)	-5.4	-5.0	-13.3	-12.8	-23.5	-23.6
Total Jack Load (kN)	-415	-391	-667	-685	-896	-842

Part B

Loading Block:	2		5		8	
Cycle:	1	3	1	6	1	6
Total Outward V-Frame Deflection (mm)	1.8	2.0	3.6	4.2	3.6	3.4
Total Jack Load (kN)	431	451	950	978	1093	1089

Table D.3 Comparison of Loading Blocks for Specimen 3

Part A

Loading Block:	2		5		8	
	1	3	1	6	1	6
Total Inward V-Frame Deflection (mm)	-4.7	-4.9	-11.5	-12.2	-22.4	-21.9
Total Jack Load (kN)	-312	-327	-642	-702	-945	-910

Part B

Loading Block:	2		5		8	
	1	3	1	6	1	6
Total Outward V-Frame Deflection (mm)	1.7	1.7	4.5	4.9	5.9	5.5
Total Jack Load (kN)	569	563	1046	1017	1079	964

Table D.4 Comparison of Loading Blocks for Specimen 4

Part A	Loading Block:	2		5		8	
	Cycle:	1	3	1	6	1	6
	Total Inward V-Frame Deflection (mm)	-5.3	-5.3	-14.2	-13.9	-24.2	-24.4
	Total Jack Load (kN)	-54	-69	-484	-479	-799	-787

Part B	Loading Block:	2		5		8	
	Cycle:	1	3	1	6	1	6
	Total Outward V-Frame Deflection (mm)	1.8	2.1	1.7	1.8	1.8	2.0
	Total Jack Load (kN)	899	902	1106	1098	1098	1087

Recent Structural Engineering Reports

Department of Civil Engineering

University of Alberta

203. *Behavior of Girth-Welded Line Pipe*, by Nader Yoosef-Ghods, Geoffery L. Kulak and David W. Murray, September 1994.
204. *Numerical Investigation of Eccentrically Loaded Tied High Strength Concrete Columns* by Jueren Xie, Alaa E. Elwi, and James G. MacGregor, October 1994.
205. *Shear Strengthening of Concrete Girders Using Carbon Fibre Reinforced Plastic Sheets* by Efrosini H. Drimoussis and J.J. Roger Cheng, October 1994.
206. *Shrinkage and Flexural Tests of a Full-Scale Composite Truss* by Michael B. Maurer and D.J. Laurie Kennedy, December 1994.
207. *Analytical Investigation of the Compressive Behavior and Strength of Steel Gusset Plate Connections* by Michael C.H. Yam and J.J. Roger Cheng, December 1994.
208. *The Effect of Tension Flange Movement on the Strength of Point Loaded I-Beams* by Dean Mullin and J.J. Roger Cheng, January 1995.
209. *Experimental Study of Transversely Loaded Continuous Steel Plates* by Kurt P. Ratzlaff and D.J. Laurie Kennedy, May 1995.
210. *Fatigue Tests of Riveted Bridge Girders* by Daniel Adamson and Geoffery L. Kulak, July 1995.
211. *Fatigue of Riveted Tension Members* by Jeffery DiBattista and Geoffery L. Kulak, November 1995.
212. *Behaviour of Masonry Cavity Walls Subjected to Vertical Eccentric Loads* by Ru Wang, Alaa E. Elwi, Michael A. Hatzinikolas and Joseph Warwaruk, February 1996.
213. *Thermal Ice Loads on Structures* by Azita Azarnejad and Terry M. Hrudehy, November 1996.
214. *Transmission of High Strength Concrete Column Loads Through Concrete Slabs* by Carlos E. Ospina and Scott D.B. Alexander, January 1997.
215. *Seismic Behaviour of Steel Plate Shear Walls* by Robert G. Driver, Geoffery L. Kulak, D.J. Laurie Kennedy and Alaa E. Elwi, February 1997.
216. *Extended End Plate Moment Connections Under Cyclic Loading* by Adey, Gilbert Grondin and J.J. Roger Cheng, June 1997.